Amazon Expedition Magazine - 1st. Edition | Manaus-Brazil (2022, Jun)

Newton Silva De Lima, Alfredo Tadeu Oliveira Coimbra, Alan dos Santos Ferreira, Aldemir Malveira De Oliveira, André Luiz Willerding, Daniel Valentim Barros Mansur Da Silva, Eriberto Barroso Façanha Filho, Fábio Raphael Moreira Cáuper, Fernanda Cabral Cidade, Guilherme Vilagelim De Souza, et al.

amazon

2022, September | 1st Year – V. 1 N. 1

Expedition MAGAZINE

amazonexpedition.zohosites.com

Black River in the La Niña Period (2020/2022) and the Climate of the Amazon: Hydrology

FRACTUS Experiment

Visit to MUSA

Observations of Gravity Wave propagation in the Equatorial Ionosphere after the Hunga Tonga–Hunga Ha'apai eruption with Ionosonde data and HYSPLIT Modeling

Reduction in water levels and regional warming of the Amazon River from Peru to the Atlantic Ocean in Brazil due to the effects of the 2016 ENSO

Amazon Expedition Magazine

First Edition: Special Edition (September 2022)

Website: (Know More)

amazonexpedition.zohosites.com

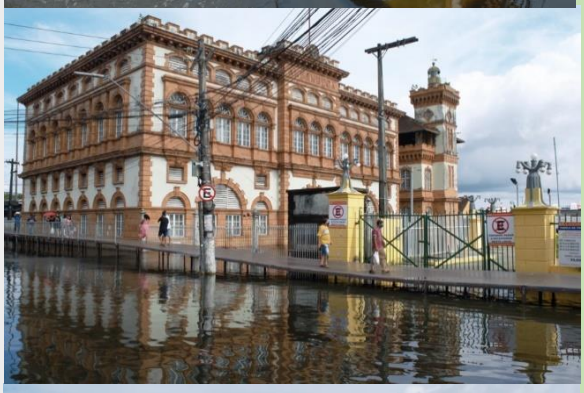

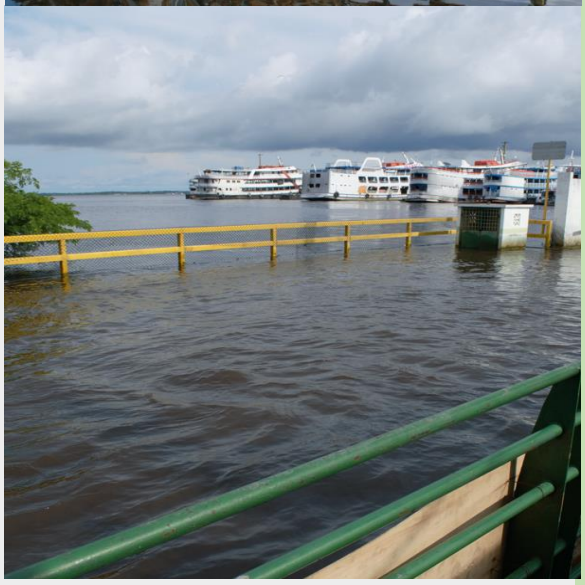

Consequences La Niña phenomenon in Manaus City – Brazil 2021-2022, June

Photos by Niels Lima: Building (imported from England in the 19th century) and Manaus Harbour

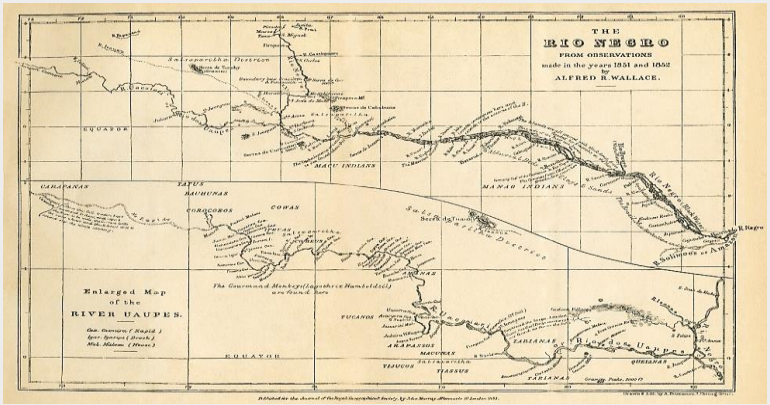

Map of the Black River (*Rio Negro*) according to Sir Alfred Russel Wallace, published in the Journal of the Geographical Society by J. M. Albermarte (London, 1895). (Copyright of Fishes of the Black River, edited by Mônica de Toledo-Piza Ragazzo, Edusp, 2002). With Climate Observations, Geological, Natural and Historical of the native peoples of the Black River, from Manaus to the Uaupés River on the border with Colombia.

September, 2022

CLIMATE

4. Black River in the La Niña Period (2020-2022) and the Climate of the Amazon: Hidrology

CLIMATE

15. FRACTUS Experiment

African dust scattering, between Sahel and Central Amazon

CLIMATE

33. Visit to MUSA (Amazon Natural Museum)

SPACE WEATHER

36. Observations of Gravity Wave propagation in the Equatorial Ionosphere after the Hunga Tonga–Hunga Ha'apai eruption with Ionosonde data and HYSPLIT Modeling

CLIMATE

47. Reduction in water levels and regional warming of the Amazon River from Peru to the Atlantic Ocean in Brazil due to the effects of the 2016 ENSO.

ENVIRONMENT

59. A brief observation of geoindicators in the Madeira River between Novo Aripuanã and Manicoré in 2018.

connections
SPACE WEATHER | CLIMATE

70. Observations with operational research on the connection of the 11-year Solar Cycle and the El Niño and La Niña phenomena and rainfall in the Amazon (1980-2030).

Cover Design and Images
Niels N C L

Editorial

The Amazon holds several adjectives of grandeur about its rainforest for having the largest river in the world, for having the greatest biodiversity of plant and animal specimens, for being the largest contributor to the capture of atmospheric CO_2, also for favoring rainfall throughout the Americas. and influence the global circulation of the atmosphere by balancing the planet's temperature. With all this status quo, it is always a subject of research and, of course, always will be.

In this first edition, a field observation involving the socio-climatic parameters in the city of Manaus - Brazil (2021-2022) of the Rio Negro floods and the consequences of the passage of the La Niña phenomenon in 2021 and 2022.

It also brings a brief description of the FRACTUS Experiment, which involves 5 different sites and the modeling of Sahel dust in the Amazon. The research team pays a visit to the Natural Museum of the Amazon. In an unprecedented aspect, it shows the Gravity Wave phenomenon on the east coast of South America after the eruption of the Hunga Tonga–Hunga Ha'apai volcano in the central pacific. Discusses the ENSO phenomenon of 2016 from the Peruvian city of Iquitos to the mouth of the river in the Atlantic Ocean during the dry period, it constitutes a recurring and interesting topic on the interaction of hydroclimatology and the biosphere - atmosphere in the Amazon, which we call the Current State.

In addition, the scope of the research describes the social and economic view of the Amazon River of the phenomena within the Surface Boundary Layer in the diffusion of localized and non-localized turbulence, wind speed and air temperature, among others.

Newton Silva de Lima (Chief-Editor)

Consequences La Niña phenomenon in Manaus City – Brazil 2021-2022, June

Image by Robson Calazães: Negro (Black) River - Manaus Harbour.

View of the Port of São Raimundo from the Bridge over the Black (Negro) River in front of Manaus

Black River in the La Niña Period (2020-2022) and the Climate of the Amazon: Hydrology

Lima[(1)], N S; Malveira, A O; Façanha[(1)], E; Ferreira[(1)], A S; Oliveira[(1)], L G S; Figueredo[(1)] R.; Calazães[(1)], R; Coimbra, A T O; Ramos, N L; Vale, R; Mansur, D V B.

Lutheran University Center of Manaus - CEULM | ULBRA[(1)]

Ave. Carlos Drummond de Andrade, 1460 - Conjunto Atílio Andreazza – Japiim
CEP 69077-730 - Manaus/AM – Brazil - Telephone: +55 (92) 3616-9800

· e-mail: acsmao@ulbra.br
· e-mail: alfredocoimbra@seduc.net
· e-mail: newton.lima@ulbra.br
· e-mail: liliam.oliveira@ulbra.br
· e-mail: naiana.Lopes.r@gmaim.com (Université de Genève -Faculté Sciences- Switzerland)
·e-mail: rics.fig@gmail.com
· e-mail: alan.ferreira@ulbra.br
· e- mail: danielvmansur@gmail.com (Martha Falcão College - Wyden – AM | Brazil)
· e-mail: matoscalazaes@gmial.com
· e-mail: roseilsondovale@gmail.com (Oeste do Pará Federal University | Brazil)
· e-mail: eriberto.filho@ulbra.br
· e-mail: amoliveira@gmai.com (Amazonas Federal University | Brazil)

Introduction

The Black River (Rio Negro) is a river that rises in the Guyanese shield in North South America in Colombian territory (Guainia River) and comes towards the great Amazon River (Brazil), where it has its mouth, where its black waters meet the waters of the Solimões river in front of the city of Manaus (Latitude: - 3.10719 Longitude: - 60.0261). Its volume is strongly influenced by the seasonal climatological phenomena of El Niño, when it reaches 13.63 m and in the La Niña period, it reaches up to 30.00 m, as the normal elevation oscillates between 17.54 m and 21.77 m, in relation to sea level, which is distant from its mouth, another 1,054 km to the Atlantic Ocean. It is the largest tributary on the left bank of the Amazon River, being the seventh largest river in the world by volume of water, responsible for 7% of the water it discharges into the Atlantic, the Black drains an area corresponding to 10% of the 7 million kilometers squares of the Amazon Basin. In, Zeidemann, 2001, more water flows through its bed than flows in all the rivers in Europe combined.

In this observation period (June, 2021-2022) indicates the increase in the level in the Black basin, which reached a record level of 30.00 m in Manaus (Brazil), the year of La Niña. At the meteorological stations in sequence to Manaus coming from São Gabriel da Cachoeira, the height ruler is 12.23 m, (average 9 m), in Santa Isabel do Rio Negro it is 7.78 m (average 6.70 m) and in Barcelos it is at 9.39 m (average 6 m), being the next in Manaus. (Brazilian Geological Survay - BGS, 2021).

From November 2020 to June 2022, the La Niña phenomenon, and the warming of the South Atlantic in the tropical region, plus the formation of the Intertropical Convergence Zone - ITCZ parking over the region in this period, favored greater rainfall intensities over the Amazon and the entire sector North of South America.

From then onwards (second half of June), the Black River (Rio Negro) tends to start its ebb process until it reaches its minimum level. The end of the ebb, in turn, does not have a preferential period, and may occur between October and January of the next year.

The present work shows the climatic phenomenology of the Manaus region (Brazil) at the meeting of the waters of the Black River with the Solimões River (Rio Solimões). The Black flows near Manaus over soil from the Mesozoic Geological Era in the Cretaceous Period (144 – 66 million years) after the Jurassic period, while the Solimões River runs over the ground of the Quaternary of the Cenozoic Era (1.8 – 0.15 million years old), in this convergence of two geological formations, the beds are of different depths and ages. At this meeting of the waters, the Black has a depth during the flood period of approximately 90 m and the Solimões 42 m. (3D simulation with Sankey Diagram and didactic view of the Underground Diagram - Subway), to better understand the positions and locations of the cities around the rivers, in addition to the bathymetry at the meeting of the waters shown here in the history of 1978, 1988, 1998 and 2013, illustrating the changes and dynamics of the profiles and turbulence at the site of observations.

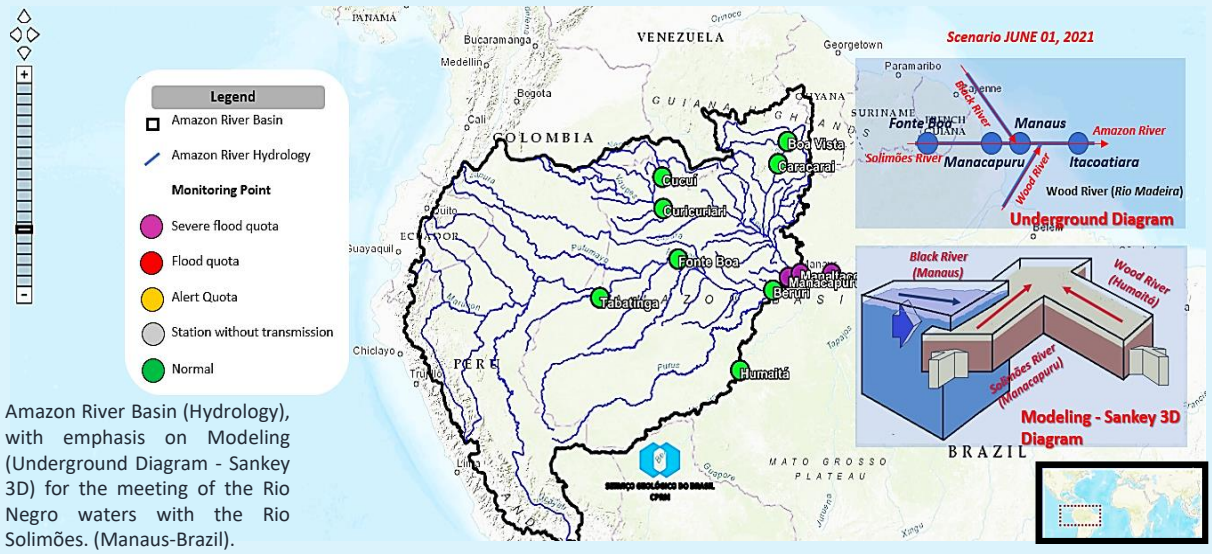

Amazon River Basin (Hydrology), with emphasis on Modeling (Underground Diagram - Sankey 3D) for the meeting of the Rio Negro waters with the Rio Solimões. (Manaus-Brazil).

Route from Rio Negro from Colombia to Manaus-Brazil

1. **Manaus** – Novo Airão : 154,8 km (2 h 52 min) (3h)*
2. **Novo Airão** – Barcelos: 276 km (5 h~ 6 h)*
3. **Barcelos** – Santa Isabel: 220 km (5 h ~ 6 h)*
4. **Santa Isabel** – S. Gabriel: 222 km (5 h~ 6 h)*
5. **São Gabriel da Cachoeira**

(*) in speedboat

1. Lat: 03° 05' 34" S, Lon: 060° 02' 24" W
2. Lat: 02° 37' 09" S, Lon: 060° 56' 43" W
3. Lat: 00° 58' 26" S, Lon: 062° 54' 58" W
4. Lat: 00° 25' 04" S, Lon: 065° 01' 14" W
5. Lat: 00° 08' 04" S, Lon: 067° 04' 46" W

Comparative images between El Niño and La Niña periods on the Black (Negro) River in Manaus (Brazil).

In the first half of December 2021, a trip up and down the Rio Negro was carried out through its multichannels, from Manaus to São Gabriel da Cachoeira. The purpose was to observe the present state of the river, after a record flood in Manaus, within the period of La Niña installed over the region in early 2018, remaining established until 2022 (June), when the river is already in alert quota. of severe flooding in the city of Manaus (Northern Brazil).

During the trip along the river, both ascent and descent, a condition of heavy rain throughout the route between the cities of Manaus-São Gabriel da Cachoeira.

The meteorological conditions of the trip and the geochemical analysis of the river water were recorded (Table | Geoindicators – Black River | 2021, December).

The Black (Negro) River in this period was in a period of low tide, although for the entire route between the cities the level of its level was still high, due to the conditions of heavy rains at its head and also throughout its body of water. Noted for the navigability throughout the route. During El Niño, the headwaters of the river become not very navigable due to rock outcrops along the riverbed. They can also be seen even during the flood season on some sections of the trail. A well-noted feature occurs when approaching the head of the river, is the appearance of mountainous elevations, including in this region the largest mountain in Brazilian territory is observed, which is the Neblina peak in the Imeri mountain range (2,995.30 meters of altitude).

The location of the source of the river in the Colombian Amazon in the North of South America, has climate type “Af”, in the Köppen-Geiger classification, until close to Manaus (Brazil), that is, rainy all year round regardless of the seasonality season. . That is, it connotes this river as the highest flow tributary in the Amazon River.

Table - Geoindicators | Black (Negro) River(Dec - 2021)

Site	Temp (°C - °F)	P_{Atm} (pascal)	Alt. (m)	pH	Cond. (µS/cm)	O_2 Sat(%)	O_2 Dissipated (mg/L)
Manaus S 03°05'32.1" W 60°02'22.7" Local Time: 06h 20min	**27.6 °C (81.68 °F)**	100681 Pa	**54.01 m**	**5.14**	**53.2**	**76.6**	**5.36**
Moura| Remanso S 02°04'44.9" W 61°09'49.9" Local Time: 00h37min	**25 °C (80.6 °F)**	**100574 Pa**	**62.21 m**	**7.3**	**32.3**	**78.7**	**6.20**
Barcelos S 00°24'38.0" W 63°37'47.2" Local Time:18h43min	**24,5 °C (76,1 °F)**	**100504 Pa**	**67.91 m**	**6.9**	**37.5**	**79.1**	**6.21**
Santa Isabel do Rio Negro S 00°18'07.1" W 65°56'02.7" Local Time:12h04min	**31.4 °C (88.52 °F)**	**100440 Pa**	**73.61 m**	**6.7**	**35.7**	**78.0**	**6.21**
São Gabriel da Cachoeira S 00°07'44.0" W 67°05'25.2" Local Time: 06h	**25,4 °C (77.72 °F)**	**100515 Pa**	**67.49 m**	**6.9**	**31.7**	**78.1**	**6.26**

(Data obtained between Dec 7 - 8, 2022. Trip started in São Gabriel da Cachoeira to Manaus)

In 2021, June. *"The flow recorded (Óbidos – PA | Brazil) was 270,392.8 m³/s and is considered the highest in the data series, since the record is made with acoustic measurement equipment. With this flow rate, a city like São Paulo (Brazil) could be supplied with its water needs for one day, in 15 seconds".* (CPRM-ANA).

Óbidos (S 01°55'03" and W 55°31'05") is a city on the left bank of the Amazon River in the state of Pará (Brazil), close to the city of Nhamundá in the state of Amazonas. It is the last station to measure the flow of the river, whose distance to the mouth is approximately 1,100 km. This care is taken so that the tides do not influence the flow data.

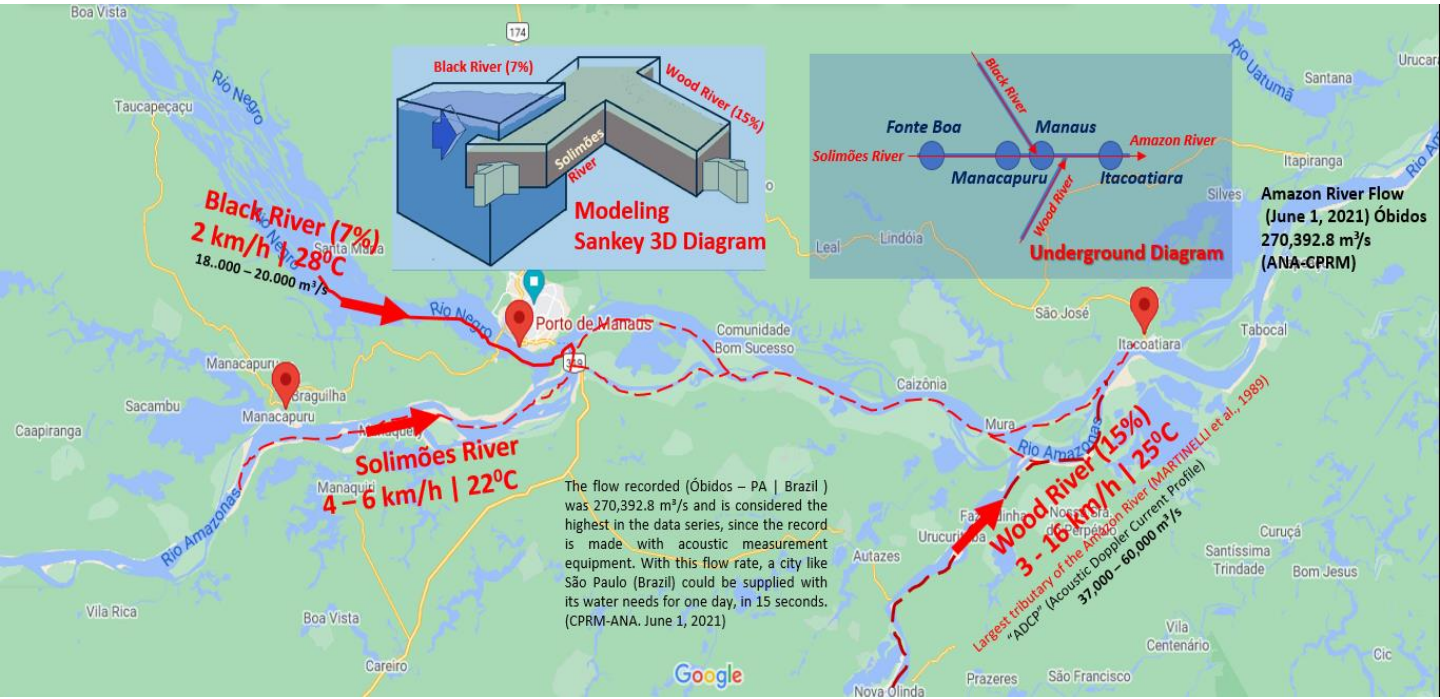

The ratio between width and depth of a river is represented for the meeting of the Black (Negro) River and Solimões River (Figure below), showing the specificities of the meeting of two rivers and their main water parameters

Black River (Rio Negro) in La Niña period in 2021, June. Photo: Natja Lima

Cross-section of the channels of the two rivers at the meeting of the waters (Black |Solimões)

Legend

WL – water level

B/h < 40 (formation of meanders is overstressed)

B >> h (open-channel)

B – width ($B = \overline{b_2\ b_2'}$)

B_c – width (of the central region)

m – varies depending on the cross-section geometry and boundary roughness.

h - depth

$\lambda - \lambda'$ – lines formed by the points where the curvature of the isovels pratically vanishes.

Sr – transverse free surface slope.

N – number row (horizontal burts)

Γ – cross-sectional circulation

ϕ –angle of repose

$\overline{b_2\ b_2'}$ - bed horizontal

$b_1 b_2$ – banks

$b_1' b_2'$ - curvilinear

C – Chézy coefficient (dimensionless)

$C = \sqrt{8g/c}$; $v = C\sqrt{SR}$; $v^* = \sqrt{gSR}$

$c = v/v^*$

c = Friction Fator = (average flow velocity by shear velocity)

$\omega \sim$ dimensionless variable determining N

S = slope

R = h = flow depth

$g = 9{,}816\ m.s^{-2}$

Width (B) and Depth (h) Ratio

I. (B/h)

II. $B - B_c - \bar{B}$

III. $Bc = B\,(1 - 2m[h/B]) \rightarrow m = (B/h).(1/N)$

IV. $N = \phi_N(\omega)$

V. $\omega \sim (B/h)/c^2 \rightarrow c = v/v_*$

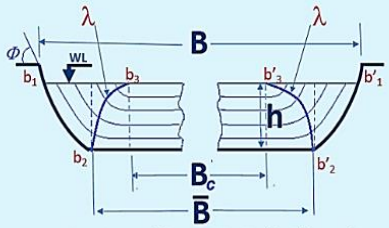

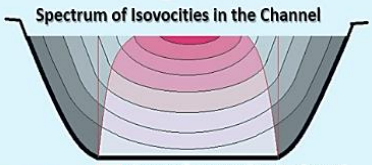

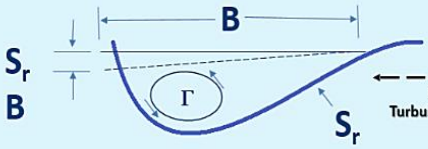

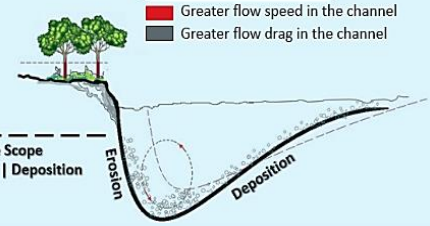

Maximum quota over sea level - 19 m
(2016 Dec) El Niño

Scenarios of El Niño and La Niña
Rio Negro (Black River) Manaus Harbour | Brazil

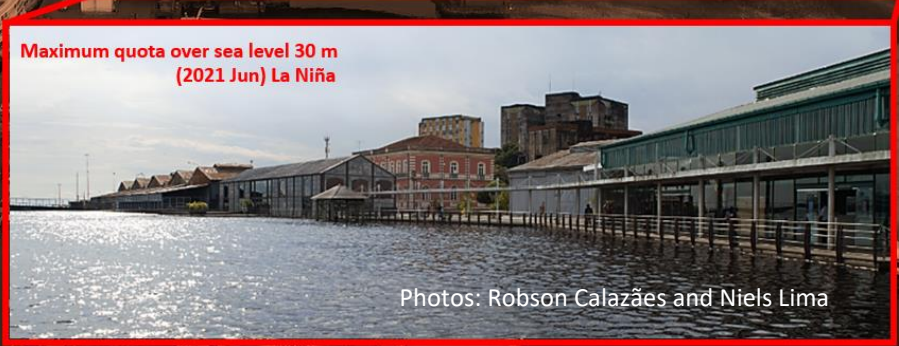

Photos: Robson Calazães and Niels Lima

Amazon Basin Modeling - Synthetic Unit Hydrographs

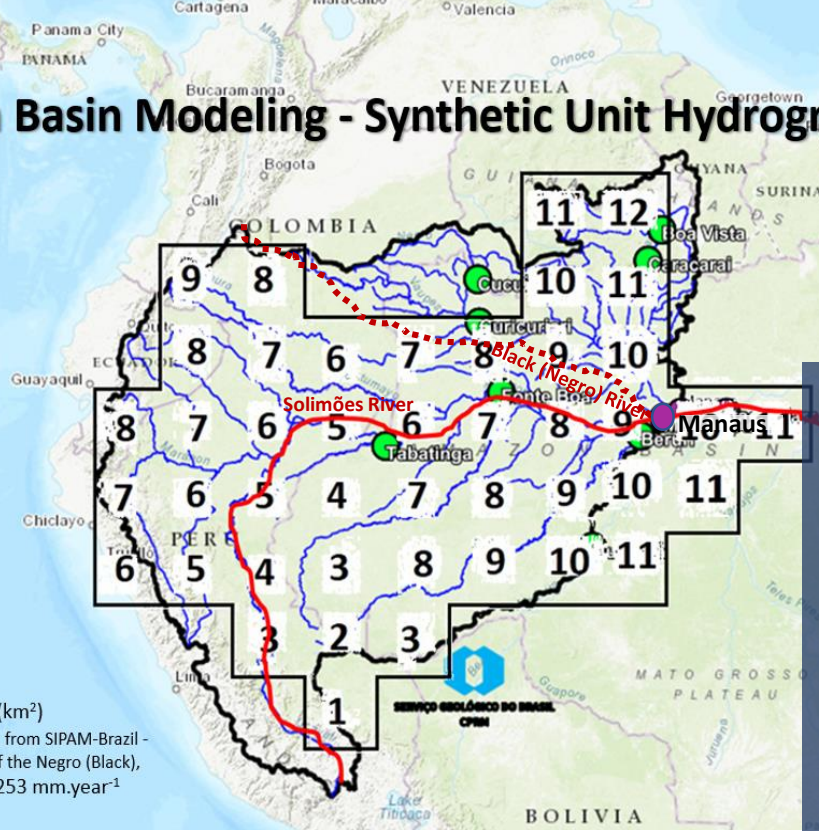

The Figure describes the influence of hydrology on major floods in Manaus-Brazil, resulting from the flooding of the Solimões River in the Amazon Basin. Especially during La Niña periods.

Features

Basin Area: 2.1 million (km²)

1 Unit Hydrograph: ~ 48 thousand (km²)

Average annual precipitation: (data from SIPAM-Brazil - considering the total area of the basins of the Negro (Black), Solimões and Madeira (Wood) rivers.) 2,253 mm.year^{-1}

Time-Area Unit Hydrograph Development

The watershed is divided into 44 subareas of equal area, all subareas contributing to the outlet within 12 time units.

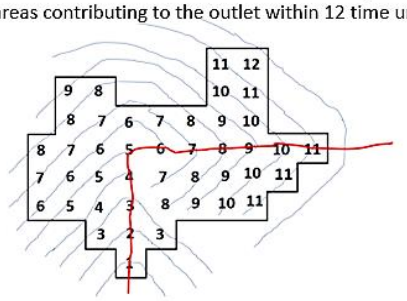

1. Watershed and Travel Times (iso-time lines)

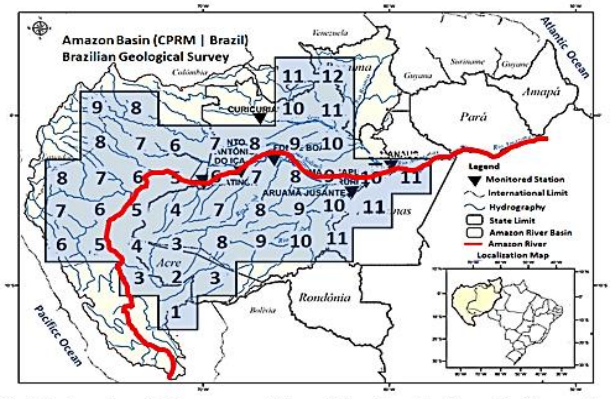

2. Watershed (Amazon River) in North South America

3. Contributing Area versus Times

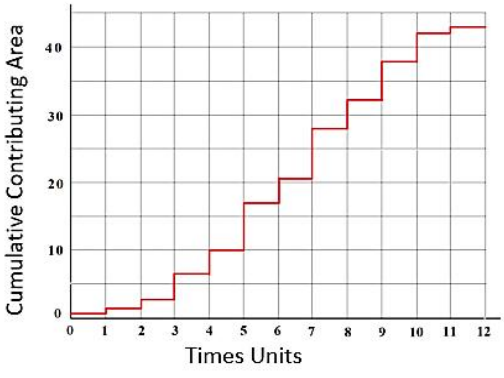

4. S-Hydrograph

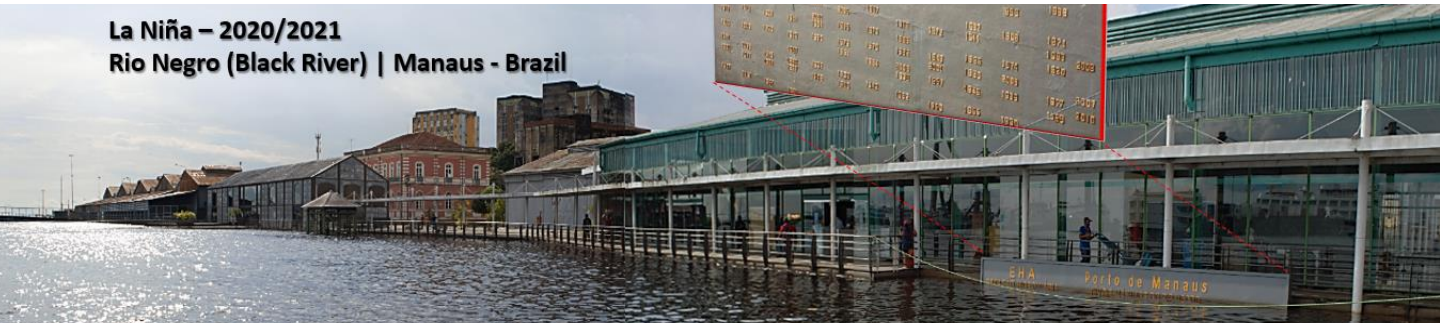

River Level and Rainfall

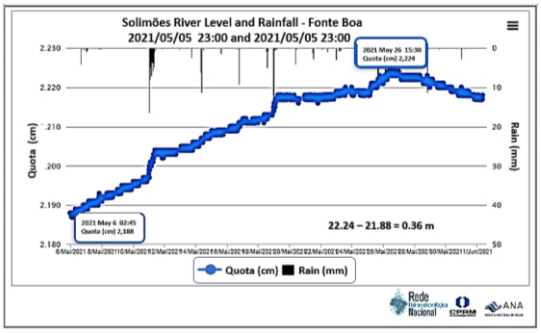

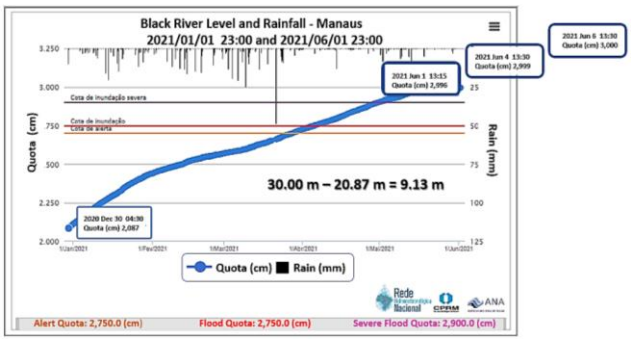

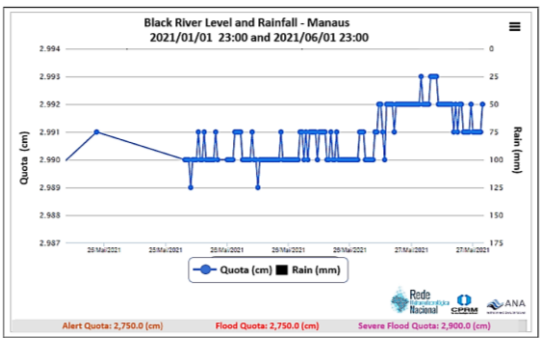

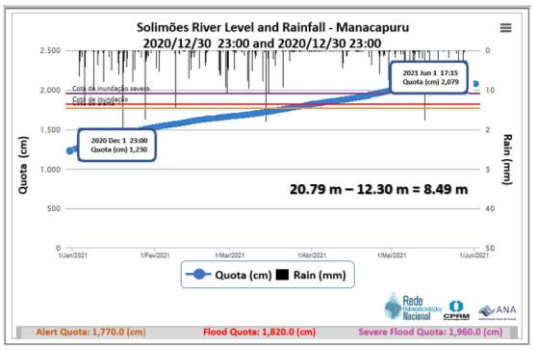

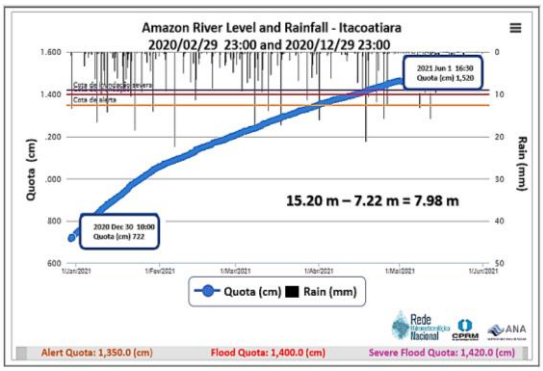

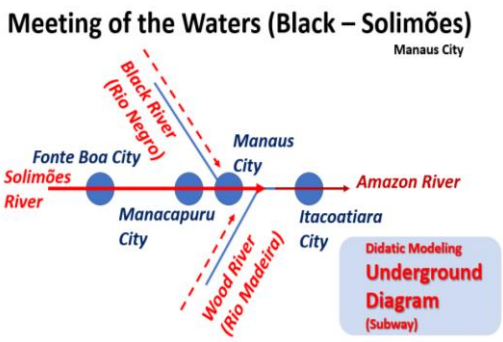

Scenario of the Meeting of the Waters showing a Sankey Flow Diagram in 3D (Map, Drawing and Graphic)

River Level 1st. Semester June 02, 2021: 29.98 m

Day	JANUARY		FEBRUARY		MARCH		APRIL		MAY		JUNE	
	Quota (m)	Filled / Leaked (cm)	Quota (m)	Filled / Leaked (cm)	Quota (m)	Filled / Leaked (cm)	Quota (m)	Filled / Leaked (cm)	Quota (m)	Filled / Leaked (cm)	Quota (m)	Filled / Leaked (cm)
1	21.26	15.00	24.49	6.00	25.79	3.00	27.34	6.00	29.08	5.00	29.98	1.00

8,72 m

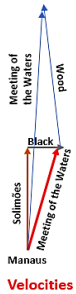

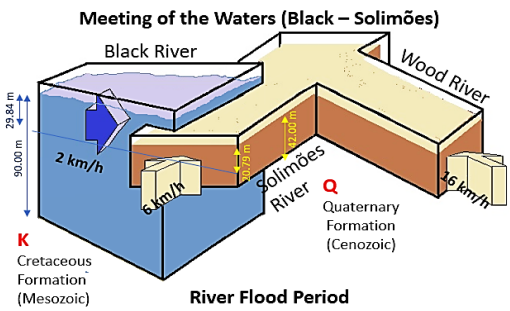

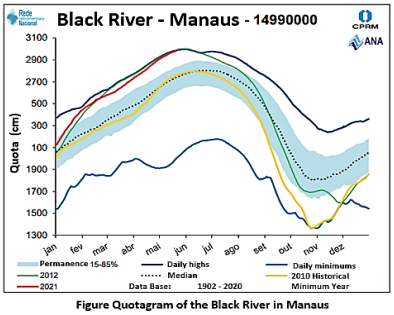

Figure Quotagram of the Black River in Manaus
Quota in June 01, 2021 : 2,984 cm

Bathymetry and dynamic analysis of the geological floor at the meeting of waters in over forty years of observations (Black - Solimões)

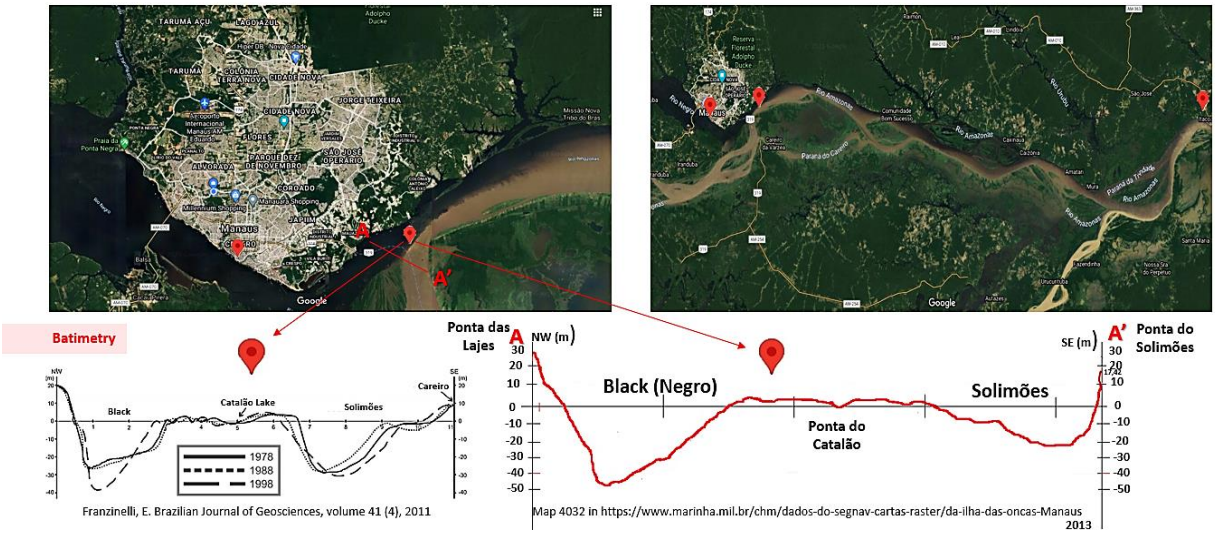

Turbulence (Meeting of the waters) - Surface View of Horizontal Turbulence

Configuration criteria: horizontal bursts of N-row at the meeting of the waters Black River (Rio Negro) with the Solimões River. (Lima, et al., 2021)

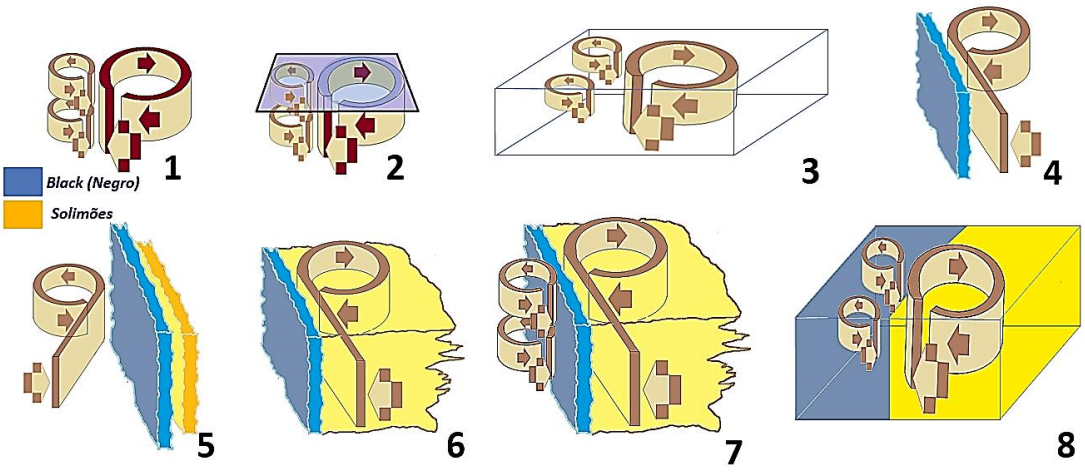

1 - Formation of coherent vortices. ***2*** - horizontal turbulent formation configuration. ***3*** - Configuration of the set of swirls that carry out shear when approaching.

4 - 5 - 6 - 7- Effects of the formation of eddies on liquid walls with different densities, temperature and speeds at the meeting of the waters. ***8*** - Artistic view of the Turbulance phenomenon.

Artistic View of Turbulence within the Channel

(Study based on Turbulence in Fluids - MARCEL LESIEUR, 2008)

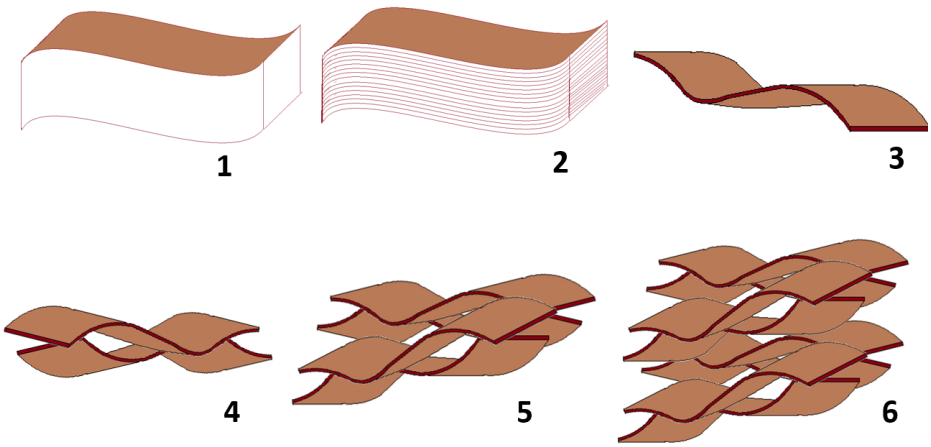

1. Continuum liquid body; 2. Horizontally quantized body; 3. n = 1; 4. n = 2; 5. n = 4.

6. n - Flow blades (twist-type turbulence). (*) n = number of blades .

Hydraulic, hydrochemical and sedimentological characteristics of the Solimões and Black rivers at the point where the waters meet.

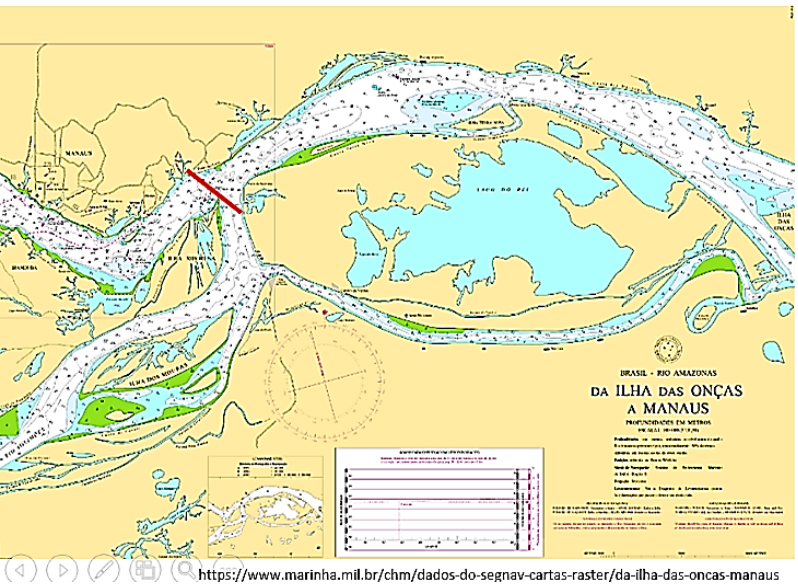

https://www.marinha.mil.br/chm/dados-do-segnav-cartas-raster/da-ilha-das-oncas-manaus

Variables	Solimões River	Black River
Basin Areas	2,200,000 km^2	600,000 km^2
Average Amplitude	2 - 5 km	3 - 20 km Maximum on the low Black River
Medium Depth	20 - 35 m	20 - 30 m 90 m maximum where the waters meet
Average Net Discharge	100,000 m^3/s	30,000 m^3/s
pH	6.2 - 7.2	3.8 - 4.9
Solid Discharge	700 x 10^8 mt/year	6 x 10^8 mt/year
Dissolved Discharge	205 x 10^6 t/year	5.7 x 10^6 t/year
Bottom Sediments	Coarse, medium and fine sand	Loose cream clay
Current Speed	0.5 - 1 m/s (2 - 2.5 m/s on the ebb)	1 cm/s
Temperature	29°C ± 1°C	30°C ± 1°C

Franzinelli, E. Brazilian Journal of Geosciences, volume 41 (4), 2011

Acknowledgments

The authors are grateful to the Northwest Navigation Survay - Brazilian Navy (NNS - Vila Buriti | Manaus-Brazil) for accessing navigation chart 4032, for bathymetry assistance, they are also grateful to the Brazilian Geological Survay (BGS) for the hydrology and climatology database from CPRM and ANA offices, and Amazon Protection System - SIPAM. Likewise, to the photographer Niels Lima, the Engineer Natja Lima and Engineer Robson Calazães for the images of the Black river and the field geochemical analyses.

References

Brazilian Geological Survey - BGS
(Critical Events Alert System) - CPRM - ANA
http://www.cprm.gov.br/sace/
Brazilian Navy. (https://www.marinha.mil.br/chm/dados-do-segnav/cartas-raster)

Franzinelli, E. Morphological characteristics of the confluence of the Black and Solimões rivers (Amazon, Brazil). Brazilian Journal of Geosciences, volume 41 (4), 2011.

Geo cities project: integrated urban environmental report: GEO report: Manaus/ Supervision: Ana Lúcia Nadalutti La Rovere, Samyra Crespo; Coordination: Rui Velloso. Rio de Janeiro: Consortium Partnership 21, 2002. 188 p.: 21 cm

Horbe, Adriana and Collaborators. Geochemistry of the waters of the middle and lower Wood River and its main tributaries - Amazon – Brazil. ACTA AMAZONICA. VOL. 43(4) 2013: 489 – 504.

HAS - Hydrological Alert Service (CPRM - ANA)
BULLETIN ON HYDROLOGICAL MONITORING OF THE WOOD RIVER BASIN BULLETIN No. 14/2021 May 7, 2021 –

Lesieur, Marcel. Turbulence in Fluids Fourth Revised and Enlarged Edition. Library of Congress Control Number: 200794115. All Rights Reserved © 2008 Springer.

Martinelli et al., Discharge of total dissolved solids from the Amazon River and its main tributaries. Geochim. Brazil 3 (2): 141-148, 1989.

Sternberg, H. O'Reilly. 1975. The Amazon River Of Brazil. GEOGRAPHISCHE ZEITSCHRIFT. BEIHEFTE. p.78

Vivian Karina Zeidemann. Forests of the Black River. The Black Waters River. Chapter 2 – USP – Company of Letters, Paulista University and The New York Botanical Garden, 2001.
http://ecologia.ib.usp.br/guiaigapo/florestas.html

Yalin, M.S. 1992. River Mechanics. Pergamon Press. p. 220.

FRACTUS-Experiment

Amazon - Morocco

(FRaction Aerosol – Climate – Temperature USable)

Introduction

The greatest contribution to the rains in the Amazon is in the humid tropical forest, whose trees are the links of the subsoil-atmosphere connection in the transport of water and volatile organic compost that transform into rain aerosols that also mix with other aerosols that arrive in the Amazon.

The analyzes show that the trajectories of air masses departing from the Sahara between the months of January and June, between 9 days before aerosols were identified in the Amazon, carrying elements associated with the soil dust.

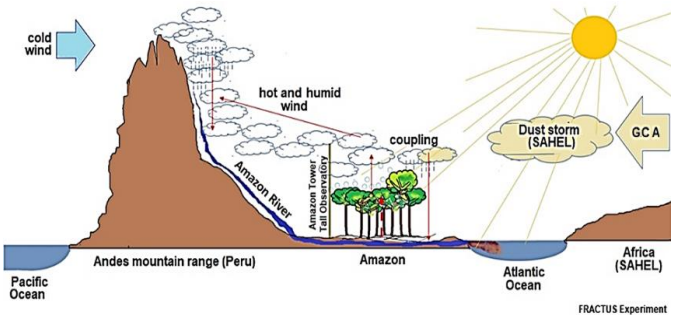

Artistic representation of the FRACTUS Experiment work scenario (Authors, 2022)

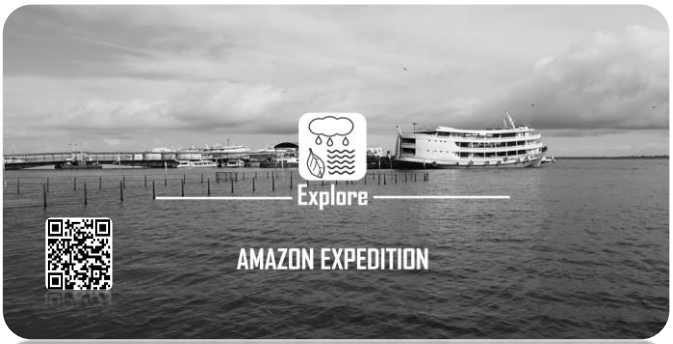

Sahel | Amazon

FRACTUS Experiment (BR)

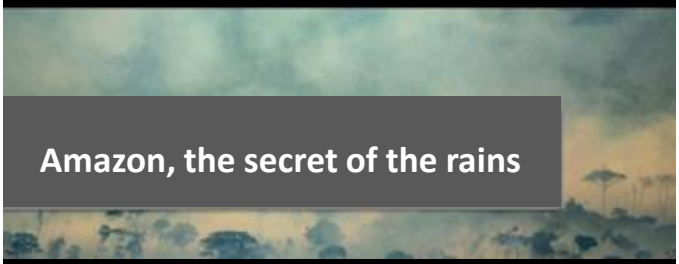

Amazon, the secret of the rains

Amazon, the secret of the rains*

(Hypothesis)

African aerosols fertilize the trees of the Adolpho Ducke Forest Reserve (Manaus-Brazil), of the Peruvian city of Iquitos, of the Pará city of Santarém (Brazil), and of the forest of the upper Black River (Rio Negro) border between Colombia and Brazil.

(*) **The FRACTUS Experiment is in field activity. Its expected completion is for the year 2025.**

amazonexpedition.zohosites.com

FRACTUS-Experiment

Amazon - Morocco

(FRaction Aerosol – Climate – Temperature USable)

FRACTUS|MOSAIC start: 2021,Dec 03. Trajectory h = 15000 m - Himalayas - Peru

FRACTUS mosaic of African dust scattering, wind trajectories between Africa and Central Amazon at 15,000 m (red) and 13,500 m (green), intermediate blue, during Amazon wet season, with HYSPLIT modeling for 7 days from January 14 to 22 January 2022. Courtesy: HYSPLIT (NOAA-NASA).

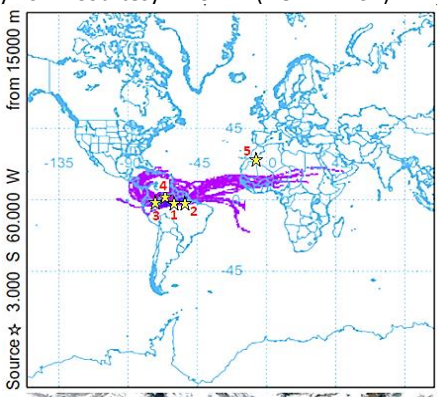

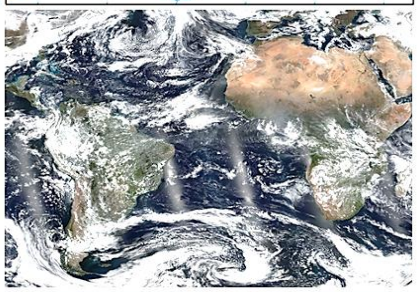

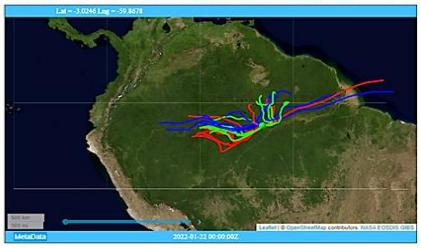

(a) Trajectory of African dust (Dust Optical Thickness) over the “hot spots”, that is, on sites in the Amazon between January 1, 2022 and January 20, 2022 (Courtesy: HYSPLIT|NOAA|NASA), (b) Image of the global circulation of the atmosphere (CGA). Courtesy: EOSDIS - NASA) from 22 Jan 2022 at 00 UTC, (c) Image of dispersion and deposition of African dust over the target in Manaus (22 Jan 2022), different colors mean different altitudes being red 15000 m (maximum) and green 12500 m (minimum). Courtesy: HYSPLIT|NOAA|NASA.

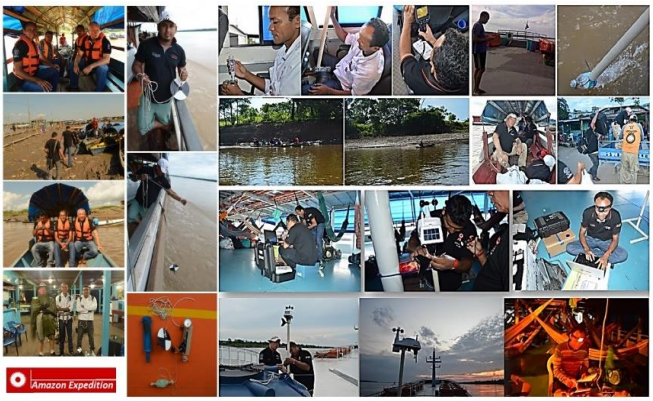

amazonexpedition.zohosites.com

FRACTUS Modeling

FRACTUS Experiment

Strongest surface dust mass concentration in North Africa with density (dark brown), > 9.0 x10 -8 kg/m3. Courtesy: MERRA-2 (Monthly) | NASA.

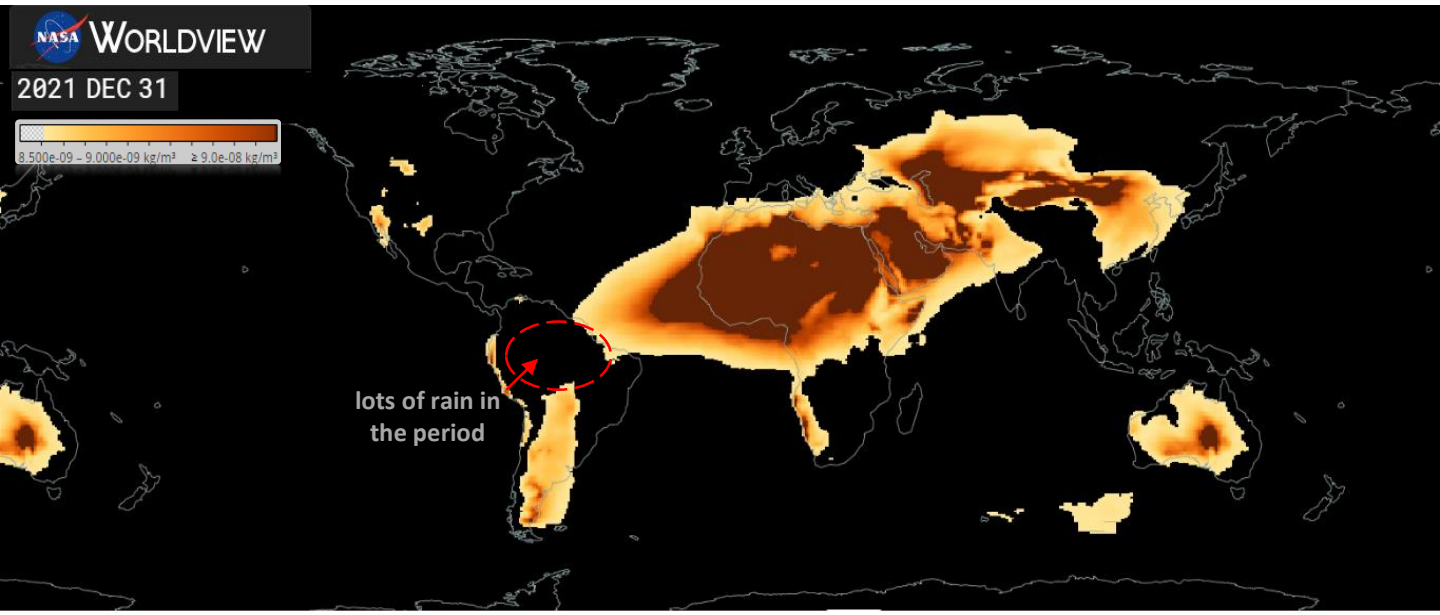

FRACTUS modeling for sites 1 - 2 - 3 – 4 - 5, for the month of January 2022, with data from NOAA HYSPLIT MODEL.

FRACTUS Experiment

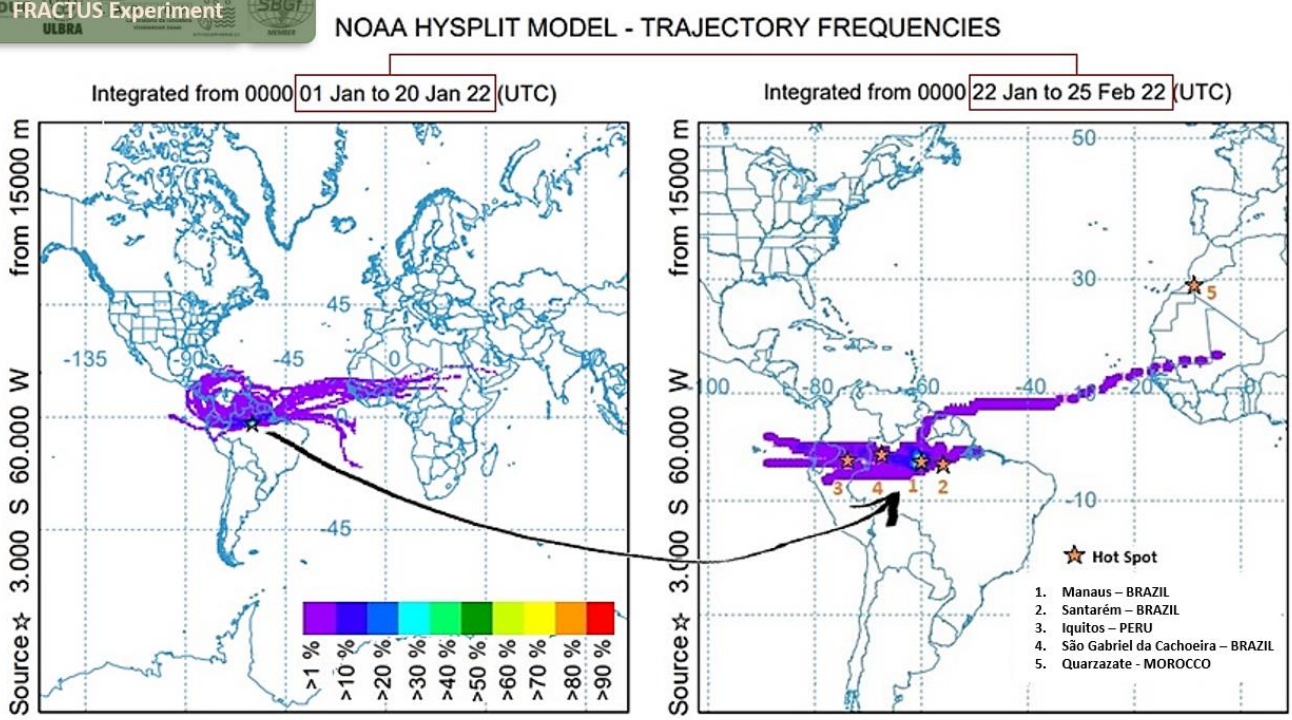

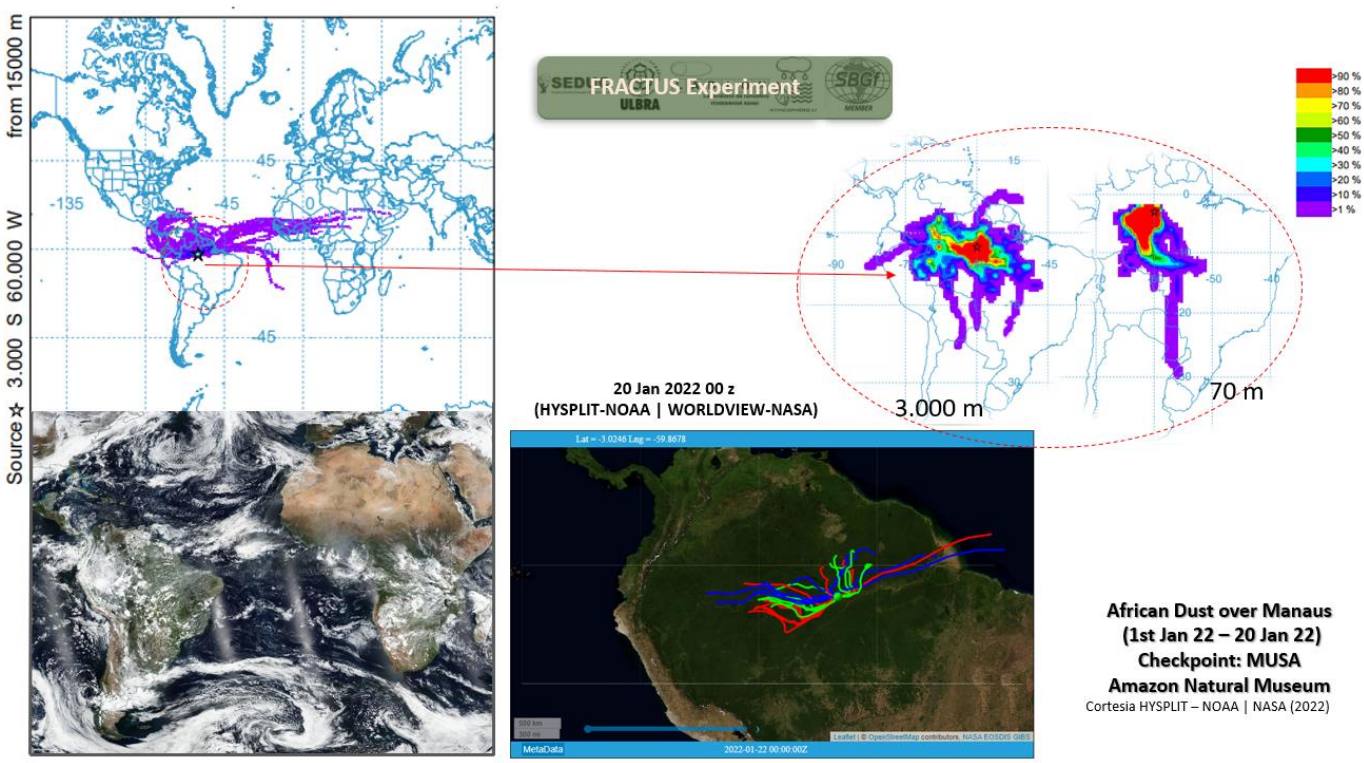

African Dust over Manaus
(1st Jan 22 – 20 Jan 22)
Checkpoint: MUSA
Amazon Natural Museum
Cortesia HYSPLIT – NOAA | NASA (2022)

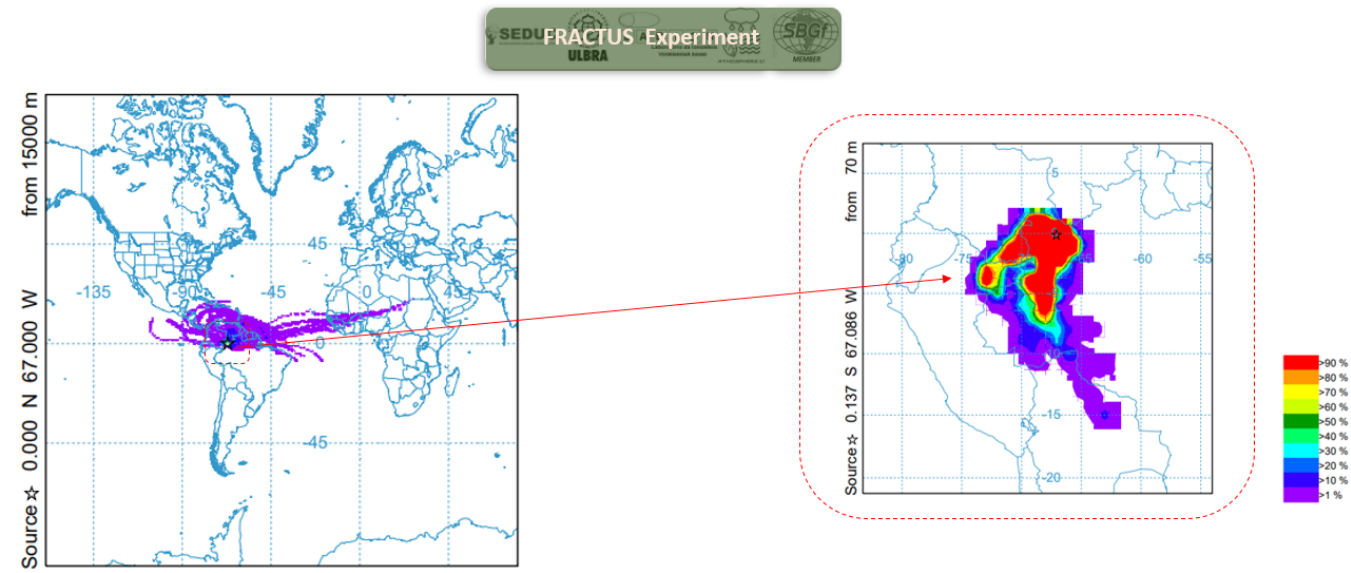

African dust over São Gabriel da Cachoeira
(1st Jan 22 - 22 Jan 22)
Checkpoint: Port Captaincy
Cortesy: HYSPLIT – NOAA | NASA (2022)

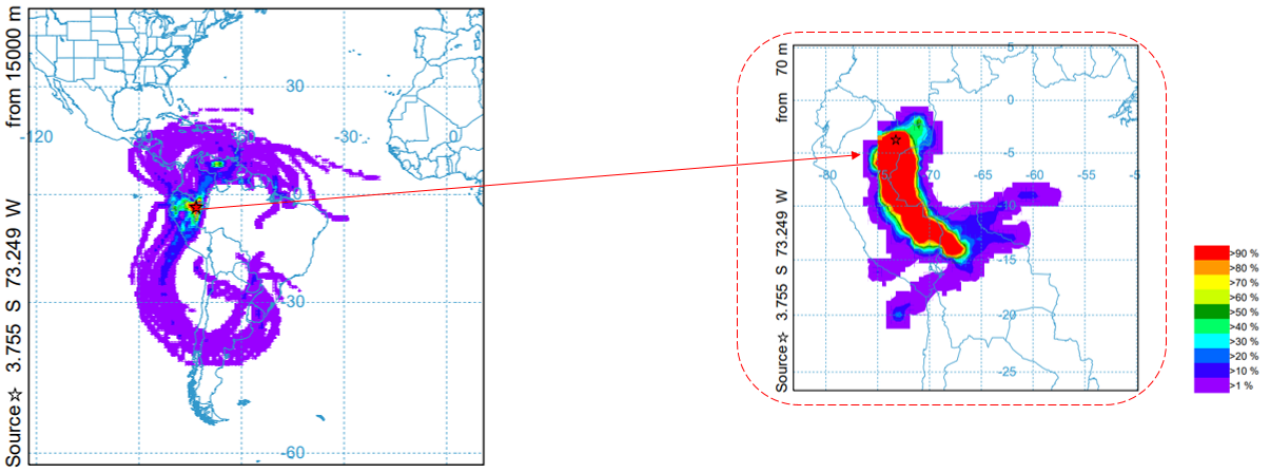

African Dust over Iquitos (Loreto - Peru)
(1st Jan 22 - 22 Jan 22)
Checkpoint: Plaza 28th of July
Cortesy: HYSPLIT – NOAA | NASA (2022)

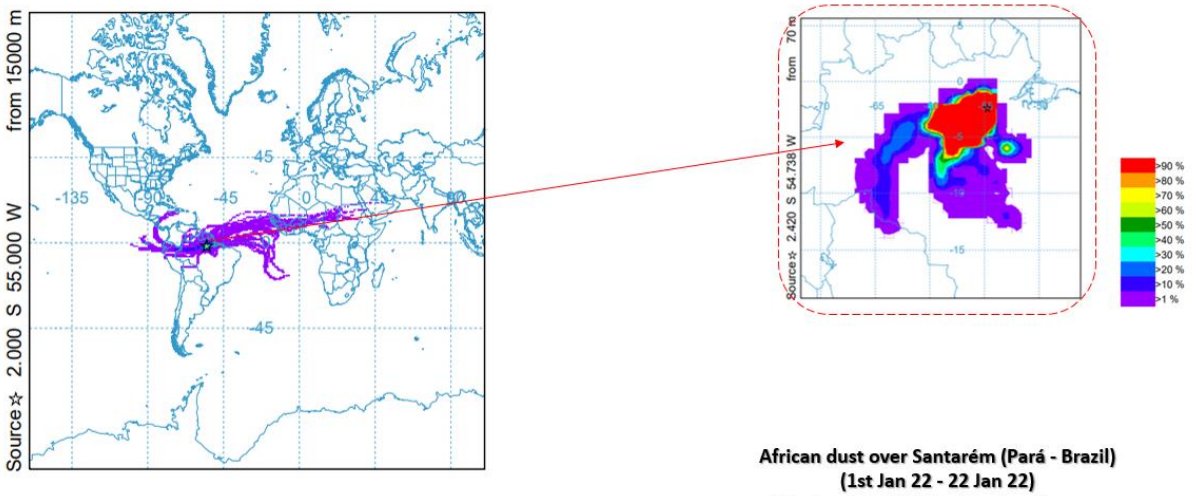

African dust over Santarém (Pará - Brazil)
(1st Jan 22 - 22 Jan 22)
Checkpoint: UFOPA – Tapajos Campus
Cortesy: HYSPLIT – NOAA | NASA (2022)

FRACTUS
FRaction **A**erosol **C**limate **T**emperature **US**able
Fraction Aérosol du Climat Température Utilisable

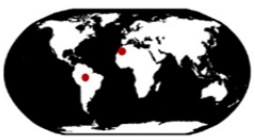

FRACTUS-Experiment
Amazon - Morocco

São Raimundo Pier (Manaus-Brazil) 2021, Dec.

Journey Overview - FRACTUS
São Gabriel da Cachoeira – SGC (Amazon|Brazil)

1. Departing from the São Raimundo Pier (Manaus-Brasil); 2. Departing from Manaus (Brazil); 3. Arriving in São Gabriel da Cachoeira - CGC (Amazon-Brazil); 4. Santa Isabel Harbour; 5. Port of CAMANAUS in SGC; 6. Fieldwork in SGC; 7. On the way between Santa Isabel do Rio Negro and Barcelos; 8. Barcelos City.

FRACTUS EXPERIMENT: AMAZON, THE SECRET OF THE RAIN

Overview

The FRACTUS Experiment began its field activities in December 2021, with the trip to the upper Rio Negro to the São Gabriel da Cachoeira City (Site 4) in the North mosaic of South America in Northwest Brazil with proximity to Colombia and Venezuela.

The climate observations on the sites under study will start with the Köppen-Geiger classification, a reference in the most widely used global climate classification system worldwide (Hasan Mahmud et al., 2015). Following the Köppen-Geiger climate classification, climatic variables and geochemical analyses, this research work is an attempt to analyze the spatial distribution pattern of climatic elements (African aerosols arriving in the Amazon) and describe the period of seasonality, scientifically quantify to categorize the climatic zones affected by African dust from the Sahel.

Seasonality and annual mean values of air temperature and precipitation are the parameters for determining the climatic types of the Köppen-Geiger classification (Peel et al., 2007). In this context, it is defined as a megathermal climate of tropical and subtropical regions – Main Group - A, with Af (tropical climate without dry season) and Am (tropical monsoon climate) being the blue color representing the main group A.

In the tropical climate (A) there is a climatic zone with two subdivisions, Af (tropical climate with no dry season | strong blue), Am (tropical monsoon climate | medium blue) covering the entire Amazon and almost the entire northern part of South America, thus translating into a tropical zone climate in which the average air temperature of the coldest month is greater than or equal to 24ºC. Af represents the tropical climate without a dry season and this climate covers the northwest area of Brazil in the locality of the city of São Gabriel da Cachoeira, a region known on the map of Brazil as, “Dog Head”.

The year 2021 in the Amazon, the La Niña phenomenon was very present, this event began effectively in July 2020 (NOAA, 2020). The year 2019 was completely neutral on the sea surface temperature (SST) in the Equatorial Pacific. So, everything indicates that in 2022, following that of 2021, the effects of the event will remain active in this region, as cities throughout the Brazilian Amazon were greatly affected by the record floods.

(See:cprm.gov.br/sace/index_bacias_monitoradas.php ?getbacia=bamazonas#), including the entire Black River channel from São Gabriel da Cachoeira to Manaus (Amazonas-Brazil), where the Black River meets the Solimões River from hence it receives the name of Rio Amazonas in Brazil. For the year of January 2022, the level of the Black River at the Black River Station in Manaus, is (54.01 m) with a water quota in relation to sea level, higher than in previous years (January 2020; quota of 20.90 m), that is, outside the average standard for the period (ANA-CPRM, 2022).

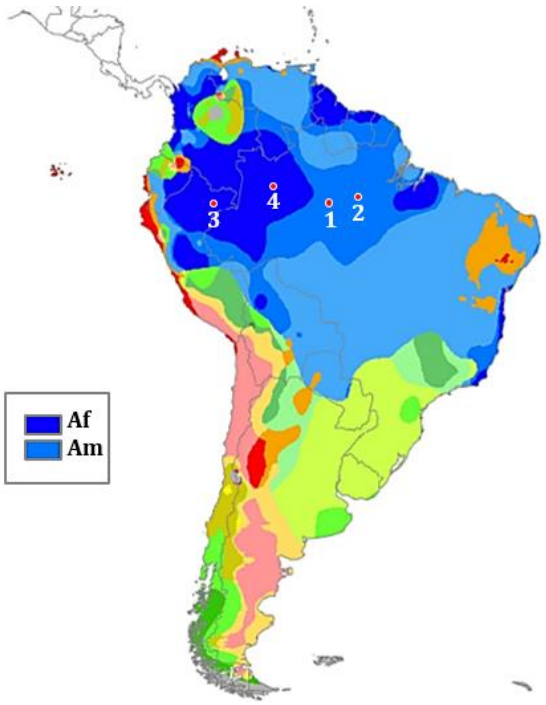

Köppen-Geiger climate type in South America, with emphasis on the Amazon, 1. Manaus City (Amazonas-Brazil); 2. Santarém City; 3. Iquitos City (Loreto-Peru); 4. São Gabriel da Cachoeira City (Amazonas-Brazil). Adapted from M. C. Peel et al.: Updated world Koppen-Geiger climate classification map, 2007.

FRACTUS EXPERIMENT: AMAZON, THE SECRET OF THE RAIN

African dust from the Sahara to spread across Europe to the Americas is a well-known theme of global monitoring by satellites and the advent of space travel that began in the 1960s. Furthermore, in BARRY and CHORLEY (2013) they comment that the tanks used in World War II in North Africa churned the surface of the desert in such a way that material transported later was visible in clouds over the Caribbean.

The connection of so-called aerosols (suspended particulate matter, measured in μg.m-3) with rainfall in the Amazon comes from studies of these particles derived from the burning of biomass in central Africa, marine aerosols and dust brought by the wind from North Africa generally reach the central part of the Amazon basin during the rainy season, a theory that gains visibility with the physicist Paulo Artaxo. Artaxo, states that 80% of the rain clouds in the period of greater intensity in the Central Amazon are constituted by African aerosols (2009 a, b).

The AQUA platform, started its operation in 2002, through the MODIS sensor (MODerate Resolution Imaging Spectroradiometer|NASA - Terrestrial Observation System - EOS), provides a product called MODIS Aerossol that performs the global monitoring of the optical thickness of the environmental aerosol in the oceans and on continents, "fine" aerosols (anthropogenic/pollution) and "ongoing" aerosols (natural particles; e.g. dust) in synoptic view of the Optical Depth of Atmospheric Aerosols image, all year round. This work uses information from the MODIS sensor (AQUA).

The transport of particulate matter on a micron scale between the African and American continents is done by the General Circulation of the Atmosphere - GCA in the equatorial belt, through the Hardley cell, resulting from the East Trade winds and the equatorial belt of greater heating (thermal equator) , on the border of the northeast and southeast trade winds between the Northern and Southern Hemispheres respectively, results in enormous instability of the convective masses due to the warming of the oceans in the summer hemisphere, giving rise to a semi-stationary region known as the Intertropical Convergence Zone - ITCZ with a predominantly oceanic feature, (Barry and Chorley, 2013).

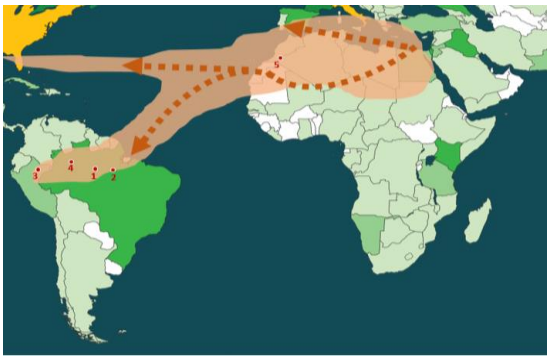

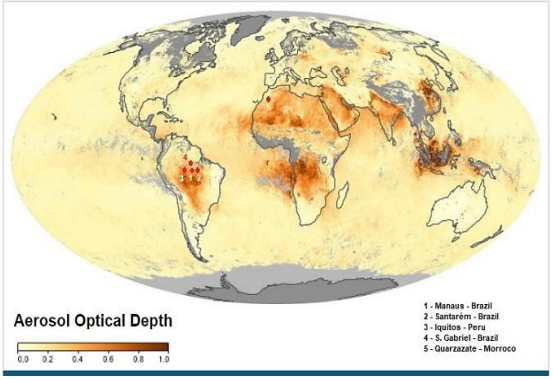

Modeling the scattering of African dust over Europe, the Atlantic Ocean and the Amazon (Adapted from L3 MODIS imagery | NASA, 2015). Optical Depth of Aerosol in the period of September 2015, for illustration of Sites 1,2,3,4 and 5. (MODIS | NASA, 2015).

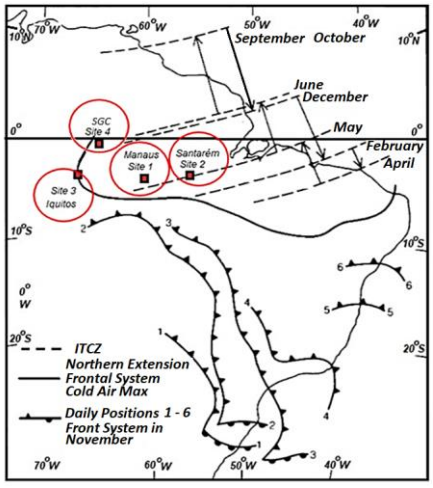

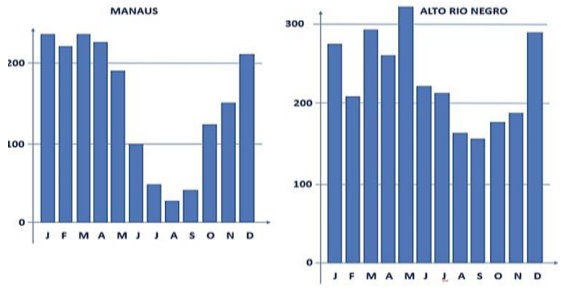

Seasonality of the ITCZ on the Central Amazon and the Climatological Normals for the Manaus City and São Gabriel da Cachoeira City– SGC. Source: Barry and Chorley, 2013; ANA-CPRM, 2022.

Research Route - FRACTUS

In images

Manaus Harbour – Brazil (2016, July)

Tabatinga | Santa Rosa

Crossing point between Tabatinga (Brazil) and Santa Rosa (Peru)

Tabatinga | Santa Rosa

Crossing point between Tabatinga (Brazil) and Santa Rosa (Peru)

2016, July

Santa Rosa Harbor – Peru (2016, July)

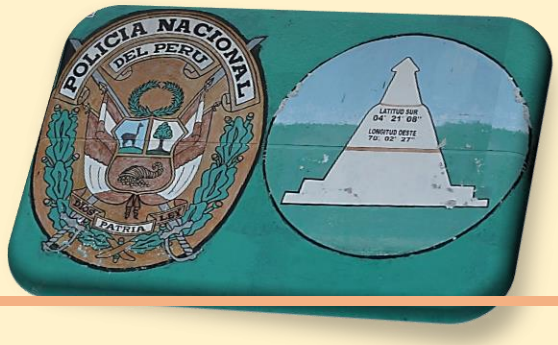

Islandia | Peru

Benjamin Constant | Brazil

Neighboring cities (connected by the Amazon River. 2016, July)

São Gabriel da Cachoeira | Brazil

Black (Negro) River. 2021, December

Santa Isabel do Rio Negro| Brazil

Black (Negro) River. 2021, December

Choachí | Colombia

Planting in mountains in the Andes, 2022, April.

Guatavita | Colombia

Guatavita Lagoon (Eldorado Ceremony. 2022, April)

Manaus | Brazil

Black (Negro) River Hydrographic Station in Manaus, (July 2022). La Niña period.

The FRACTUS Experiment should start from July 2016 to 2019. Discontinued in 2019 until 2021. Now it continues until 2026.
To learn more about the survey, go to: HAL Id: hal-03130887
https://hal.archives-ouvertes.fr/hal-03130887

Manaus | Brazil

Port region in the La Niña period. (July 2022).

amazonexpedition.zohosites.com

Amazon Research NEWS

Atmosphere Office 101



Visit to MUSA

The research team from the Atmosphere Office 101 (Yogeshwar Sahai Laboratory) went to Amazon Natural Museum (MUSA) to verify the possibility of developing observations on climate and environment at the MUSA in a dry and wet season in Central Amazon (Brazil), North of South America. The team made a brief observation of the scenery and conditions of collection of atmospheric information at the location, in order to understand the behavior of direction, vertical wind profile, humidity, atmospheric pressure, rainfall, temperature and greenhouse gases. Such investigations will become relevant climate and environment information for the Amazon Natural.


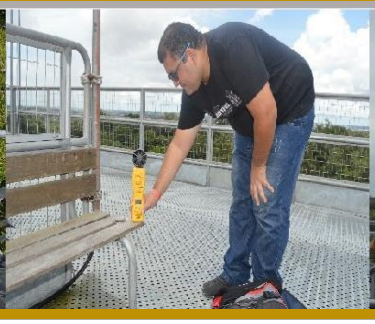

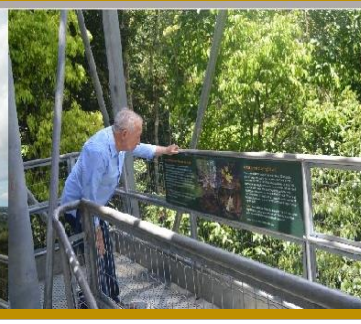

Site Fieldwork

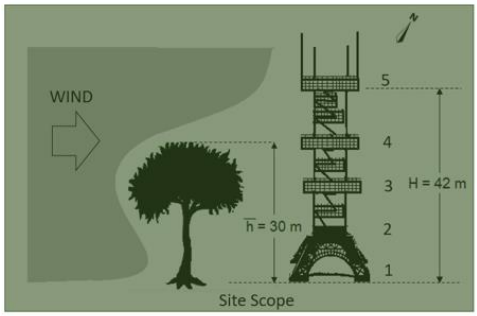

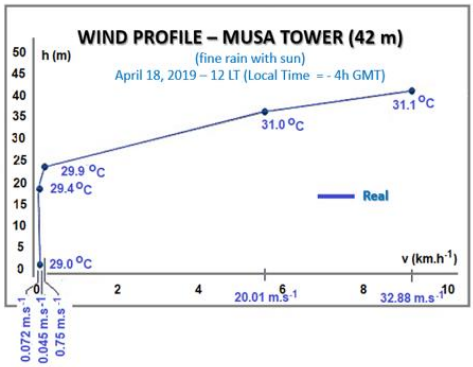

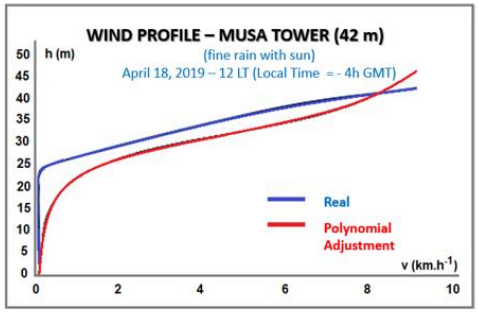

Source: Atmosphere Office 101

Site Climatology

The climate observations at MUSA will be developed with the support of the Climate and Environment of the Y. Sahai Laboratory team, in the field of Geosciences. Together they intend to build an Orthomosaic GIS for the Museum area with several layers that reflect the climate and environment of the scenario.

Acccess: amazonexpedition.zohosites.com

https://www.google.com/maps/Hunga+Tonga/@-20.569987,-175.3975096,14z/

Observations of Gravity Wave propagation in the Equatorial Ionosphere after the Hunga Tonga–Hunga Ha'apai eruption with Ionosonde data and HYSPLIT Modeling

Newton Silva de Lima[1,2], Alan Ferreira dos Santos[1], Eriberto Barroso Façanha Filho[1,2], Liliam Gleicy de Souza Oliveira[1], Aldemir Malveira de Oliveira[2,3], Daniel Barros Valentim Mansur da Silva[4].

(1) Lutheran University Center of Manaus – CEULM/ULBRA
Av. Carlos Drummund de Andrade, 1460. Conj. Atilio Andreazza – Japiim II – CEP 69077-730. Manaus, Amazonas - Brazil. Tel: (+55 92 3616-9800). Email: acsmao@ulbra.br

(2) Secretary of State for Education and Sports of the State of Amazonas
Street: Waldomiro Lustosa, 250 - Japiim II, Manaus – Amazonas. Brazil. CEP 69076-830 Manaus, Amazonas - Brazil. https://www.seduc.am.gov.br/

(3) University Center for Higher Education of Amazonas - CIESA
Rua Pedro Dias, 203 – Flores. CEP 69058-818 Manaus – Amazonas – Brazil. Tel. (+55 92 99401-6229). Email: academico@ciesa.br

(4) Martha Falcão College - Wyden
Rua Natal, 300 – Adrianópolis - Manaus – Amazonas – Brazil. CEP 69057-090. Tel.: (+55 (92) 2121-0929).

e-mail: newton.lima@ulbra.br; alan.ferreira@ulbra.edu.br; eriberto.filho@ulbra.br; liliam_gso@yahoo.com.br; amoliveira@gmail.com, danielvmansur@gmail.com.

Abstract

This article reports the propagation of gravity waves in the Ionosphere over the west coast of South America (-11.9523954; -76.8757172) as of 01:03 UTC, after the eruption of the Hunga Tonga-Hunga Ha'apai volcano (-20.8229 ; -175.4376) using Ionosonde (VIPIR) (PEZZOPANE and SCOTTO, 2005) and HYSPLIT Modeling for January 15, 2022 (17:00 UTC). It was observed the real accuracy of this instrumentation for the verification of gravity waves in the Equatorial Ionosphere.

Keywords: Layers F1, F2, F3, Es; Magnetic Equator; ionograms (VIPIR).

Introduction

In Lima (2009) and Lima et. al., (2011), he says that oscillating ionospheric disturbances such as gravity waves (GW) and traveling ionospheric disturbances (TID - Traveling Ionospheric Disturbances), are treated by some researchers as synonyms (KELLEY, 1989, HARGREAVES, 1992). TIDs, which are oscillations with a period on the order of hours to minutes, are produced in geomagnetic periods disturbed by the Joule effect at high latitudes and travel in the equatorial direction, while GW generally have their origins in the lower atmosphere by tropospheric winds, fronts cold weather or tropical convection (FAGUNDES et al., 2007) and according to Hines (1960), can also be caused by meteors entering the Earth's atmosphere, rocket launches in the F region of the ionosphere or by Solar Eclipse. In addition to nuclear explosion, volcanic eruption (FERREIRA et al., 2018; KOMJATHY et al., 2012, MINSTER, 1996; ROW, 1967). Hegai et al., (2006), investigated disturbances in the F2 region at mid-latitude during nighttime in the ionosphere that were produced by internal gravity waves generated before a strong earthquake through Joule heating due to the electric field of short duration seismogenics, in the Region D, of the ionosphere. Hines (1974) adds that GW originate by transfer of momentum and pressure and gravity gradients in an anisotropic medium.

During propagation of gravity waves in the neutral atmosphere, depending on the type of forcing in the ionospheric plasma, the time in the region of maximum anomaly (in this study, on the magnetic equator) the appearance of stratification for an F3 layer, is sometimes present. , a fact also discussed by Klausner and Fagundes (2005) and shown in Mendoza et al., (2021).

Fagundes et al., (2008) proposes to study gravity waves, through ionograms obtained by digital Ionsonde that simulate the same RADAR sounding, so sounding analyzes with high temporal resolution (100 seconds, for example) should be used. In Pillat and Guimarães, (2014), the technology and data acquisition by ionosondes are in the radio frequency range from 1 to 20-30 MHz. The radio frequency signals transmitted by ionosondes are reflected when the transmitted frequency is equal to the natural frequency. of the ionospheric plasma, that is, the echoes return to the Earth's surface, whose graphs resulting from these echoes when performing a frequency sweep are called ionograms. In this work we use a digital Ionosonde composed of several antennas (Vertical Incidence Pulsed Ionospheric Radar – VIPIR), (MENDOZA et al., 2021, TSAI, et al., 2014), and HYSPLIT - (Hybrid Single Particle Lagragian Integrated) modeling.

Materials and Method

The site

Observations were carried out between coordinates (-20.570; -175.398) and (-11.9523954; -76.8757172), near the center of the Equatorial Pacific Ocean and the west coast of South America over Peru, respectively.

Gravity Waves (GW)

Study the morphological aspects of the GW, that is, seasonal variation, preferential propagation direction, wavelengths, periods and characteristic propagation speed, mainly in the equatorial region of the event (January 15, 2022) with the aid of Trajectory, dispersion, deposition modeling and Ionograms, were performed in this observation. The dynamics of the lower and upper atmosphere, which were excited after the strong volcanic eruption of the Hunga Tonga-Hunga Ha'apai, mainly in the transport of momentum and energy through clouds of ash, steam and gas up to 30 km into the atmosphere at the beginning of the eruption , the plume that initially spread across 260 km in diameter before being distorted by wind and seismic magnitude of M4.8. (NASA; usgs.gov; IRIS – (2022).

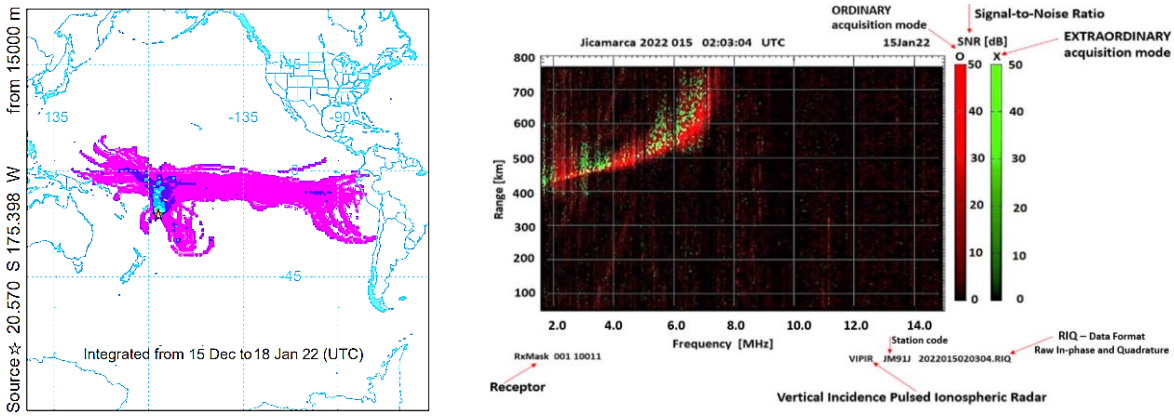

Fig. 1 – (A) The Site: Mosaic of the Observation Site between the Hunga Tonga-Huga Ha'apai volcano and the west coast of South America, wind trajectory modeling for possible dispersion and deposition of ash at tropospheric altitude between days 15 December 2021 to January 18, 2022. Courtesy: HYSPLIT – NASA, (2022). (B) Ionogram of January 15, 2022 at 02:03:04 UTC, in Jicamarca (Peru), using the VIPIR technique. Courtesy: LISN/IGP, (2022).

Ionsonde – VIPIR (Vertical Incidence Pulsed Ionospheric Radar)

VIPIR is a fully digital frequency radar that operates between 0.3 and 26 MHz. It has 8 digital receivers and a digital transmission exciter. It has extremely high-performance analog receiving electronics and a 4 kW solid-state amplifier provide an interface to the real world. This work shows an application of ionograms recorded by this Ionosonde (Fig. 2). Due to the Earth's magnetic field, the ionosphere is birefringent at radio frequencies - there are two possible propagation modes, called ordinary (O) and extraordinary (X) mode. This means that there is a high frequency (HF) radio band sweep, normally they find two distinct ionospheric returns for each frequency. For automatic scaling of ionograms, it is highly desirable to be able to separate the two modes (HARRIS and PEDERICK, 2017).

The acquisition of the ionograms was carried out by the Low-Latitude Ionospheric Sensor Network – Instituto Geofisico del Perú - IGP, at the Jicamarca Radio Observatory (JRO) JM91J, (Lima - Peru), as it has a VIPIR acquisition technique system (Fig. 2), and be ideal for viewing the Magnetic Equator proximity anomaly.

Fig.2 - Equipment set (Double-sided): Model – VIPIR: Vertical Incidence Pulsed Ionospheric Radar Very high interference immunity: IP3 > 45 dBm; High Dynamic Range: 115(I) +30(V) dB; Direct RF sampling 14 bits at 80 MHz; Fully digital conversion, receiver and exciter; Waveform Agility: 2 µs to 2 ms pulse/chip width; USB-2 Data and Command/Control Interfaces; 8 coherent receive channels; Frequency: 0.3 – 26 MHz; 4 kW class AB pulse amplifier; 3rd harmonic < -30 dBc; Precise GPS timing possible for bi-static operation; Radar software Open Source C code; runs under Linux. Cortesy: National Oceanic and Atmospheric Administration – NOAA and National Geophysical Data Center | Terence.Bullet@colorado.edu (2018).

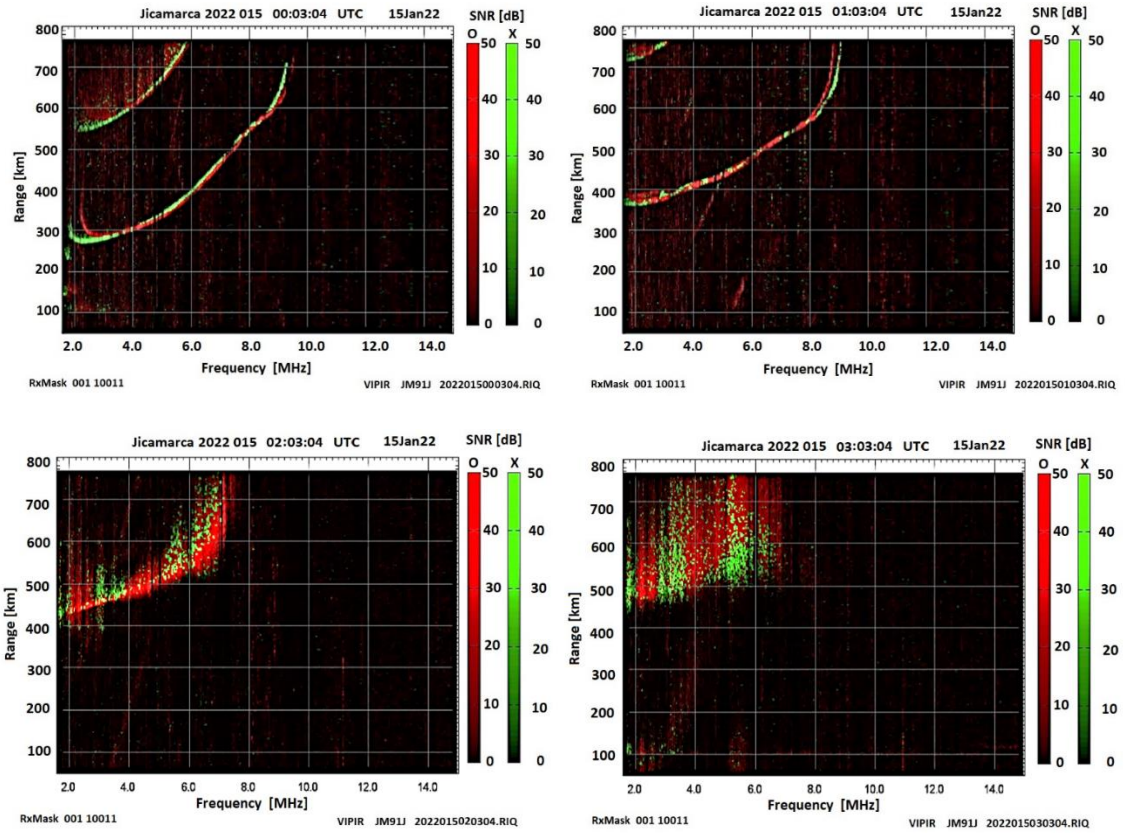

Fig. 3 - Panel of Ionograms of the times (00 UTC; 01 UTC; 02 UTC and 03 UTC) in Jicamarca for January 15, 2022. Courtesy: LISN | IGP, 2022.

Results and Discussion

In order to understand the results of the ionograms and modeling, we will have to start our observations with the records of Geoscience research agencies (NASA, NOAA, INGV, USGS) that justifies the phenomenon recorded on the volcanic eruption event that occurred in the Central Pacific near the island. of Tonga on January 15, 2022.

Comparing the energy of the volcanic explosion with that released by another type of explosion, such as the Hiroshima bomb (Mw = 4.8), the magnitude Mw = 5.7 calculated for the Tonga eruption corresponds to a load of 355,000 tons of TNT (equivalent to TNT), therefore, at least 25 times larger than the Hiroshima explosion (equivalent to 15,000 tons of TNT), (INVG, 2022).
For this observation, Ionosonda Digital - VIPIR in Jicamarca records the day of January 15, 2022, (Fig. 3), in the first four ionograms of a total of 24 ionograms in the 1 h time sequence between them, for this work.

The event in the Central Pacific began at 17 UTC. At this time on the west coast of South America (Jicamarca – Peru) it was 01 UTC, (Peru is -5 UTC).

In Fig. 3, at the time of (00:03:04 UTC) it is 19 HL and the Pre-Reverse Peak is taking place in the Electric Field, that is, the inversion of the direction of the Terrestrial Electric Field is taking place, whose effect is a strong elevation altitude of the F layer, at this moment the ionogram registers strong echoes over the F layer, that is, defined close to 300 km of altitude. At, (01:03:04 UTC) there is an echo decrease over the VIPIR signal (transmission) with more definition of the F layer at 350 km altitude. At, (02:03:04 UTC) there is an appearance of Spread-F (Plasma Bubbles) in the signal with altitude 420 km altitude. In, (03:03:04 UTC) F layer wrapped in full Spread-F (Plasma Bubble) at 480 km altitude.

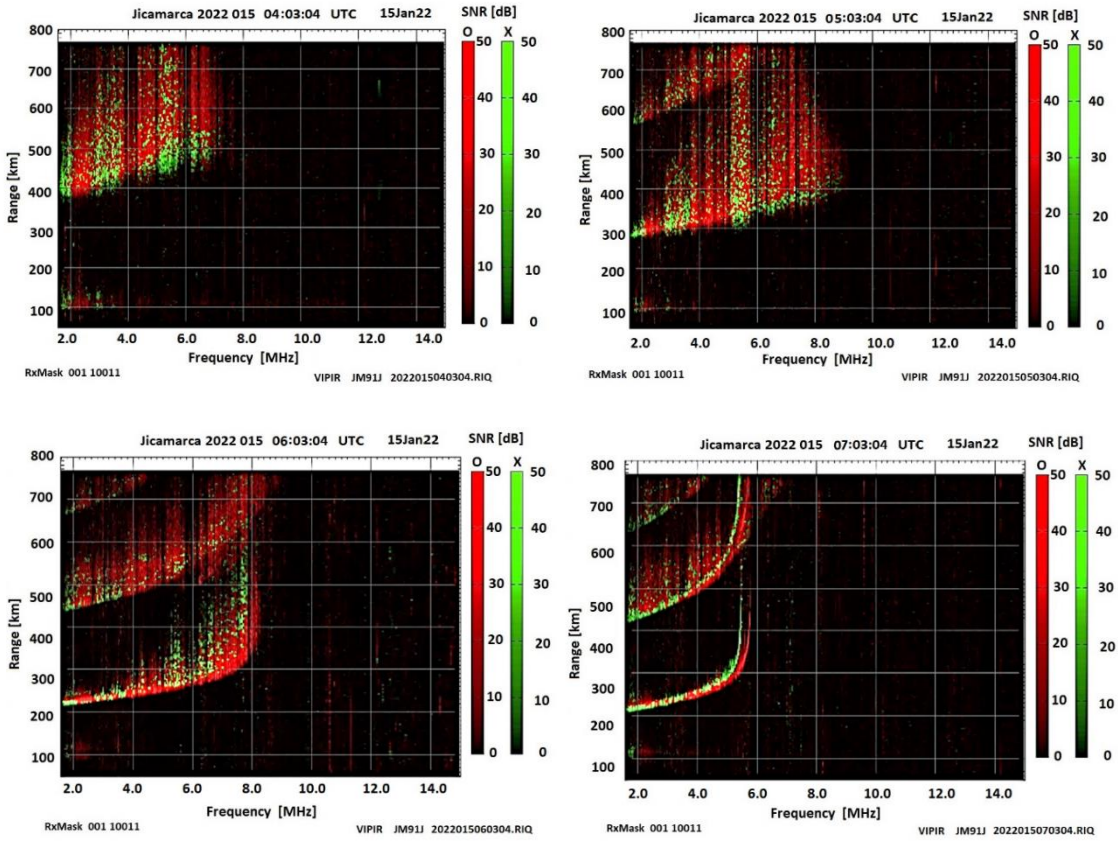

Fig. 4 - Ionogram Panel of the times (04 UTC; 05 UTC; 06 UTC and 07 UTC) in Jicamarca for January 15, 2022. Courtesy: LISN | IGP, 2022.

In Fig. 4, we have at (04:03:04 UTC) a fully diffused signal in Spread-F, close to 400 km of altitude. In, (05:03:04 UTC) Plasma bubbles involved in the F layer with strong echo in the Radar signal - VIPIR. At, (06:03:04 UTC) very strong echoes for all sweep frequencies of the Ionsonde Plasma Bubble formation. (07:03:04) decreases the Plasma Bubbles and the ordinary and extraordinary signals now appear to be more defined for F1 and F2 and signal reflection for F2 with ionospheric plasma scattering.

For Fig. 5, from (08:03:04 UTC) the Radar signal (VIPIR) tends to disappear, remaining thus at (09:03:04 UTC) and (10:03:04 UTC), returning slowly appearing at (11:03:04 UTC), but for the low frequencies of Ionosonde at 300 km altitude. This effect on the ionograms is strongly linked to Gravity Waves (GW) brought to the Ionosphere by tropospheric winds from the eruption of the Hunga Tonga-Hunga Ha'apai volcano at 08 UTC, in the Central Pacific.

At, Fig. 6, (12:03:04 UTC), the GW remain in the high atmosphere environment scattering the ionospheric plasma and begin to appear at an altitude of 100 km approximately in the form of a sporadic E layer, with the radar signal producing strong echoes and the definition of the heights of layers F1 and F2 confused at this time. For the times of (13:03:04 UTC), (14:03:04 UTC) and (15:03:04 UTC) in the range of 4 h to 6 h from the beginning of the volcano eruption, a strong connection is noted of the reflected signal from the plasma between 100 km to 600 km with definition of F1 and F2 and the acquisition signals of O and X, well defined. It is known that when the ionosphere has regions with very rarefied plasma density, the acquisitions (O and X) are more difficult to define the heights of the F1 and F2 layers.

In Fig. 7, at (16:03:04 UTC), (17:03:04 UTC), (18:03:04 UTC) and (19:03:04 UTC) we observe the influence of GW on the ionospheric plasma, with Es formation for all Ionosonde scanning frequencies and F3 layer formation after 17 UTC.

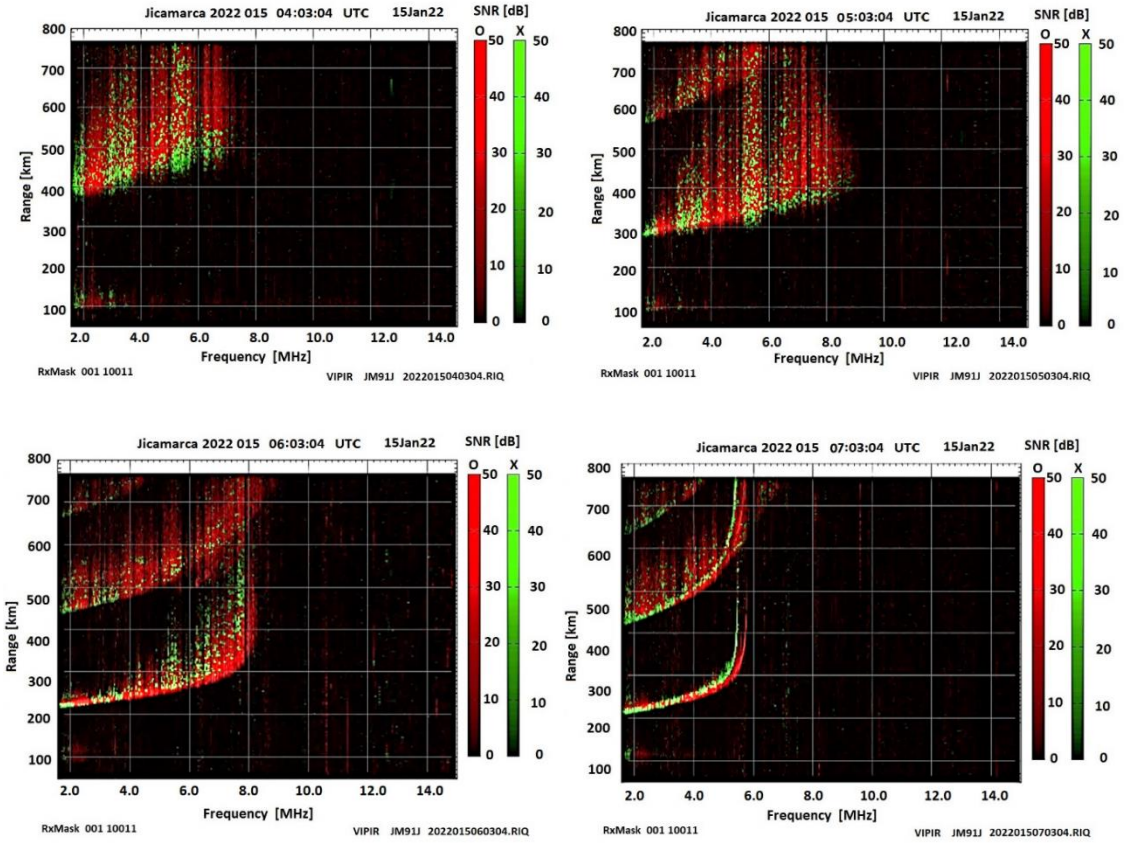

Fig. 4 - Ionogram Panel of the times (04 UTC; 05 UTC; 06 UTC and 07 UTC) in Jicamarca for January 15, 2022. Courtesy: LISN | IGP, 2022.

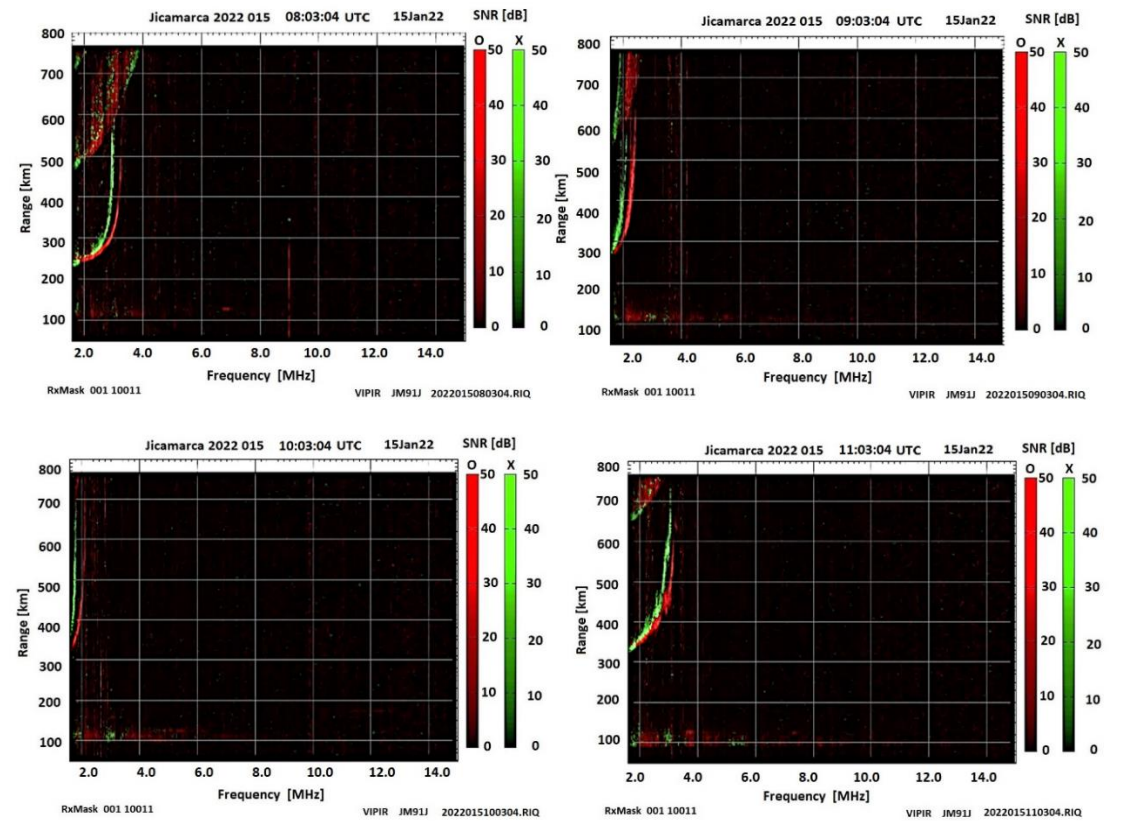

Fig. 5 – Timetable Ionogram Panel (08 UTC; 09 UTC; 10 UTC and 11 UTC) in Jicamarca for January 15, 2022. Courtesy: LISN | IGP, 2022.

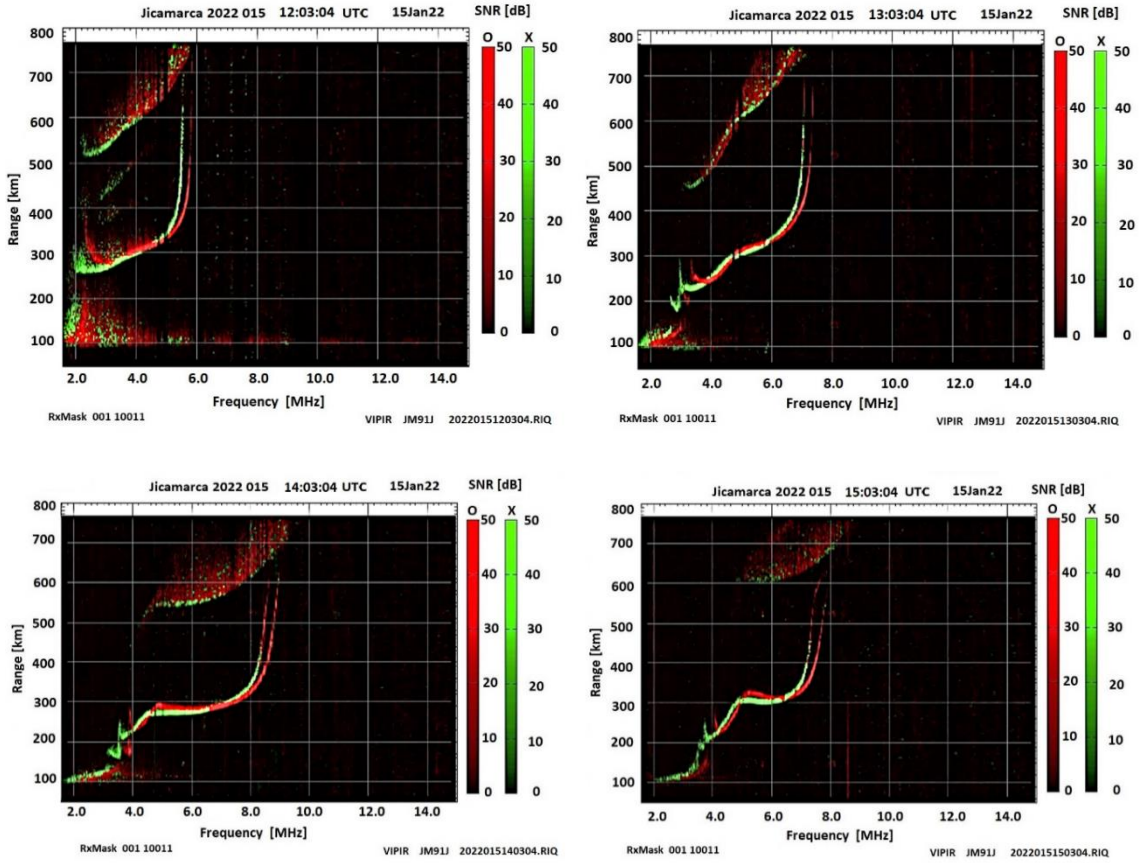

Fig. 6 - Timetable Ionogram Panel (12 UTC; 13 UTC; 14 UTC and 15 UTC) in Jicamarca for January 15, 2022. Courtesy: LISN | IGP, 2022.

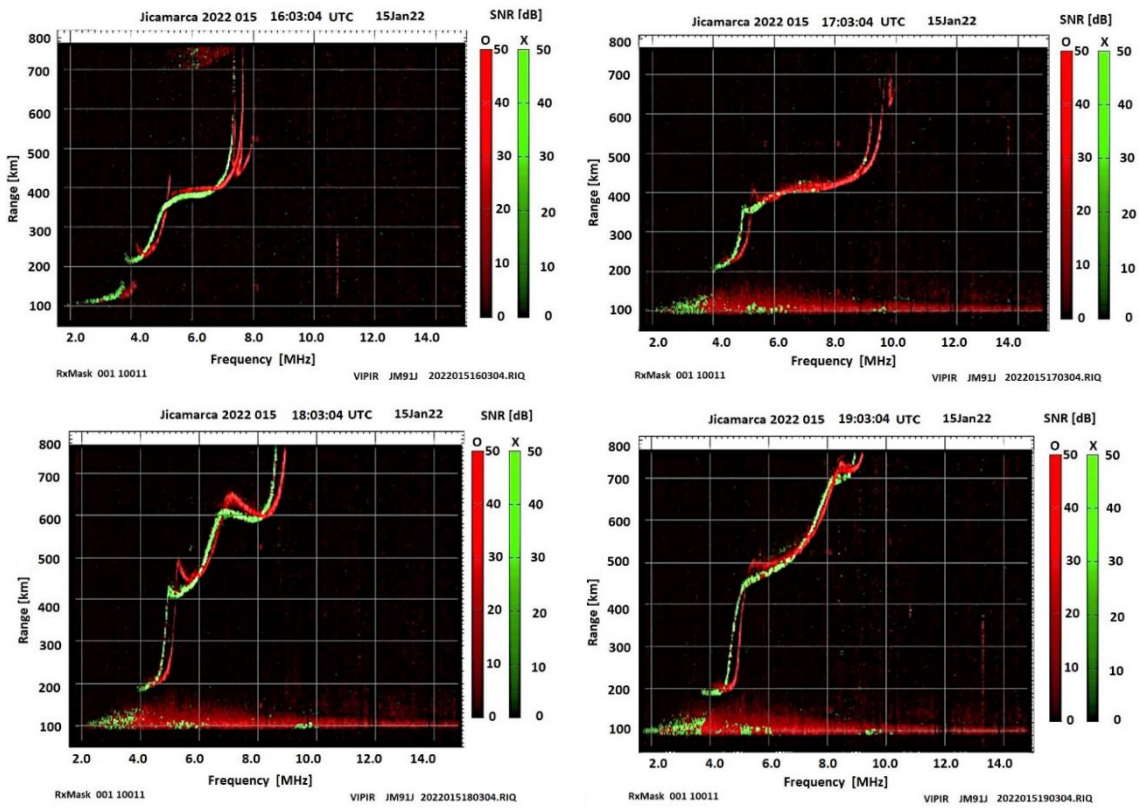

Fig.7 - Timetable Ionogram Panel (16 UTC; 17 UTC; 18 UTC and 19 UTC) in Jicamarca for January 15, 2022. Courtesy: LISN | IGP, 2022.

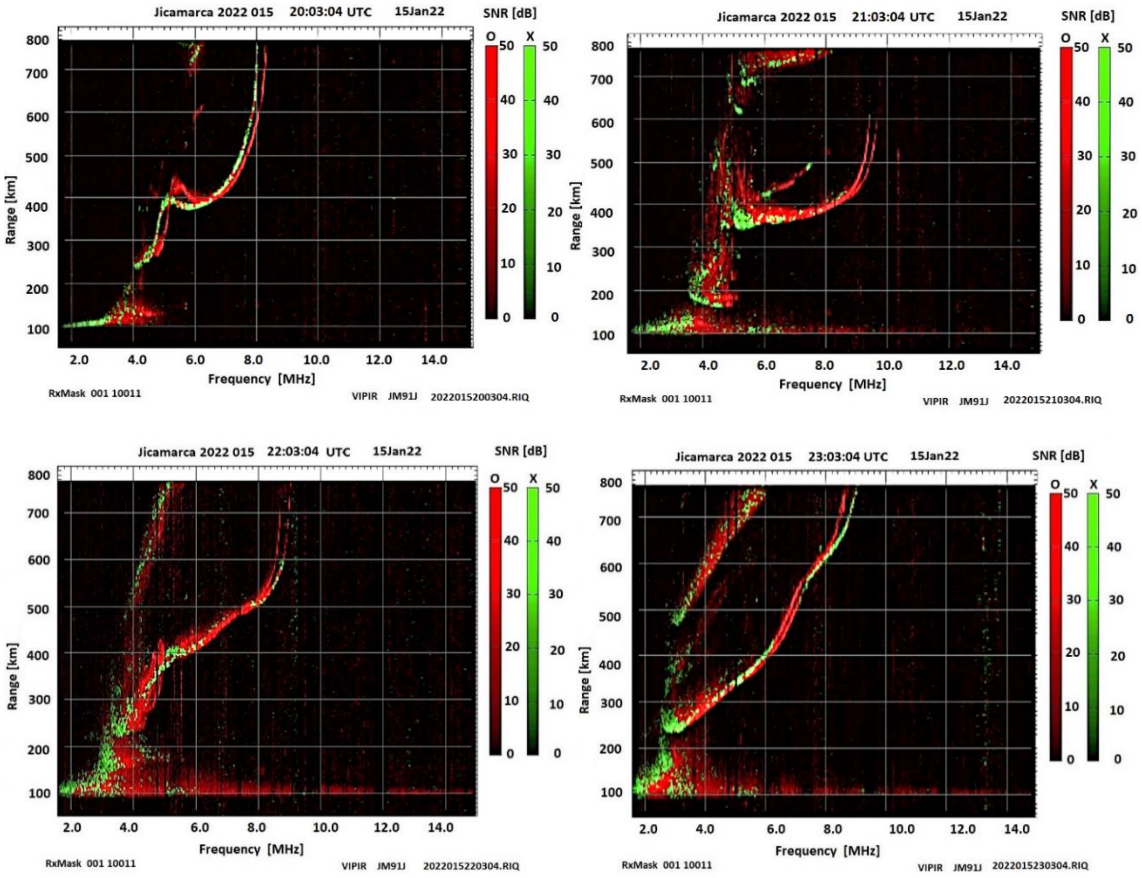

Fig. 8 - Timetable Ionogram Panel (20 UTC; 21 UTC; 22 UTC and 23 UTC) in Jicamarca for January 15, 2022. Courtesy: LISN | IGP, 2022.

The modeling of the dispersion and deposition of volcanic ash shows the global dimension of the phenomenon. Comparing the energy of the volcanic explosion with that released by another type of explosion, such as the Hiroshima bomb (Mw = 4.8), the magnitude Mw = 5.7 calculated for the Tonga eruption corresponds to a load of 355,000 tons of TNT (equivalent to TNT), therefore at least 25 times greater than the Hiroshima explosion (equivalent to 15,000 tons of TNT) and P and S seismic waves, traveling at speeds between > 340 m/s (in air) at 1450 m/s (in water). (INGV, 2022). The consequence of the shock wave at the ocean-atmosphere interface is devastating and produces a large difference in pressure, rumble and ejection of particulate matter that are projected in the first moment at an altitude greater than 15 km (NASA Earth Observatory System, 2022).

Fig. 9 shows the modeling in the volcano scenario and the ash dispersion to 15 km of altitude in the first 12 h of the event, if we compare the aerial of the spot, with the city of São Paulo in Brazil, which is 1,521 km2, the largest city in South America, the spot is more than 36 times bigger, even in the first 12 hours.

Conclusion

Observations in the Equatorial Ionosphere using Digital Ionosonde – VIPIR in Jicamarca (-11.9523954; -76.8757172) and HYSPLIT Modeling of trajectory and ash dispersion, showed efficient and strong accuracy. They also showed the propagation of Gravity Waves, shortly after the eruption of the Hunga Tonga-Hunga Ha'apai volcano (17 HL Tonga, 08 HL London and 03 HL Jicamarca).

This work begins by announcing a series of 24 Ionograms with a 1 h interval, which described the behavior of the Equatorial Ionosphere very close to (or over) the Magnetic Equator on the west coast of South America. Confirming the point location anomaly (-11.9523954); -76.8757172), by enabling the visualization by Ionograms at the time of (00:03:04 UTC to 07:03:04 UTC) the development of Ionospheric Plasma Bubbles throughout the dawn of January 15, 2022. It also identifies the propagation of Gravity Waves in the equatorial position during (08:03:04 UTC and 10:03:04 UTC) the visual identification by Ionograms, through the disappearance or removal (profile of the F layer) in the target of the echoes that should return to the Radar Digital, ie the scanning of the VIPIR

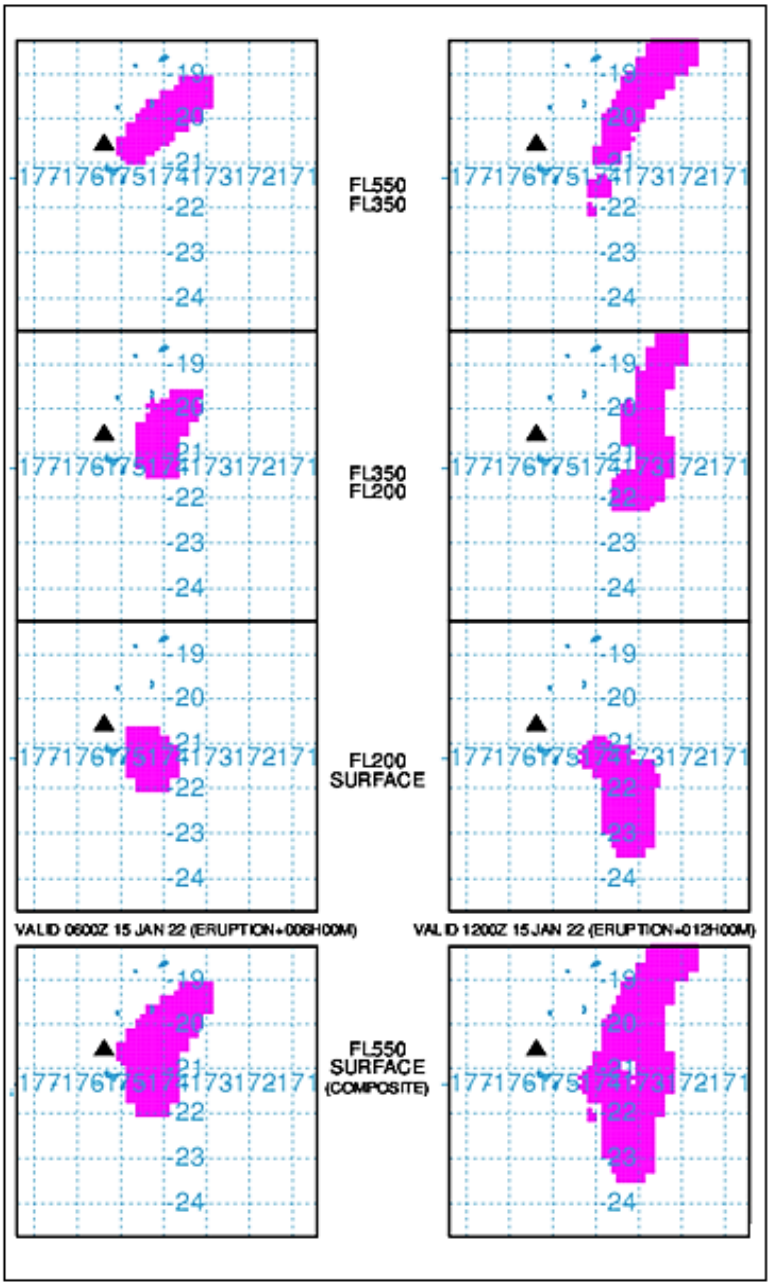

Fig. 9 – Modeling of the dispersion and deposition of ash from the Hunga Tonga-Huga Ha'apai volcano (-20.8229; -175.4376) for the first 12 h of the beginning of the event, at an altitude of 15 km. Courtesy: HYSPLIT – Vulcan Ash. (NASA).

frequency range (0.3 – 26 MHz) was compromised by GW. The profiles very slowly return to appear on the VIPIR screen at (11:03:04 UTC). Tropospheric winds of > 340 m/s in the atmosphere (NASA, USGS, INGV) (with a certain inclination, shear with stratospheric winds, also with a certain inclination within the atmospheric envelope of the Earth Magnetic Field, inducing an altitude of approximately 100 km (on Screen of VIPIR) the formation of a Sporadic layer – Es. A fact already discussed by Hines, 1964, confirming Lorentz's theory for particles or charges immersed with great speed in a magnetic field, the effect of rotation and displacement. volcano expels particulate material rich in metallic ions (HERRMANN, et al., 1978), which rise and favor the construction of Es throughout 15 January 2022. Also, during the daytime phase (18:03:04 UTC – 14 HL), formation of a third layer F (F3) appears and remains until (20:03:04 UTC). of the Hunga Tonga-Hunga Ha'apai, in the range of (07:03:04 UTC to 23:03:04). During the day phase, the acquisition of information by the O/X signal (ordinary and extraordinary) are well defined in the ionograms, since, during the night, the Spread-F formation is constant, confusing the visualization of a given signal.

The trajectory HYSPLIT Modeling (Fig. 1-A) and ash dispersion (Fig. 9) confirm the efficiency and accuracy of the VIPIR in Jicamarca.

The authors, however, indicate that more information can be extracted with these two instruments used in this observation.

(Authors' Note: Although on January 14, 2022, magnetometer (forecasting and monitoring) data from the WDC (World Data Center - Kyoto | Japan) indicated a geomagnetic storm (-88 nT at 24 GMT) in comparison with of the same time of the Auroral Electrojet (WDC data), for the equatorial latitude it is not possible to inform a strong influence of this storm. Therefore, the disturbances in the equatorial ionosphere east of South America (January 15, 2022) are strongly affected by Gravity Waves resulting from the explosion of the Hunga Tonga-Huga Ha'apai volcano as shown in Fig. 1A and Fig. 9 of this paper viewed by HYSPLIT modeling).

Acknowledgments

The authors are immensely grateful for the courtesy of Low-Latitude Ionospheric Sensor Network – LISN, Instituto Geofisico del Perú – IGP and the Ministry of the Environment of Peru, for making the information available by Ionograms (VIPIR | O/X) from Station JM91J: Jicamarca Radio Observatory – JRO. We also thank the Air Resources Laboratory (NOAA-NASA) for making available the HYSPLIT - models that simulate the dispersion and trajectory of substances transported and dispersed through our atmosphere, on local to global scales. We thank the support of the researchers' institution: CEULM/ULBRA – SEDUC-AM – CIESA – FMF-Wyden, Dr. Evandro Barbosa Brandão (CEULM/ULBRA-Manaus-Brasil) to Dr. Troy Beldini (UFOPA-Santarém-Brazil), the agencies NASA, NOAA, INGV, USGS for relevant information about the research object of the article.

References

BULLETT, T., MALAGNINI, A., PEZZOPANE M., SCOTTO C (2010). Application of Autoscala to ionograms recorded by the VIPIR ionosonde. Advances in Space Research. Volume 45, Issue 9, 3 May 2010, Pages 1156-1172.

FAGUNDES, P.R., KLAUSNER, V., SAHAI, Y., PILLAT, V. G., BECKER-GUEDES, F., BERTONI, F.C., BOLZAN, M. J. A., ABALDE, J. R. (2007). Observations of daytime F2-layer stratification under the southern crest of the equatorial ionization anomaly region, Journal of Geophysical Research, vol 112, doi:10.1029/2006JA011888.

FAGUNDES, P.R., MUELLE, M. T. A. H., BITTENCOURT, J. A., SAHAI, Y., LIMA, W. L. C., GUARNIERI, F. L., PILLAT, V. G., BECKER-GUEDES, FERREIRA, A. S., LIMA, N. S. (2008) - Nighttime ionosphere–thermosphere coupling observed during an intense geomagnetic storm, Advances in Space Research 41, 539–547.

FERREIRA, A., LIMA, N., SILVA, R., GÓES, K., FARIAS, T. (2018). Investigation of the propagation of gravity waves in the earthquake in PERU on 26 November 2015 at 05:45:18 (UTC) observed at GPS stations in the Amazon. VII Brazilian Geophysics Symposium – (Ouro Preto – MG – Brazil).

H**ARGREAVES, J. K. (1992).** The solar-terrestrial environment, Cambridge: Cambridge University Press, v.5, 420p.

HARRIS, T. J., PEDERICK, L. H. (2017). A Robust Automatic Ionospheric *O*/*X* Mode Separation Technique for Vertical Incidence Sounders. Radio Science. https://doi.org/10.1002/2017RS006279.

HEGAI, V. V.; LIU, J. Y.; KIM, V.P. (2006) The ionospheric effect of atmospheric gravity waves excited prior to strong earthquake. Advances in Space Research 37-653-659. Available at: https://www.researchgate.Net/publication/222556220.

HERRMANN, U., EBERHARDT, P., HIDALGO, M. A., KOPP, E., SMITH, L. G. (1978). Metal ions and isotopes in sporadic E-layers during the Perseid meteor shower. Space Res. 18, 249.

HINES, C. O. et al. (1974). The upper atmosphere in motion, Canadian Journal of Geophysical, American Geophysical Union, Washington, D.C, v.75, 2563-2586.
HINES, C. O., (1964). The formation of mid-latitude sporatic-E layers. Journal Geophysical Research. Volume 69, Issue 5. 1 Mar 1964. Pages 1018-1019. https://doi.org/10.1029/JZ069i005p01018.

HINES, C.O. (1960). Internal atmospheric gravity waves at ionospheric heights. Canadian Journal of Physics, 38, 1441-1481.

HYSPLIT. Hybrid Single-Particle Lagrangian Integrated Trajectory (2015). Models simulate the dispersion and trajectory of substances transported and dispersed through our atmosphere, over local to global scales. https://doi.org/10.1175/BAMS-D-14-00110.1.
https://www.ready.noaa.gov/HYSPLIT.php. Accessed on January 15, 2022.

INGV - ISTITUTO NAZIONALE DI GEOFISICA E VULCANOLOGIA, (2022). Boletim INGV | nº 01 | 2022 | ano XVI (/it/ingv-newsletter-n-01-2022-anno-xvi) - Un redação do presidente

IRIS - Incorporated Research Institutions for Seismology, (2022). https://www.iris.edu/hq/. Accessed on January 22, 2022.

KELLEY, M. C. (1989). The Earth´s Ionosphere Plasma Physics and Eletrodynamics, Academic Press, San Diego – USA – California, 487p.

KLAUSNER, V., FAGUNDES, P. R. (2005). Observations of Gravity Waves in Region F during the day period. X Latin American Meeting of Scientific Initiation and VI Latin American Postgraduate Meeting – University of Vale do Paraíba. (São José dos Campos, SP, Brazil).

KOMJATHY, J.A.; GALVAN, V.D.A.; STEPHENS, P.; BUTALA, M.D.; AKOPIAN, V.; WILSON, B.; VERKHOGLYADOVA, O.; MANNUCCI, A.J.; HICKEY, M. (2012). Detecting ionospheric TEC perturbations caused by natural hazards using a global network of GPS receivers: The Tohoku case study. Earth Planets Space. 64, 1287–1294.

LIMA, N. S., FERREIRA, A. S., ARAÚJO, R. C., YAMAMOTO, K. C. (2011). Observations of MSTIDs/GWs at the F2 layer heights in the near equatorial region. Geophysical Research Abstracts Vol. 13, EGU2011-122, 2011 EGU General Assembly.

LIMA, N. S., (2009). Study of the Propagation of Gravity Waves in the Equatorial Ionosphere, using Observations in Manaus (2.9^{O}S, 60^{O}W), Master's Dissertation in Geosciences, Federal University of Amazonas, UFAM/Brazil.
(Available in: https://tede.ufam.edu.br/handle/tede/3275).

LISN - Low Latitude Ionospheric Sensor Network. In collaboration of Instituto Geofísico del Peru (IGP) and Jicamarca Radio Observatory (JRO) (2022). http://lisn.igp.gob.pe/ Accessed on January (15-31), **2022.**

NASA - Earth System Observatory, (2022). Dramatic Changes at Hunga Tonga-Hunga Ha‘apai. https://science.nasa.gov/earth-science/earth-system-observatory Accessed on January 22, 2022.

MENDOZA, M. M., CHANG, Y., DMITRIEV, A. V., LIN, C., TSAI, L., LI, Y., HSIEH, M., HSU, H., HUANG, G., Lin, Y. and TSOGTBAATAR, E. (2021). Recovery of Ionospheric Signals Using Fully Convolutional DenseNet and Its Challenges. Recovery of Ionospheric Signals Using Fully Convolutional DenseNet and Its Challenges. Sensors 2021, 21, 6482. https://doi.org/10.3390/s21196482.

MINSTER, J. BERNARD. (1995) GPS detection of ionospheric perturbations following the January 17, 1994, Northridge Earthquake. DOI: 10.1029/95GL00168. Geophysical Research Letters. Vol. 22. Pages 1045– 1048, May 1995.

NOAA - National Oceanic and Atmospheric Administration - Air Resources Laboratory’s (ARL); https://www.ready.noaa.gov. Accessed on January (15 – 31), 2022.

PEZZOPANE, M. and SCOTT, C. (2005). The INGV software for the automatic scaling of foF2 and MUF (3000) F2 from ionograms: A performance comparison with ARTIST 4.01 from Rome data. Journal of Atmospheric and Solar-Terrestrial Physics 67, 1063–1073.

PILLAT, V.G. and GUIMARÃES, L.N.F. (2014). Identification of the Ionosphere Profile Using Fuzzy Logic: Part I. Trends in Applied and Computational Mathematics, 15, N.1, 47-57. doi: 10.5540/tema.2014.015.01.0047.

ROW, R. V. (1967). Acoustic gravity waves in upper atmosphere due to a nuclear and an earthquake. Journal of Geophysical Research, 72 (5); 1599.

STEIN, A. F., DRAXLER, R. R., ROLPH, G. D., STUNDER, B. J. B., COHEN, M. D., and NGAN, F. (2015). NOAA’S HYSPLIT Atmospheric Transport and Dispersion Modeling System. AMERICAN METEOROLOGICAL SOCIETY. December – BAMS | 2059.

TSAI, L.C.; TIEN, M.H.; CHEN, G.H.; ZHANG, Y., (2014). HF radio angle-of-arrival measurements and ionosonde positioning. Terr. Atmos. Ocean. Sci. 25, 401–413.

USGS - United States Geological Survey - https://earthquake.usgs.gov/earthquakes/ma/. Accessed on January 22, 2022.

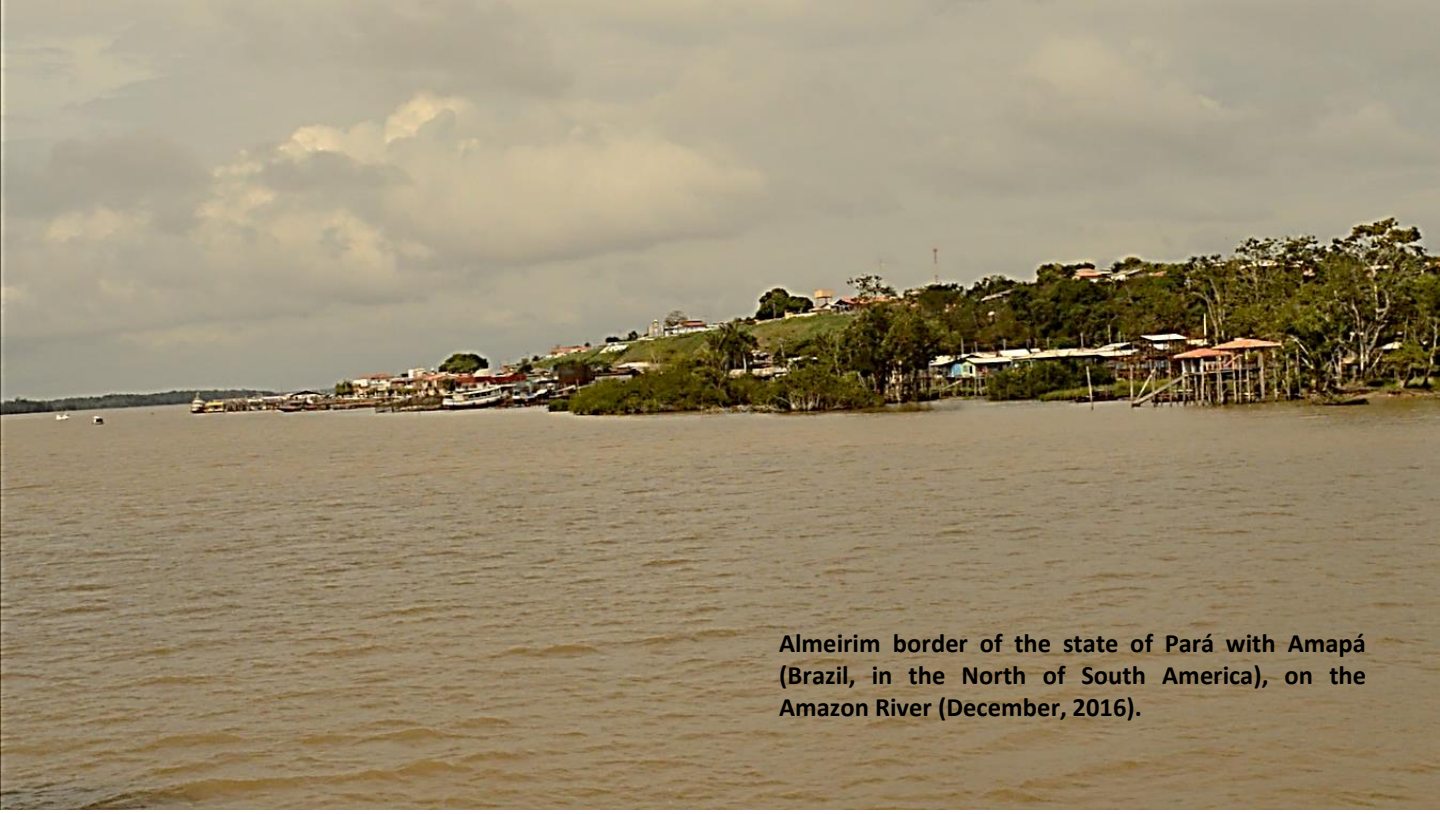

Almeirim border of the state of Pará with Amapá (Brazil, in the North of South America), on the Amazon River (December, 2016).

Reduction in water levels and regional warming of the Amazon River from Peru to the Atlantic Ocean in Brazil due to the effects of the 2016 ENSO.

Lima, NS.; Malveira, AO.; Façanha, EF.; Braga, OS.; Pietzsch, MR.; Figueiredo, RS.; Calazães, RM.; Quispe, WD; Ferreira, AS.

Abstract

In situ observations of the tendencies of the prolonged ENSO (El Niño Southern Oscillation) phenomenon combined with a trend of regional warming in both western and eastern Amazonia were registered by the Amazon River Peru-Brazil Expedition on the Amazon River. Temperatures were taken at four positions on the river (edge, middle of the canal, 1 m deep below the surface, and ambient air temperature), air pressure and humidity, and the velocity and direction of the wind were the parameters that were sampled from the Peruvian city of Iquitos beginning in July 2016, to the Brazilian city of Macapá at the mouth of the Amazon River in December 2016. The results suggest that there was a decline in water levels along the river during the entire observation period due to the prolonged El Niño event that occurred in 2014, 15 and 16.

Introduction

Changes in atmospheric circulation in the tropical zone (Walker cell) induce change in rainfall patterns, devastating floods, and severe droughts that can drastically affect the lives of millions of people (MOHTADI *et al,* 2017). In the mosaic of landscapes that is tropical South America the tendencies for rainfall, in the Amazon in eastern Brazil, to the northwest of Peru are well-defined by long-term hydrological data for the Amazon basin that were recorded during the 20th century. During this period the tendency for rainfall during the three most humid months and for the subsequent superficial runoff rate during the three months with the greatest runoff for the northeastern region of Brazil demonstrated a slow increase over long periods (MAREGO, TOMASELLA, UVO, 1998). In 2016 the Amazon River Expedition from Peru to Brazil observed tendencies in which a prolonged ENSO event combined with a trend of regional warming increased the demand for water from the reservoirs of Brazilian hydroelectric plants in the Northeast, Central-West, and Southeastern regions of Brazil (CCEE, 2017), and caused strong rains in the Southern region of Brazil (CPTEC, 2016).

According to Jiménez-Muñoz *et al* (2016), this event was associated with warming that was without precedent and an extreme drought in the Amazon, compared to other strong ENSO events in 1982/83 and 1997/98. The typical conditions of drought caused by the ENSO were observed and described by Jiménez-Muñuz *et al,* (2016), as occurring only in the eastern Amazon, while in the western region of the Amazon there prevailed an uncommon level of humidity. For researchers this situation can be attributed to the humid-dry dipole at the location of maximum warming of the surface of the equatorial central Pacific Ocean. This humid-dry dipole was also confirmed in the current study through a time series of temperature readings at 4 distinct points (edge, middle of the canal, 1 m deep below the surface, and ambient air temperature) along the Amazon River from the west in Iquitos, Peru, to the east in Macapá, Brazil by the research team of the Amazon River Expedition from Peru to Brazil in 2016. According to Erfanian, Wang and Fomenko (2016), the empirical relationships between rainfall and sea surface temperatures (SST) in the Pacific and Atlantic Oceans represent the factors of tropical ocean variability responsible for the observed precipitation anomalies. These results indicate that the warmer than normal SST for the tropical Pacific and Atlantic Oceans (including El Niño events) were the principal causes of extreme droughts in South America, however, researchers are still unable to explain the severity of the precipitation deficits observed in 2016 in a substantial portion of the Amazon region. Therefore, hydroclimatic variability in South America is strongly coupled, on a large scale, to oceanic and atmospheric phenomena. Specifically, the El Niño Southern Oscillation (ENSO) that affects climatological and hydrological conditions has a “terrestrial – atmospheric” mechanism that forms a bridge between these two domains and connects the anomalies of SST of the Pacific and Atlantic Oceans (Paveda and Mesa, 1997).

Material and Methods

Map of the Expedition (Arequipa-Peru; Iquitos-Peru; Macapá-Brazil)

Fig. 1: Image of the mosaic of regions of tropical South America and the 2016 route of the Amazon River Expedition from Peru to Brazil (solid line), and the 2017/18 route (dotted line) (3rd phase, modified route).

Fig. 2: Ships used in the Amazon River Expedition (A) Voyager III (Manaus-Tabatinga). (B) M. Monteiro II (Tabatinga-Manaus). (C) *Flipper* (Santa Rosa-Iquitos-Santa Rosa). (D) S. Bartolomeu III and IV, (Manaus– Santarém–Santana—Manuas) July through December, 2016.

An automatic meteorological station was installed on roof of the five passenger transport ships (Fig. 2) used in this research expedition (Fig. 1). The station was free from obstacles that would impede accurate measurement of the variables of interest (temperature, humidity, pressure, wind speed and direction, dew point, and rainfall).

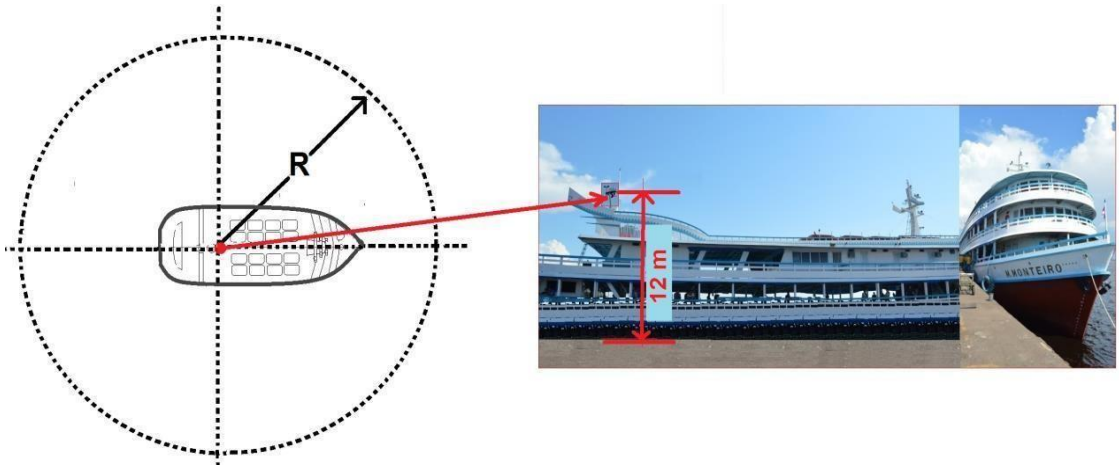

Fig. 3 - ***Footprint*** **of the boat-mounted meteorological station,** *Lagragian Footprint Model*, *Weather Station* - DAVIS - *Vantage – Vue*, ***300 m ≤ R ≤ 500 m,*** on the ship M. Monteiro II, July 2016.

Sampling and chronogram

For monitoring of weather and climate during the period of the research, a I - FLIR-E60 thermal imager, (Tab. 1), and II –Mira digital thermometer– LASER, Minipa MT-360 sensors were used. Measurement of ambient air temperature, and the temperature at the edge of the river, middle of the canal, and at 1.0 m below the river´s surface a Davis meteorological station with uninterrupted recording (15 days + 15 days) with data collection (ambient air temperature, humidity, pressure, wind speed and direction, dew point) were measured every 5 minutes, and *in situ* two liter water samples were taken at each sampling point along the entire river.

Temperature values are a composite of 10 *in situ* readings taken at each sampling point. The geographic coordinates of the sampling points were taken along with a description of the weather (climate) and the time at the moment of collection, and samples were labeled accordingly (Steps 1 and 2 of the Amazon River Expedition protocol).

Laboratory analysis of water samples (method used in parentheses)*

1-Alkalinity (APHA, 2003; GOLTERMAN, 1970); 2-Calcium (Ca^{+}), hardness, and Magnesium (Mg^{+}) APHA, 1985; GOLTERMAN & CLYMO, 1978); 3 – Chlorides ((FENANTHROLINE – FIA) (MACKERETH, et. al., 1978: GOLTERMAN & CLYMO, 1971); 4-DQO with potassium dichromate (APHA, 2003; MACKERETH, et. al., 1978); 5 – Total and Dissolved iron (FIA) (APHA, 2003); 6 - Phosphate (PO4) (APHA, 2003; GOLTERMAN, 1970; 7 - Total phosphorus and nitrogen (N and P-TOTAL) (VALDERRAMA, 1980); 8 – Total phosphorus (FIASTAR) (APHA, 2003, ISO 5861, s/d);
9 – Nitrate (FIA) (GOLTERMAN, 1971); 10 – Ammoniacal nitrogen (NH3) (FIA - *Flow Injection Analysis*) Nessler reagent method; – 11 –Silicates (Silica – Molybdenum blue method) (GOLTERMAN, 1980, MACKERETH, et. al., 1978); 12 – pH (hydrogen ion concentration) (APHA, 2003), 13 – Potassium and sodium by flame emission spectroscopy (MACKERETH, et. al., 1978), 14 – Total suspended solids (STS) (APHA, 2003), 15 – Sulfate (APHA, 2003), 16 – Temperature (FLIR-E60); 17 – Turbidity (turbidity meter); 18 - Color (Spectrophotometer).
(*) Done only between Manaus (Brazil) and Macapá (Brazil).

Additionally, *in situ* analyses of pH, O_2, conductivity, and O_2 saturation were conducted on all water samples.

Table 1. Physical characteristics of the FLIR-E60 thermal imager.

MATERIAL	SPECIFICATION	TEMP. (°C)	ELECTROMAGNETIC SPECTRUM	EMISSIVITY
WATER	LAYER THICKNESS > 0.1 mm	0 - 100	ALL	0.95 - 0.98

Statistical modeling and georeferencing of data.

The time series of temperature reading along the Amazon River were processed and analyzed using the *Marine Modeling and Analysis Branch Oper. H. R.* (Verification ensemble) of NOAA/NWS/NCEP/EMC, (ftp://ftpprd.ncep.noaa.gov/pub/data/nccf/com/gfs/prod). For the characterization of the composition of the El Niño event during this period the temperature gradients of the SST of the equatorial Atlantic and the eastern equatorial Pacific were constructed. All sampling points were georeferenced using a GPS (GARMIN – E60 and the *software TrackMaker*®), and the creation of a thematic map for sampling points was done using *ArqGis*®. Flux measurements (temperature, humidity, pressure, wind speed and direction) were taken using a meteorological station (Vantage-Vue/*DAVIS Instruments Corporation, WeatherLink* 6.0.3), using the static method (Lima, 2017), for covariances (*Eddy Covariance*).

Results and Discussion

Figure 4 below shows systems that were responsible for the atmosphere dynamics on July 26, 2016 between 05:00 LT and 17:0 LT, the first day of the Amazon River Expedition when it left Iquitos, Peru, for Manaus, Brazil. The Intertropical Convergence Zone (ITCZ) is in the north of South America and reaches the Amazon region, and there is a cold front that is developing in the southern Atlantic Ocean and is penetrating the southern region of Brazil.

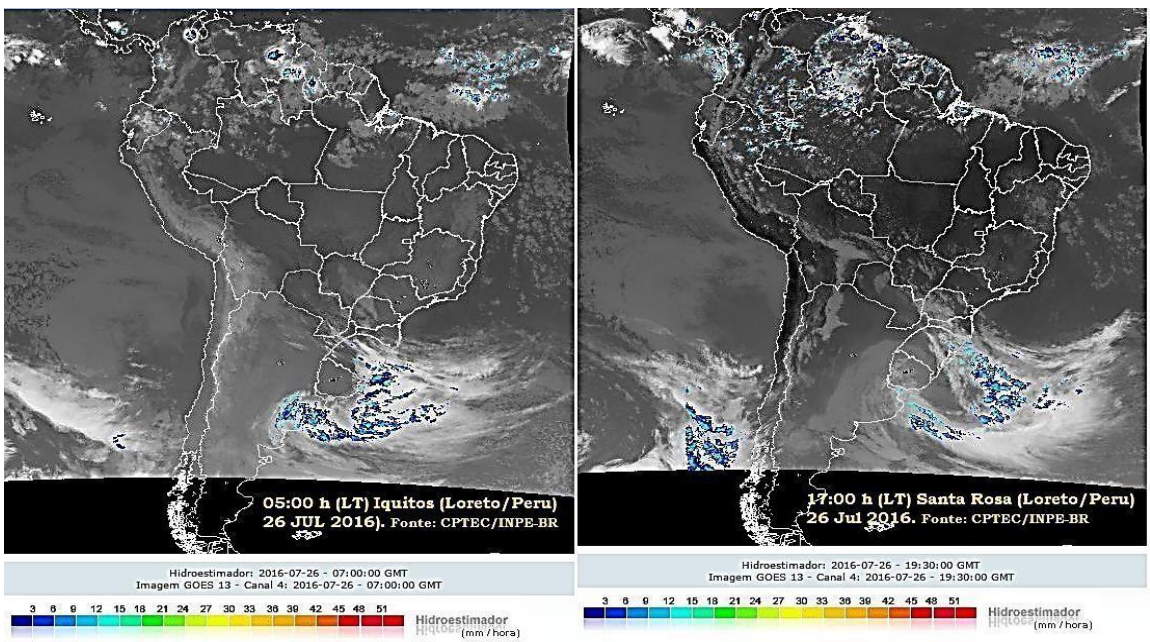

Fig.4: Meteorological conditions on July 26, 2016, between 05:00 LT and 17:00 LT for South America. (Source: CPTEC/INPE, 2016).

Figure 5 shows a graphical rhythmic analysis of weather types between Iquitos (Loreto-Peru), Tabatinga and São Paulo de Oliveira (State of Amazonas-Brazil) on July 26, 2016, between 05:00 LT and 18:00 LT in Peru, and July 27 and 28, 2016 (12:00 h to 03:00 h LT, in Brazil), in which the climatic elements involved in this analysis of atmosphere dynamics are evident (CPTEC/INPE).

Figure 6 shows the time series of temperature that was taken at three positions (ambient temperature at the ship – 100 m from the edge of the canal – middle of the canal) during the first stage of the expedition (Iquitos/Peru – Manaus/Brazil), using the FLIR E60 thermal imager. The image next to the time series shows SST in Real Time Global (RTG), High Resolution (HR) and was obtained by NOAA/NCEP/NWS by analyzing satellite images, ocean floats, sea ice cover, salinity, and conducting mathematical modeling in a second degree polynomial series (Branch analysis method), ftp://ftpprd.ncep.noaa.gov/pub/data/nccf/com/gfs/prod), and indicates correlation with the results obtained by the Amazon River Expedition.

The observations from this study suggest regional warming of temperature gradients in the stretch between Iquitos-Peru to Manaus-Brazil) in July, 2016, (dry season), with average ambient temperature at the ship (in the shade) of 30.41^{0}C, at the river´s surface (100 m from the edge) of 27.34^{0}C, and at the middle of the canal of 24.73^{0}C, (Fig.6).

During the 2nd stage of the Expedition (Manaus-Brazil to Macapá-Brazil) in December 2016, the rainy season had already begun and average temperatures were slightly reduced, with average ambient temperature at the ship of 28.97^{0}C, at the river´s surface (100 m from the edge) of 26.06^{0}C, and at the middle of the canal of 24.04^{0}C. The interval between the first and second stages was taken in order to be able to verify the effect of drought on the river due to the time necessary for water to flow across the large distance from Iquitos-Peru to Macapá-Brazil (Fig.7). The margin of error is shown in Figures 6 and 7 and in Table 1.

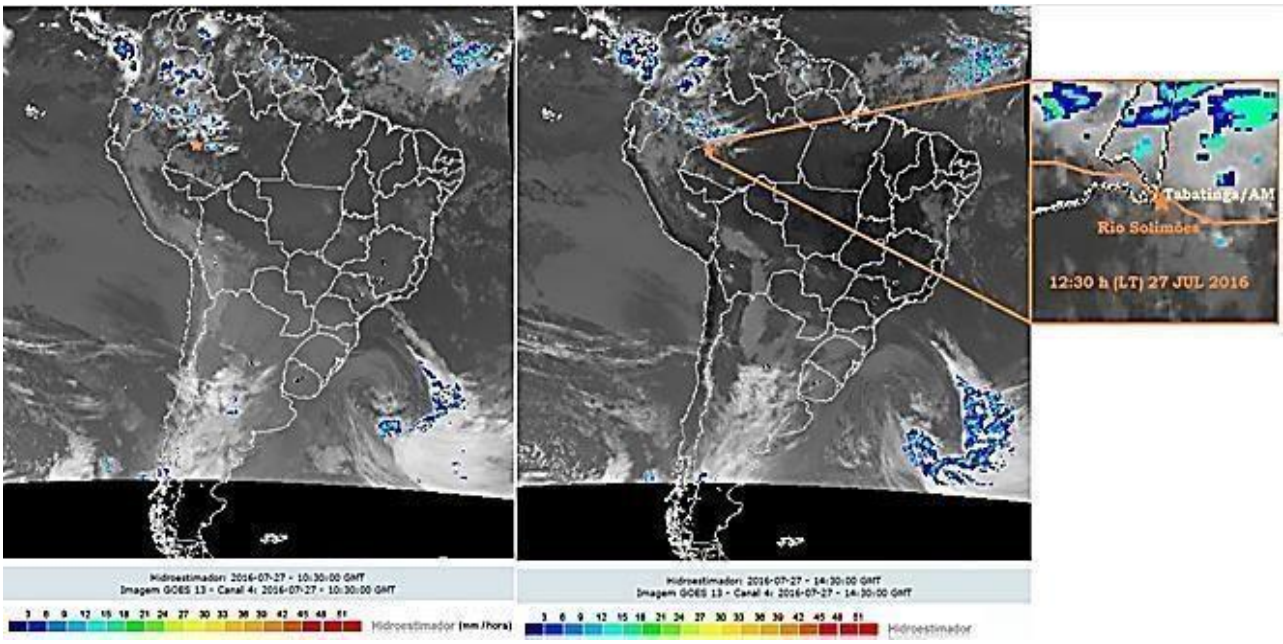

Fig.5: Meteorological conditions on July 27, 2016, between 10:30 and 14:30 GMT, for South America. (Source: CPTEC/INPE, 2016).

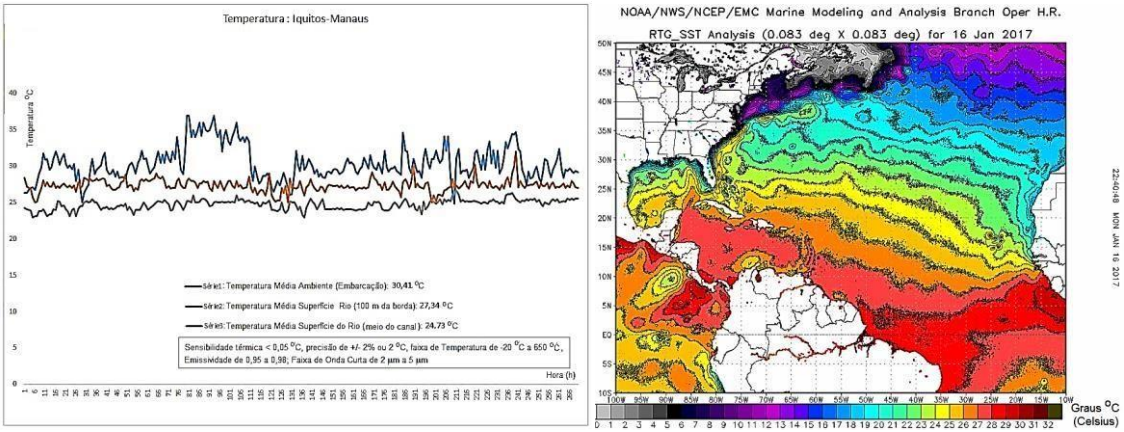

Fig. 6: Time series of temperature along the Amazon River during the first stage of the Expedition (Iquitos/Peru – Manaus/Brazil), and compared to data from the *Marine Modeling and Analysis Branch Oper. H. R.* (Verification Ensembles) of NOAA/NWS/NCEP/EMC. Source: Amazon River Expedition and NOAA, 2016.

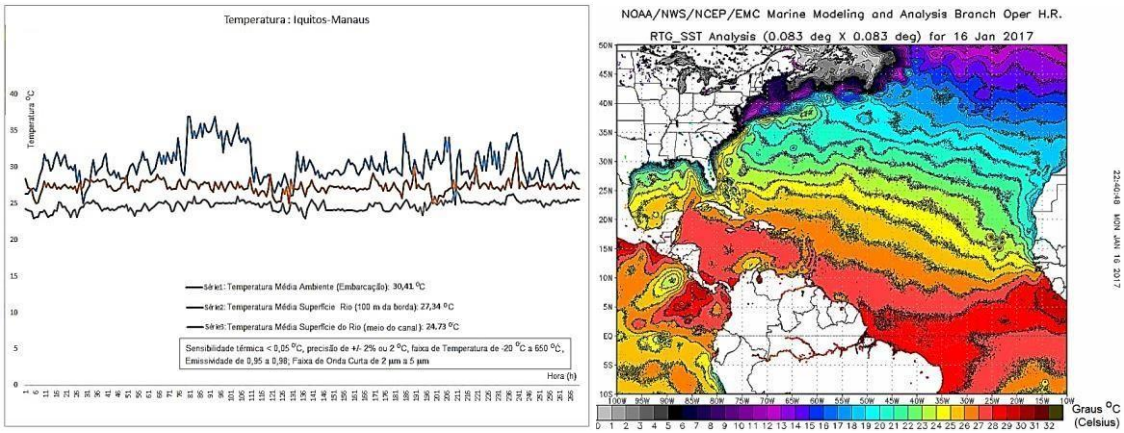

Fig. 7: Time series of temperature along the Amazon River during the second stage of the Expedition (Manaus/Brasil – Macapá/Brasil), and compared to data from the *Marine Modeling and Analysis Branch Oper. H. R.* (Verification Ensembles) of NOAA/NWS/NCEP/EMC. Source: Amazon River Expedition and NOAA, 2016.

Fig. 7: Time series of temperature along the Amazon River during the second stage of the Expedition (Manaus/Brasil – Macapá/Brasil), and compared to data from the *Marine Modeling and Analysis Branch Oper. H. R.* (Verification Ensembles) of NOAA/NWS/NCEP/EMC. Source: Amazon River Expedition and NOAA, 2016.

The analyses of the water samples from both stages of the expedition are list in Tables 2 (1st stage) and 3 (2nd stage), and these data describe the "actual state" of the Amazon River in 2016 during the dry season in the Amazon. In Tabatinga at the entry of the Amazon River into Brazil, during the month of July 2016, the level of the Solimões River (the name given to the river from this point to Manaus, Brazil) was 5.54 m (at the end of the rainy season it was 11.62 m at this sampling point in May 2016), and the highest level recorded here was in May 1999 when the depth was 13.38 m with respect to sea level (ANA/CPRM/SIPAM, 2017). During this period of the expedition the El Niño climate phenomenon was already firmly established in the region since it had begun in 2014, lasted for all of 2015, and was still strong in 2016. The effects of this drought were clearly visible during the entire voyage along the river from Peru to the Atlantic, principally due to the marks left on trees in the *várzea* areas at the river's edge by the previous high-water season.

However, the quality of the water from the Amazon River at the 39 georeferenced sample points was satisfactory and within the standard for potable water for human consumption by communities adjacent to the river's edge from the western portion of the basin to the Atlantic, although basic sanitation services are a preoccupation for all the communities located at these 39 sampling points, including for Iquitos (Peru), Manaus, Santarém and Macapá (Brazil).

At the end of December 2016, the Tapajós River in Santarém, Pará, Brazil, located in the lower Amazon region, was more than 6 m below the base of the contention dike that serves as a waterfront walkway for urban dwellers along the Tapajós' edge in front of the city. A vertical line near the pier in front of the church of *Nossa Senhora da Conceição* approximately 5m above the base of this dike represented the maximum extent of the previous high-water mark, and this mark extended for more than 60 m horizontally to near the municipal fish market. Rainfall is still sporadic during this period of the year in Santarém and almost always occurs early in the first hours of the morning before sunrise or at the end of the afternoon, but is always brief in duration.

Nearing the mouth of the Amazon River, the weather was constantly cloudy with grey and dark, low nimbostratus (Ns) clouds at about 2,000 to 3,000 m, with a constant fine rain near Prainha (Pará/Brazil) and Almeirim (Pará/Brazil), (08:20 LT), and the air temperature and the dew point temperature at the level of the river's surface were very similar, indicating a condition of saturation. There was fog on the horizon, and this fog goes by the name of hot fog because the drops are well above the freezing temperature. It was most likely an advective fog in function of the horizontal dynamic of atmospheric migration that was in a situation that was more adequate for saturation, since, being nearer to the Atlantic Ocean (approximately 300 km), the ocean breeze that penetrates the coast of Amapá at Macapá (Brazilian Atlantic coast), in this period of the year has favorable conditions for the trade winds, including for the ITCZ, that can stimulate the development of climatic ariation in this region of the Amazon River.

Recommendation

At the site (https://amazonexpedition.zohosites.com) there is more information about the "actual state" of the Amazon River in 2016, not only with respect to climatology, but also with respect to the life of people in the communities in this region.

Conclusion

The Amazon River, during the dry season of 2016, was influenced by a prolonged El Niño climatic tendency (2014, 2015 and 2016). The results show that there was a reduction in water levels along the entire sampling trip on the river, from the city of Iquitos in Peru to the Brazilian city of Macapá near the interface of Brazil and the Atlantic Ocean. The sea surface temperature stimulated the establishment of an increasing temperature gradient in the equatorial region along the river, up to its mouth at the Atlantic Ocean, where the river accompanied the same temperature regime as the ocean during this period. This gradient established the climatic phenomenon called the wet-dry dipole, combined with a tendency for regional warming during the El Niño event of 2016.

Acknowledgements

The authors are grateful to the Lutheran University Center of Manaus (Centro Universitário Luterano, Manaus, (CEULM/ULBRA)) for the help with setting up this bi-national research trip, the Brazilian Navy in the Amazon (western and eastern regiments) for information that helped with navigation, the Foundation for the Support of Research of the State of Amazonas (Fundação de Amparo e Pesquisa do Amazonas (FAPEAM)) that provided a scholarship student to conduct the water analyses, the Max Planck Chemistry Institute (Mainz- Germany) for support with the chemical analyses, and the Mauá group at INPA in Manaus/Brazil. Furthermore, we thank the Secretary of Education and Quality of Teaching of the State of Amazonas, that through the DEPPE,

provided logistical support in sampling areas in the State of Amazonas, Brazil, and the Environmental Engineering sector of Honda of the Amazon, the engineers Feijão, Mirian, Mário, and Murakami for physical support with material used in the field, and also the Consul of Peru in Manaus, Dr. Javier Arteta Valencia for his orientation, and the Consul of Brazil Dr. Salvador R. Vecchio in Iquitos for providing access to sites in Peru. Additionally, the authors thank the Institute of Investigation of the Peruvian Amazon (IIAP) in Iquitos, Peru, specificaly the Director Dr. Luis Campo Baca and his team, for the logistical support and the dissemination and promotion of this reasearch expedition, the Superintendency of the Federal Police –Tabatinga-Amazonas/Brazil, the Migration and Foreign Visitor Service of Peru (Manaus, Santa Rosa and Iquitos), and the collaborators Eliomar Oliveira, Maurício Benzecry, Abrahão Barros, Gilberto Carvalho, and Francisco Santana.

References

APHA - American Public Health Association. Standard Methods for the examination of water and wastewater. 19th ed, Washington DC, USA. 1985.

APHA - American Public Health Association. Standard Methods for the examination of water and wastewater. 19th ed, Washington DC, USA. 2003.

ANA – CPRM - SIPAM: Monitoramento Hidrológico. Agência Nacional de Água – Serviço Geológico do Brasil - Sistema de Proteção da Amazônia. Boletim no. 18 (2016). Disponível em;
https://www.cprm.gov.br/sace/boletins/Amazonas/20160513_19-20160513%20-%20191650.pdf EE

Câmara de Comercialização de Energia Elétrica. Em
https::://economia.uol.com.br/noticias/Reuters/2017/09/20.

CPTEC – INPE: Centro de Previsão de Tempo e Estudos Climáticos – INSTITUTO NACIONAL DE PESQUISAS ESPACIAIS: Em, http://satelite.cptec.inpe.br/home/index.jsp, (acesso em julho e dezembro 2016).

ERFANIAN, A.; WANG, G.; FOMENKO, L. Unprecedented drought over tropical South América in 2016: significantly under-predicted by tropical SST. Scientific Reports. 5811(2017) doi: 10.1038/s415998-017- 05373-2.

GOLTERMAN, H.L., CLYNO, R.S. & OHNSTAD, M.A.M. Methods for physical and chemical analysis of freshwaters. 2nd ed. Blackwell, Oxford, 1978.

GOLTERMAN, H. L. (Edit., with the assistance of R. S. Clymo): Methods for Chemical Analysis of Fresh Waters—IBP Handbook No. 8—Oxford & Edinburgh (Blackwell Scientific Publications), 1971.

JIMÉNEZ-MUÑOZ, J.; MATTAR, C.; BARICHIVICH, J.; SANTAMARIA-ARTIGAS, A.; TAKAHASHI, K.; MALHI, Y.;
SOBRINO, J. A.; SCHRIER G. Record-breaking warming and extreme drought in the Amazon rainforest during course of El Niño 2015-2016. Scientific Reports. 33130 (2016) doi: 10.1038/srep33130.

LIMA N.S., TÓTA J., BOLZAN, M.J.A., FERREIRA, A.S. and PIETZSCH, M.R. A brief observation of the formation of coherent structures and turbulence over a rain forest área in central Amazonia: THE ATTO-CLAIRE/IOP – 1/2012 EXPERIMENT. Revista Brasileira de Geofísica (2017) 35(3): 187-199. (2017) Sociedade Brasileira de Geofísica. ISSN 0102- 261X, www.scielo.br/rbg. DOI: http://dx.doi.org/10.22564/rbgf.v35i3.882.

MACKERETH, F.J.H., Heron, J. & Talling, J.F. Water analysis: some revised methods for limnologists. Freshwater Biological Association, London. (Scientific Publications, 36), 1978.

MAREGO J.A.; TOMASELLA J.; UVO, C.R. Trends in streamflow and rainfall in tropical South America, eastern Brazil, and northwestern. Journal of Geophysical Research Atmospheres. 103: (D2) 1775-1783 (1998).

MOHTADI, M.; PRANGE, M.; SCFUB, E.; JENNERJAHN, T. Circulation in Southeastern South America and it's influence from El Niño events. Journal of the Meteorological Society of Japan, 80, 21-22. Article number: 1015 (2017) doi: 10.1038/s41467-017-00855-3n, *Nature Communications*.

NOAA/NCEP/NWS/EMC: In, ftp://ftpprd.ncep.noaa.gov/pub/data/nccf/com/gfs/prod, (acess: July/December, 2016/July, 2017).

POVEDA G.; MESA, O. J. Feedbacks between hydrological processes in tropical South America and large-scale ocean-atmospheric phenomena. Journal of Climate. 2690-2702 (1997).

VALDERRAMA, J. G. The similaritons analysis of total nitrogen and total phosphorus in natural waters. Mar. Chem, v.10, 1981

Transport of Soy on the Madeira River between Porto Velho and Manaus (Brazil)

A brief observation of geoindicators in the Madeira River between Novo Aripuanã and Manicoré in 2018.

Newton Silva de Lima[1,2], Alan Ferreira dos Santos[1], Eriberto Barroso Façanha Filho[1,2], Liliam Gleicy de Souza Oliveira[1], Aldemir Malveira de Oliveira[2,3], Daniel Barros Valentim Mansur da Silva[4].

(1) Lutheran University Center of Manaus – CEULM/ULBRA
Av. Carlos Drummund de Andrade, 1460. Conj. Atilio Andreazza – Japiim II – CEP 69077-730. Manaus, Amazonas - Brazil. Tel: (+55 92 3616-9800). Email: acsmao@ulbra.br

(2) Secretary of State for Education and Sports of the State of Amazonas
Street: Waldomiro Lustosa, 250 - Japiim II, Manaus – Amazonas. Brazil. CEP 69076-830
Manaus, Amazonas - Brazil. https://www.seduc.am.gov.br/

(3) University Center for Higher Education of Amazonas - CIESA
Rua Pedro Dias, 203 – Flores. CEP 69058-818 Manaus – Amazonas – Brazil. Tel. (+55 92 99401-6229). Email: academico@ciesa.br

(4) Martha Falcão College - Wyden
Rua Natal, 300 – Adrianópolis - Manaus – Amazonas – Brazil. CEP 69057-090. Tel.: (+55 (92) 2121-0929).

e-mail: newton.lima@ulbra.br; alan.ferreira@ulbra.edu.br; eriberto.filho@ulbra.br; liliam_gso@yahoo.com.br; amoliveira@gmail.com, danielvmansur@gmail.com.

ABSTRACT

The presence of toxic metals in the gold mining process conducted in the region of the Madeira River and its effect on fish metabolism and contamination of the várzea floodplain environment and the vegetables that are grown there is a relevant factor for the need for geoindicators to monitor gold mining activities in this watershed, especially between Novo Aripuanã and Manicoré. The objective of this study was to identify geoindicators and concentrations of the metals Cu, Cd, Cr, Co, Pb, Zn, Mn and Ni in the fish called pacu (*Mylossoma spp*), plankton, and vegetables and fruits such as squash, watermelon, and banana in the adjacent floodplain communities of Jenipapo, Vencedor, and Providência. The risk of contamination was analyzed, and a brief evaluation of the current state of the water taken from the Madeira River by these communities was made. Samples of fish, plankton, and vegetables and fruits were taken in these floodplain communities along the Madeira River between Novo Aripuanã and Manicoré, along with water samples and depth at each community. Atomic absorption was used to analyze the metal concentrations, and geochemical analysis of water samples was done, including pH, conductivity, associated O_2 and oxygen concentration for *in situ* determination of water quality. The results show that the geoindicators require further fieldwork to better describe the parameters necessary for monitoring of water, vegetable, and fruit consumption by these communities. The necessary adjustments include improving the use of taxonomy of larger fish during field collection work for more specific analysis of gills, liver, and kidneys of specimens, collection work for more specific analysis of gills, liver, and kidneys of specimens, collection in other habitats in the floodplain environment, and inclusion of mercury (Hg) in the aquatic field sampling.

Keywords: toxic metals, contamination, várzea floodplain, atomic absorption

Introduction

"Egypt is a gift of the Nile", an observation that is identical in relation to a habitat in the western world in South America, specifically communities in the north of Brazil such as Porto Velho, Humaitá, Manicoré, Novo Aripuanã, Borba and Nova Olinda do Norte, which can be thought of as gifts from the Madeira River. The Madeira River is the most inhabited and commercially exploited of the tributaries of the right (southern) bank of the Solimões-Amazonas River system (RAPP PY-DANIEL, 2007). The river received this name because of the enormous quantity of tree trunks that its waters carry throughout the entire year (STERNBERG, 1975). The true grandeur of this river lies in its richness in fish species (DORIA *et al.*, 2012) along it margins, vast alluvial plains have developed through deposition of sediments carried in the water (HORBE *et al.*, 2013), which also contain gold. Its geographic location allows for a shipping route for soybeans produced in the Center-West region of Brazil to the Atlantic Ocean (Correa and Ramos, 2010), besides providing ample hydroelectrical energy through the dams at Jirau (**Fig. 01**) and Santo Antônio, which do not use conventional reservoirs (ANEEL).

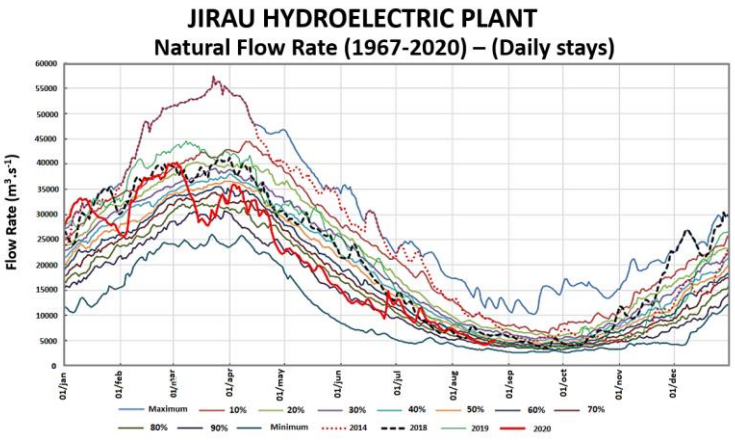

Fig. 01 – Control of the natural flow rate at the Jirau hydroelectric dam (1967-2020). Source: ANA – National Water and Sanitation Agency, 2020.

The establishment of geoindicators, according to Berger and Iams (1996), and VALLADARES SOARES, *et al*., (2006), involves estimating a temporal range of effects and disturbances in an ecosystem. Investigations of the behavior of the Madeira River, which flows carrying great quantities of alluvium, is a highly challenging undertaking because the natural conditions of this river are far from simple, with the flow varying in time and space, and the granular structure and cohesive properties of the alluvium are rarely homogeneous along its course (YALIN, 1992). Mining activities that exist along the Madeira River are intense and require monitoring, a theme that is discussed in detail by BASTOS and LACERDA (2004). This mining activity makes the elaboration of geoindicators of contamination of the elements that compose this ubiquitous aquatic ecosystem an important priority.

According to Stumm and Morgan (1981), since the industrial revolution, the burning of fossil fuels, production of paper and cement, mining, among other human activities have caused an increase in the levels of metals in aquatic ecosystems around the world. McDonald and Wood (1993) related that the potentially toxic metals in aquatic ecosystems that affect fish are, in decreasing order of severity, Hg, Pb, Cd, Cu, Zn, Al, Mn and Cr. In the current study, all these metals were investigated, except for mercury (Hg). The motive for omitting Hg was to focus on other metals since Hg receives an inordinate amount of attention in studies of environmental contamination in this region, especially because it is essential to gold mining activities in the region and would therefore be relevant as a geoindicator. The effects of exposition to potentially toxic metals in aquatic ecosystems affects fish morphology as well as physiology, according to Mazon *et al*. (1999), and Val and Almeida-Val (1999).

Material and Methods

Sites along the Madeira River

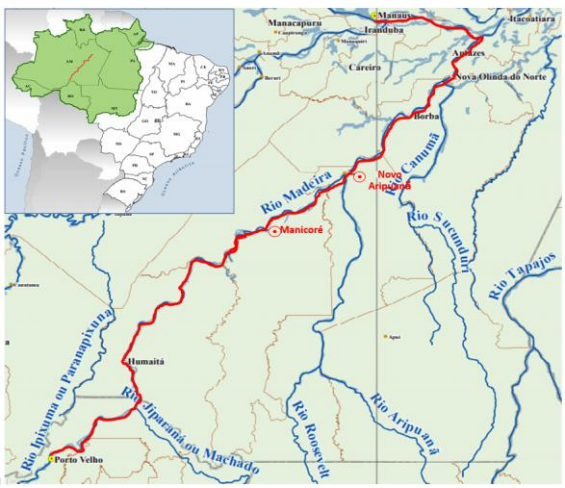

Fig. 02 – Map of the Amazon River watershed, with the Madeira River in detail. Source: ANA – National Water and Sanitation Agency, 2018.

Figure 2 shows the delimitation of the research area along the Madeira River from Porto Velho to Manaus (**Fig. 02).** The stretch of river between the cities of Novo Aripuanã and Manicoré is where samples were collected of fish, fruit, vegetables, and plankton. Water samples were collected from Manicoré to Manaus.

The Madeira is an alluvial river is with meanders, floodplains, and erosion along its banks, known as *terras caídas* in Portuguese (**Fig. 03**). This geofluvial scenario has allowed for the development of gold mining along the river (**Figs. 04 A - B**). The choice of the sample collection regions (**Tab. 01**) is a function of the strategic position of Novo Aripuanã, which is on the river with the same name. This river is a tributary of the Madeira, and the confluence of these two rivers is in front of Novo Aripuanã. The Aripuanã River has the Roosevelt River as a tributary, and the city of Manicoré (S $5^0$58’32” W$61^0$18’00”) (**Fig. 05**) is the nearest city upriver from Novo Aripuanã (S $5^0$08’00” W $60^0$22’30”).

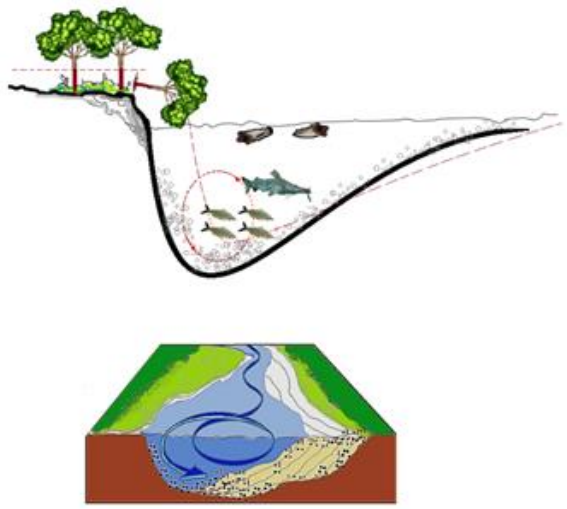

Fig. 03 – Artistic representation of the profiles of the geoindicators for terrestrial and aquatic ecosystems along the Madeira River, with emphasis on the effects of erosion caused by vortices as observed in the 2018 field campaign, (not to scale).

Fig. 05 – Aerial view in the direction Porto Velho to Manaus of the city of Manicoré on the Madeira River in July 2018.

Figs. 04 A - B – Madeira River Alluvial Gold Mining (A). In detail, 15 active mining plants, cross-section cut and bathymetry of the georeferenced location on the map of the region - S 05^0 17' 52.0'' W 060^0 41' 14.3'' (B). (2017DEC24 – 11:32:24 LT). (Source: SHNN-09/Map 4726.tif – Madeira River; Google Maps, 2018)

Sample collection

Sample collection occurred between the cities of Manicoré and Novo Aripuanã (**Fig. 06**), with sampling trips in different communities. In the public market of Manicoré ten specimens of Characiformes - *Mylossoma spp* that are commonly marketed in the community of Rosarinho (upriver from Manicoré, on the Manicoré River, 20 min by motorboat). An additional ten specimens (*Mylossoma spp*) were collected at Fazenda Providência which were captured in Xadá Lake, between Manicoré and Novo Aripuanã. Although there were species of the order Siluriformes available during the sample collection, the choice of species of the order Characiforme was made due to the abundance of these fish during the study period, and also because these species are greatly appreciated by the local communities and therefore economically support fishing activities. Collection of fruits and vegetables occurred near the community of Vencedor (S 05° 20.130' W060° 44.776') before Novo Aripuanã, and included watermelon (*Citrullus lanatus*), squash from the family Cucurbitaceae – order Cucurbitales, which are native to várzea floodplain areas in the Amazon and are abundant in the month of July. Along the banks of the Madeira River in the community of Jenipapo (S 05^0 34.598' W 060^0 55.803') plankton (*limnoplâncton*) were collected based on Raunkiaer *et al*. (1934), in according to Gonçalves and Lorenzi (2011). The banana called pacovã (*Musa paradisíaca*) is a pseudoberry or an epigynous berry from the community of Providência (S 05^0 34.797' W 060^0 55.801') along the stretch of river from Manicoré - Novo Aripuanã (**Tab. 01**). This banana sample was collected at Borba, where it was being sold in the market. Water sample collection occurred during the entire trajectory between the cities along the Madeira River to Manaus.

Fig. 06 – Panel of sample collection in the field: (1) squash and watermelon in the community Vencedor. (2) water sample collection in Providência. (3) mining plant in Providência. (4) cataloging fish (*Mylossoma spp)* in Manicoré. (5) bananas being shipped in Providência. (6) weighing of fish in the public market of Manicoré. (7) public fish market (species of Characiformes and Siluriformes) in Manicoré. (8) Plankton collection in Jenipapo. (9) water collection in Novo Aripuanã. (10) Bananas in Borba. All the products that were being shipped on the Madeira River were destined for the Municipal Market of Manaus.

Geochemical analysis method for potentially toxic metals

After collection, the samples were sent to the where they were washed with tap water then with distilled water and prepared for analysis. Samples of fish gills and pieces of fruits and vegetables were used for the atomic absorption analysis, while plankton were analyzed in their whole form, and all samples were dried at 65°C for 48 h. From each sample a subsample of 0.5000 g was taken in duplicate and digested in 10 mL of (Synth) on a heating plate at 90 °C for 1 hour. The digested sample were filtered, quantitatively transferred to a 50 mL volumetric flask and the volume was completed with distilled water.

Subsequently, the samples were stored in flasks and refrigerated until the atomic absorption analysis. The same procedures were conducted for the control and blank samples.

The standard concentrations used were (mg/mL): Cu (0.5, 1.0, 2.0, and 3.0), Pb (1.0, 3.0, and 5.0), Zn (0.1, 1.0, 3.0) and 6.0, Cd (0.5, 2.0, and 3.0), Ni (1.0, 3.0, and 6.0), Mn (0.1, 0.5, 1.0 and 2.0), Cr (1.0, 3.0, and 5.0), Co (1.0, 5.0, 10, and 20).

All biogeochemical analyses followed the procedures described by Bruno (2014).

Table 01 – Sample points during the on the Madeira River between Novo Aripuanã and Manicoré in 2018 (N$^{er.}$ of samples).

YEAR	LOCATION	LAT	LONG	WATER	FISH	PLANKTON	GREEN	FRUIT
2017-2018	Nova Olinda do Norte	S 03° 53' 10.8"	W 059° 05' 34.6"	2	-	-	-	-
2017-2018	Borba	S 04° 23' 01.1"	W 059° 35' 36.9"	2	-	-	-	10
2017-2018	Novo Aripuanã	S 05° 08' 00"	W 060° 22'30"	3	-	-	-	-
2017-2018	Manicoré	S 05° 58' 32"	W 061°18'00"	3	-	-	-	-
2018	Rosarinho[1](Mercado Público)	S 05° 58' 32"	W 061° 18'00"	-	10	-	-	-
2018	Jenipapo[2]	S 05° 48.519'	W 060° 55.803'	1	-	10	-	10
2018	Vencedor[2]	S 05° 20.131'	W 060° 44.776'	1	-	-	-	-
2018	Fz. Providência-Lagoa Xadá[2]	S 05° 34.800'	W 60° 55.799'	1	10	-	10	-

Water quality analysis at the collection points

All the parameters for geoindicators of water quality were measured *in situ*, thus allowing for a sampling scheme that was able to accurately capture the characteristics of the Madeira river-atmosphere ecosystem for the data collection period of December 2017, and January and July of 2018. The sampled parameters are shown in (**Tab. 03**), with their respective geochemical analyses (pH, conductivity, associated oxygen, and oxygen concentration) and water temperature, for the Madeira River to the Negro River in Manaus. Additionally, bathymetric profiles were conducted with the aid of maps in raster and tiff formats from Northwest Hydrology and Navigation Service – (SHNN-09) for the sample collection points. This sampling will serve to describe the current state of the bed of the Madeira River from Manicoré to Nova Olinda do Norte, which is the last city before the mouth of the river, between the cities of Autazes (right bank) and Itacoatiara (left bank), each coming after Manaus, on the Amazon River.

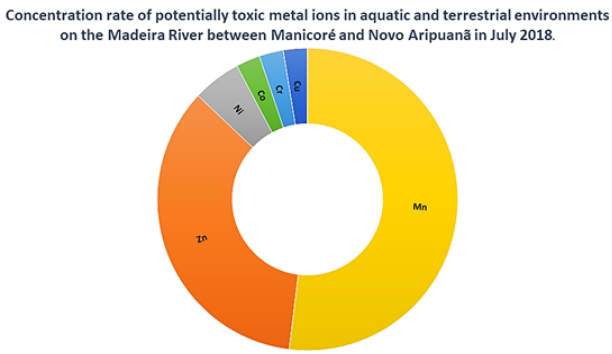

Fig. 07 –Concentration toxic metal ions in aquatic and terrestrial environments on the Madeira River between the cities of Manicoré and Novo Aripuanã in July 2018.

Results and Discussion

The description of geoindicators is shown in (Tab. 02) for the eight (8) analyzed chemical elements (Fig. 07). Zn and Mn have the largest values, but only for the fish (*Mylossoma spp),* and Cd, Cr, Co and Ni had the lowest values. The Ministerial Order 2914/2011 of the Brazilian Ministry of Health determines that the values of the peaks shown in (Fig. 08) for Zn and Mn are above the acceptable limits for human consumption. For zinc the recommended concentration is 5 mg/L and acceptable levels are in the range of 10 – 40 mg/L. For manganese the recommended concentration is 0.1 mg/L and acceptable levels are within 0.2 mg/L. Recommended concentrations for human consumption the recommended acceptable levels are in the range of 1 – 10 mg/L, and for nickel the recommended concentration limit established by the World Health Organization (WHO) is 0.07 mg/L; however, the Ministerial Order 2914/2011 does not establish a recommended concentration for nickel.

There is a total absence of Cd (cadmium) for all sampled species, which, according to the WHO (2010) and the Food and Agriculture Organization (FAO; 1997) the Provisional Tolerable Weekly Intake (PTWI) is 400-500 mg, or 7 mg / kg of body mass (assuming a body mass of 60 kg). The presence of cadmium in foods is a result of soil and water contamination from natural as well as anthropogenic sources. Is known that cadmium accumulates in tissues, particularly the liver and kidney, in terrestrial as well as aquatic animals, especially those that feed on detritus, such as mollusks and Siluriforme species like catfish.

Table 02 – Concentration of toxic metal ions in aquatic and terrestrial environments on the Madeira River between the cities of Manicoré and Novo Aripuanã during the dry season in July 2018.

METAL	LOCATION						
	ROSARINHO	XADÁ LAGOON	XADÁ LAGOON	BORBA	JENIPAPO	PLANKTON (JENIPAPO)	
	FISH- 1	FISH -2	GREEN (pumpkin)	BANANA	WATERMELON	ROOT	LOAF
	CONCENTRATION (mg/mL)						
Cu	0.002	0.002	0.010	0.006	0.004	0.005	0.034
Pb	0.000	0.005	0.000	0.000	0.002	0.007	0.009
Zn	0.027	0.031	0.084	0.037	0.082	0.076	0.110
Cd	0.000	0.000	0.000	0.000	0.000	0.000	0.000
Ni	0.004	0.005	0.020	0.004	0.003	0.004	0.007
Mn	0.040	0.003	0.040	0.082	0.002	0.094	1.210
Cr	0.002	0.002	0.000	0.000	0;001	0.001	0.001
Co	0.002	0.002	0.003	0.003	0.002	0.004	0.003

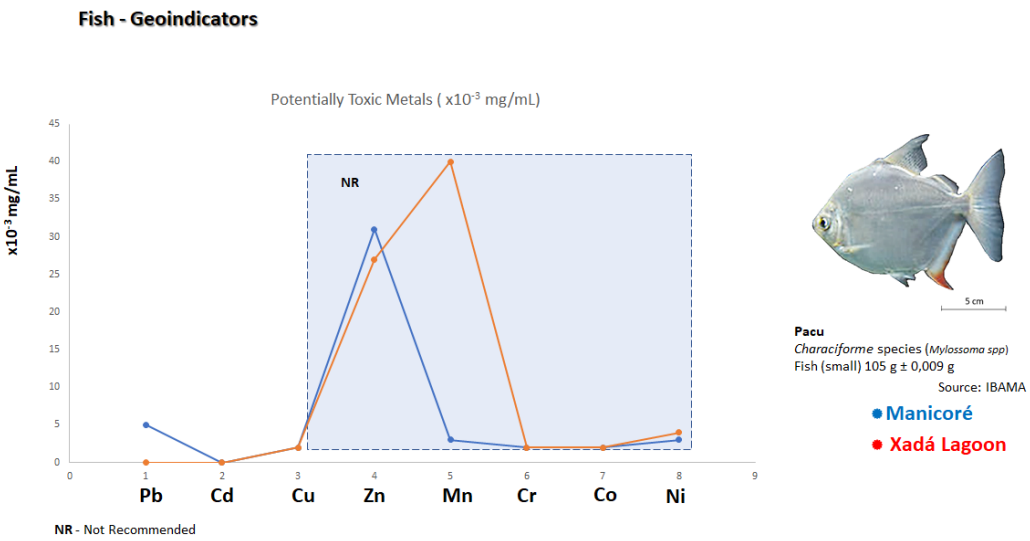

Fig. 08 – Indices of potentially toxic metals in the fish pacu - *Mylossoma spp,* in the Rosarinho community (Manicoré River) in blue, and the Xadá Lagoon in red, July 2018.

The plankton had higher values for the concentrations of the elements Cu, Pb, Zn and Mn (**Fig. 09**).

The concentrations of Mn (manganese) were high in all the species sampled in this study, and it is known that there is an antagonistic interaction between Mn and iron (Fe) wherein an excess of Mn in the diet will reduce the absorption of Fe, causing anemia, and affects the central nervous system as well as the reproductive and respiratory systems (SOARES, 2009). The Mn geoindicator is strong for concentration in fish species in Xadá Lake, as well as for most species sampled in this study, except for fish and watermelon from Manicoré. Ni (nickel) had a significant peak only for squash.

According to the Environmental Agency of the State of São Paulo (CETESB; Appendix E-2016), conductivity is the numerical expression of the capacity of water to conduct an electrical current. This capacity depends on ionic concentration and temperature, and indicates the quantity of salts present in the water column and is therefore an indirect measure of pollutant concentration. In general, levels above 100 µS/cm (**Fig. 10**) indicate impacted environments (metals). The data taken in front of the city of Manicoré (104 µS/cm), show that this aquatic ecosystem has been impacted, and this may be a result of the operations of the port which involve manipulation of contaminating fluids and fuels that contain oil and gasoline (**Tab. 03**). Observations made of the mining plants on the Madeira River from Porto Velho to Borba revealed that all these plants use a diesel generator to generate electricity, and very few of them use gasoline powered generators, and then only to power lights and small electronic equipment. The filling of storage tanks with fuel and equipment maintenance is done at the mining site and spilling of contaminants into the river commonly occurs. There are frequently from 3 up to 20 mining plants operating in close proximity, and in this way water, plankton, and fish are constantly in contact with contaminating material discarded into the river during mining activities.

Temperature is influenced by variables such as latitude, altitude, seasonality, time of day, water flow rate, and depth (**Fig. 11**). The conditions of the Madeira River drastically change with depth and flow rate every six months. The pH geoindicator for water from the Madeira River showed that it is alkaline (6.4 to 7.7) up to its mouth at the Amazon River, and is much more acid at Manaus (5.45). The water-associated oxygen geoindicator had a large decrease in Autazes (1.08 mg/L) at the mouth of the Madeira, and the oxygen saturation (40.8%) peaked at the mouth of the river.

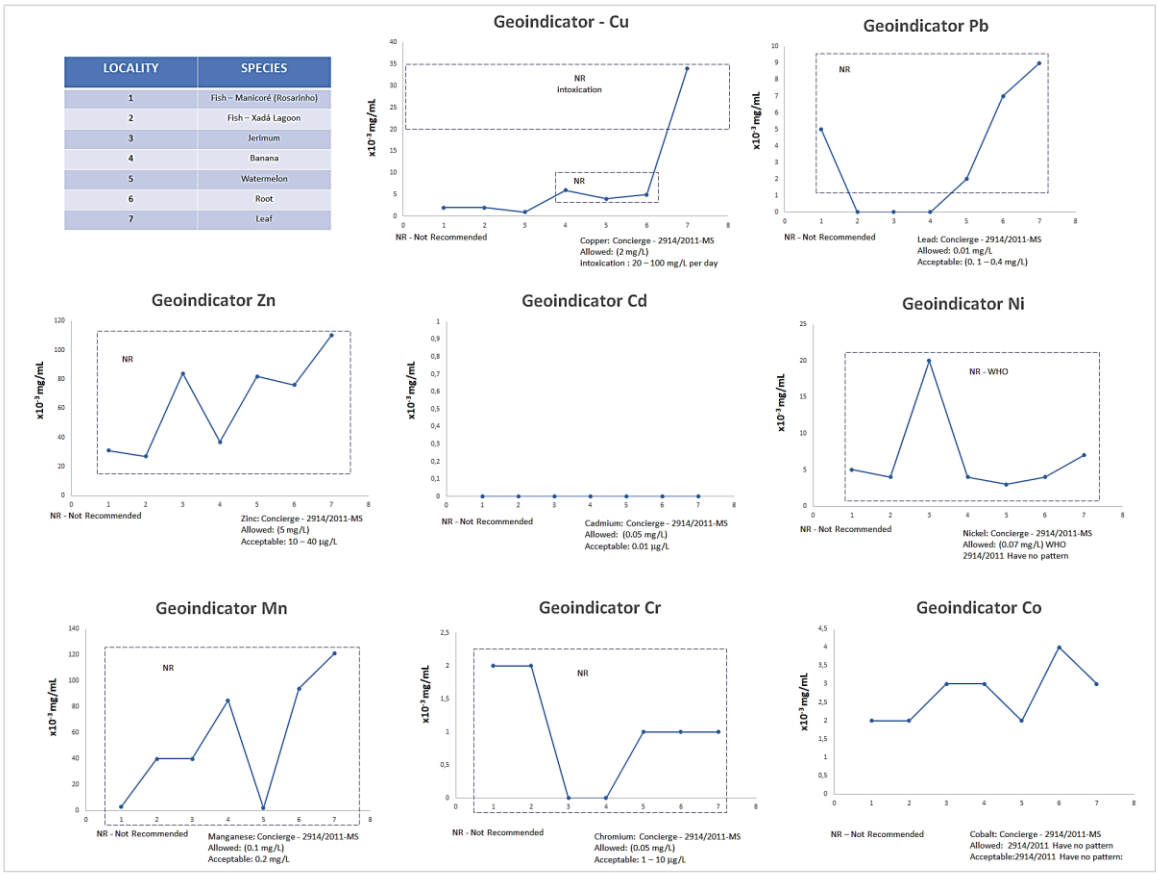

Fig. 09 – Panel showing the geoindicators for the potentially toxic metals Cu, Pb, Zn, Cd, Ni, Mn, Cr and Co, for fish, vegetables, fruits, and plankton, between Manicoré and Novo Aripuanã on the Madeira River, Brazil, in July 2018.

Table 03 – Water quality of the Madeira River in July 2018.

SAMPLE NUMBER	MUNICIPALITY	PLACE OF COLLECTION	GEOGRAPHIC COORDINATES		HOUR	DATE
			Longitude (S)	Latitude (W)		
1	Manicoré City	In front of the city (Madeira River)	S 05° 48.519'	W 061° 18.211'	12h49	2018/07/18
2	Jenipapo Community	In front of the port (Madeira River)	S 05° 34.598'	W 060° 55.803'	15h31	2018/07/18
3	Vencedor Community	In front of the port (Madeira River)	S 05° 20.130'	W 060° 44.776'	20h11	2018/07/18
4	Novo Aripuanã City	In front of the port (Madeira River)	S 05° 06.824'	W 060° 22.518'	00h20	2018/07/19
5	Borba City	In front of the port (Madeira River)	S 04° 23.092'	W 059° 35.641'	08h14	2018/07/19
6	Nova Olinda do Norte City	In front of the port (Madeira River)	S 03° 53.148'	W 059° 05.524'	12h41	2018/07/19
7	Autazes City	Beautiful Sunrise Port	S 03° 34.410'	W 059° 07.752'	17h28	2018/07/19
8	Autaz Island	Amazon River	S 03° 22.030'	W 058° 53.846'	18h45	2018/07/19
9	Manaus City	Demétrio of the Port (Black River)	S 03° 08.499'	W 060° 01.484'	05h56	2018/07/20

SAMPLE NUMBER	WEATHER	pH	TEMPERATURE	CONDUCTIVITY	OXYGEN	OXYGEN SATURATION
(continue)			°C	(µS/cm)	mg/L	%
1	Partly Sunny	7.7	26.5	104	2.5	32.65
2	Partly Sunny	6.9	28	58	2.4	33
3	Overcast	6.8	26	76	1.72	23.4
4	Clear	6.5	27	23	2.8	34.4
5	Partly Sunny	6.9	27	66	2.71	34.1
6	Partly Sunny	6.9	28	68	2.69	36.9
7	Partly Sunny	6.4	26	43.5	1.08	14.27
8	Clear	6.9	29	69	2.71	40.8
9	Fog	5.45	26	14	2.15	27.8

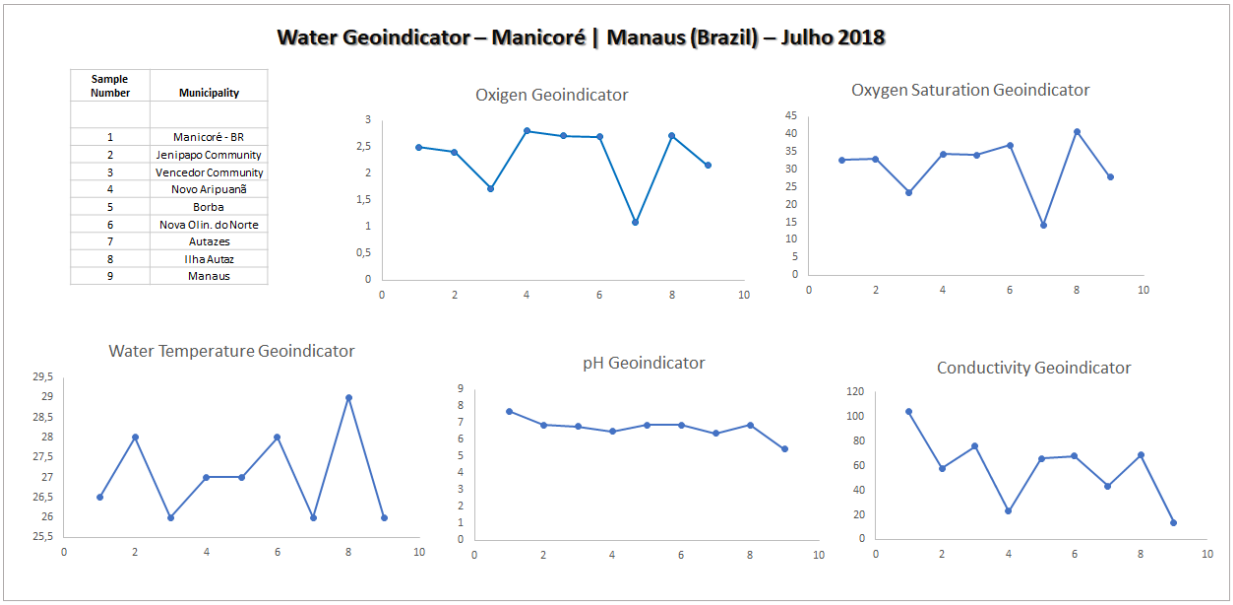

Fig. 10 – Water quality of the Madeira River between Manicoré and Manaus – Brazil, in July 2018.

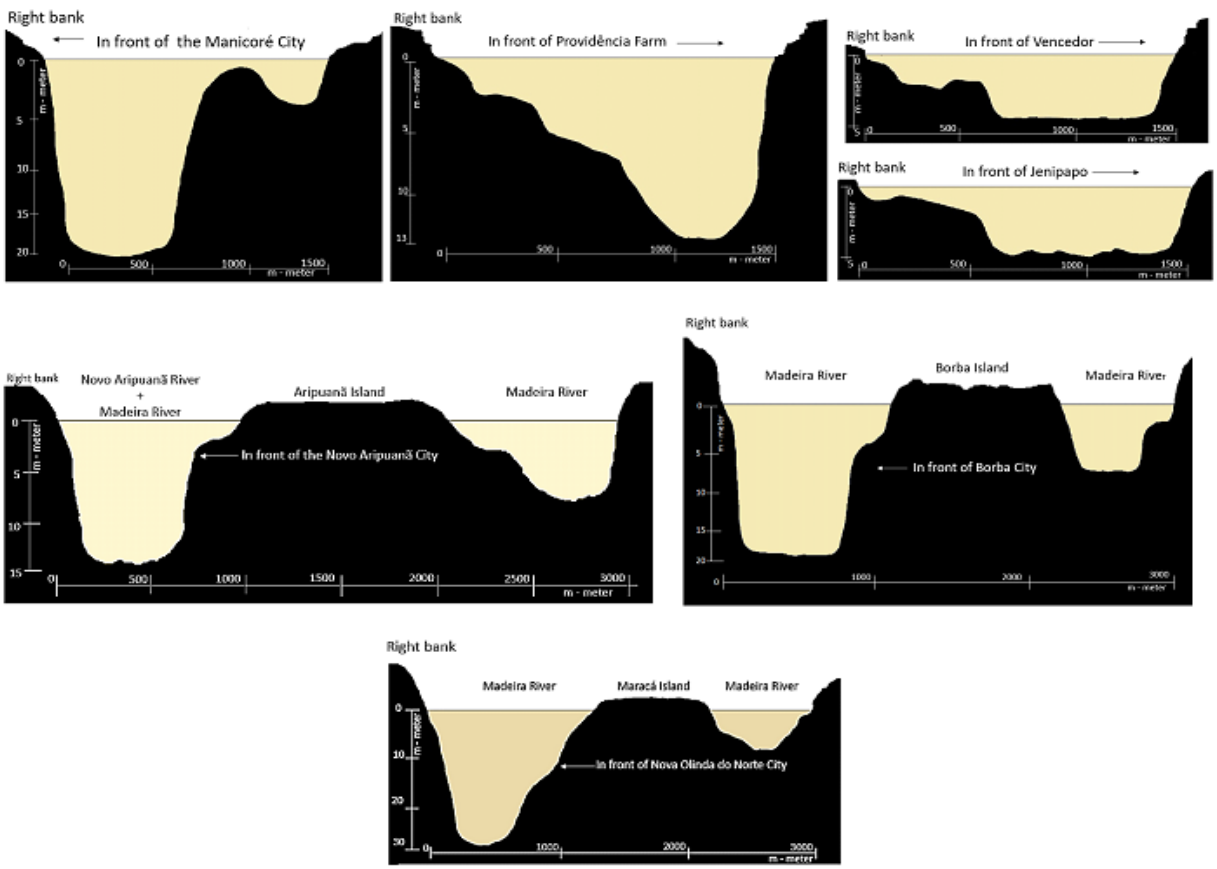

Fig. 11 – Panel showing transversal cross sections and bathymetry profiles of the Madeira River and the sampling points at indicated cities between Manicoré and Nova Olinda do Norte. (Source: Northwest Hydrology and Navigation Service – 09, Brazilian Navy, 2018).

Conclusion

This study of geoindicators of potentially toxic metals conducted on the Madeira River between Manicoré and Novo Aripuanã followed the guidelines established by the FAO (Report FSF/FOS 97.5) / the WHO (Technical Report – Series 960), National Health Foundation (FUNASA; Water Analysis Manual – 4ª. Ed.), CETESB (Appendices D and E – Environmental and Sanitary Importance of Water Quality Variables and of Sediments, and Analytic and Sampling Methods), the Minsterial Order 2914/2011 – of the Brazilian Ministry of Health, besides the contributions of Brazilian governmental agencies such as ANA, ANEEL, IBAMA, SHNN-09.

However, the use of geoindicators to collect data in the field should be frequently conducted in order to maintain robust, updated scientific information that can help to improve the lives of the populations that live along the Madeira River. It is also important to state that the omission of the metal Hg in this study should be corrected so it is included in future studies since gold mining activities in the region are in continuous operation and depend on the use of Hg due to its ability to rapidly amalgamate gold, although it contaminates the user as well as the surrounding aquatic environment and also enters the atmosphere to be subsequently deposited into waters and land at the sites visited in this study.

Future studies could include Siluriforme species such as (catfish, and surubim (*Pseudoplatystoma* species)) for gill, liver, and kidney analyses, since these fish are bottom feeders and feed on detritus and smaller fish.

These results reveal the current state of the Madeira River between Manicoré and Novo Aripuanã, and the analyzed material provides an initial slate of parameters that should be investigated using the geoindicators developed in this study in order to support decision-making with respect to use and conservation of aquatic and terrestrial ecosystems in the study region. Since this study is of a preliminary character, it is nevertheless important, and it should be emphasized that future studies should complement the current one in order to reinforce the conclusions or correct possible errors made in conducting this research.

Acknowledgements

The authors are immensely grateful to the chemistry technician Eila B. Vasconcelos (CRQ-AM: 023790) for conducting the laboratory analyses, and to the Northwest Hydrology and Navigation Service – (SHNN-09) of the Brazilian Navy (Vila Buriti/Manaus) for the bathymetry maps (raster and tiff) of the Madeira River. We also thank the Biodiversity Authorization and Information System - IBAMA/ICMBio (CR-02 - km 3 of the BR-174/Manaus highway) for authorization No. 64309 to conduct scientific activities at the National Center for Research and Conservation of Continental Fish - CEPTA, and the National Civil Aviation Agency (ANAC) for registering Nº. PP- 201800724 in the Unmanned Aircraft Register System (SISANT) for non-recreational use to fly over the Madeira River. Additionally, we thank the Social Assistant and MSc. Isaque Dantas da Unidade Hospitalar of Manicoré for logistical help in Manicoré during the Period of Intense Observation (POI). We extend a warm thanks to the captain Matheus and his team for the use of the boat N/M – Lindo Amanhecer III and the small motorboat, who contributed to our work through their skills and experience in piloting on the Madeira River and its streams, bays, and flooded forests, all having many meanders and canals which can make navigation difficult.

References

ANA – Agência Nacional de Água e Saneamento Básico**:** https://www.ana.gov.br/as-12-regioes-hidrograficas-brasileiras/amazonica. (Acesso em agosto, 2020).

ANEEL - Agência Nacional de Energia Elétrica: https://www.aneel.gov.br. (Acesso em agosto, 2020).

BASTOS, W. R. & LACERDA, L. D. A contaminação por mercúrio na bacia do Madeira: Uma breve revisão. Geochim. Brasil. 18(2)099- 114. 2004.

BERGER, A. R. and **IAMS**, W. J., eds, 1996, Geoindicators—assessing rapid environmental changes in earth systems: Rotterdam, A.A. Balkema, 466p.

BRASIL. Fundação Nacional de Saúde. Manual prático de análise de água / Fundação Nacional de Saúde – 4. ed. – Brasília: Funasa, 2013. 150 p.

BRASIL. Ministério da Saúde – MS. Portaria No. 2914 de 12 de Dezembro de 2011. https://bvsms.saude.gov.br/bvs/saudelegis/gm/2011/prt2914_12_12_2011.html.

BRASIL. Serviço de Hidrografia e Navegação do Noroeste – No. 09 - (SHNN-09) (Manaus-Amazonas). Marinha do Brasil. https://www.marinha.mil.br/chm/dados-do-segnav/cartas-raster.(2018)

BRUNO, Alessandra Nejar. **Biotecnologia I: Princípios e Métodos**, Artmed Editora, 2014 ISBN 8-582-71101-8.

CETESB - Companhia Ambiental do Estado de São Paulo. Apêndice E Significado Ambiental e Sanitário das Variáveis de Qualidade das Águas e dos Sedimentos e Metodologias Analíticas e de Amostragem (Apêndice - E). https://www..gcetesb.spov.br/ - E. pdf, (2016).

CTESB - Companhia Ambiental do Estado de São Paulo. Apêndice D Significado Ambiental e Sanitário das Variáveis**E** de Qualidade. https://www.cetesb.sp.gov.br/Apêndice - D. pdf , (2014).

CHANG, Raymond. **Físico-Química - 3.ed.: Para as Ciências Químicas e Biológicas**, McGraw Hill Brasil, 2010 ISBN 8-563-30830-0.

CORREA, Vivian Helena Capacle; **RAMOS,** Pedro. A precariedade do transporte rodoviário brasileiro para o escoamento da produção de soja do Centro-Oeste: situação e perspectivas. Rev. Econ. Sociol. Rural- - vol.48 no.2 Brasília abr./jun. 2010. https://doi.org/10.1590/S0103-20032010000200009.

DORIA, Carolina Rodrigues da Costa [et al.]. A pesca comercial na bacia do rio Madeira no estado de Rondônia, Amazônia brasileira. ACTA AMAZONICA. vol. 42(1) 2012: 29 – 40.

DOWN, Randy D., **LEHR** , Jay H., Environmental Instrumentation and Analysis Handbook, John Wiley & Sons, 2005 ISBN 0-471-47332-4.

FAO/WHO – Food consumption and exposure the assessment chimicals. WHO/FSF/FOS/97.5. (Consultations and Workshops. Geneva, Switzerland, 10-17 February, 1997).

FARMER, Franklin H., **JARRETT**, Olin, **BROWN**, Clarence A., United States. National Aeronautics and Space Administration. Scientific and Technical Information Branch, Visible absorbance spectra: a basis for In Situ and passive remote sensing of phytoplankton concentration and community composition, National Aeronautics and Space Administration, Scientific and Technical Information Branch, 1983 OCLC 9839377 - Biblioteca Digital HathiTrust's,NASA.

GONÇALVES, Eduardo Gomes e **LORENZ**I, Harri. Morfologia Vegetal: organografia e dicionário ilustrado de morfologia das plantas vasculares. 2ª. Edição – São Paulo: Instituto Plantarum de Estudo da Flora, 2011.

HORBE, A. M. C., **QUEIROZ**, M. M. A., **MOURA** C. A. V., **TORO**, M. A. G. Geoquímica das águas do médio e baixo rio Madeira e seus principais tributários - Amazonas – Brasil. ACTA AMAZONICA, VOL. 43(4) 2013: 489 – 504.

IUPAC – International Union of Pure and Applied Chemistry (2020) - https://iupac.org/

KAMAT, Prashant and **SCHATZ**, George C. How to Make Your Next Paper Scientifically Effective". J. Phys. Chem. Lett. (4): 1578−1581. 2013. doi:10.1021/jz4006916. 2013.

LAKOWICZ, Joseph R, **Principles of fluorescence spectroscopy**, 3ª edição, Springer, 2009. ISBN978-0-387-46312-4 doi:10.1007/s00216-007-1822-x ISSN 1618-2642. Livro, ISSN 1618-2650 e-Book

MAZON, A. F. et al. (1999). Acute copper exposure in freshwater fish: Morphological and physiological efffects. (In Biology of Tropical Fishes. Edited by A. L. Val and V. M. F. Almeida-Val. Chapter 21, pp. 263 – 275, INPA, Manaus, 1999).

MORAES, Érica Siani – Histórias (Heródoto e o Egito. Tradução e Comentários do Livro II) Dissertação de Mestrado - UNICAMP, 1999.

RAPP PY-DANIEL, Lucia [et al.]. Biodiversidade do médio Madeira: bases científicas para propostas de conservação – Manaus; INPA; [Brasília]: MMA: MCT, 2007.

RAUNKIAER, Christen Christensen; **FAUSBØL**, Annie Ingeborg; **GILVERT-CARTER**, Humphrey; **TANSLEY** Sir– The life forms of plants and statistical plant geography. Clarendon Presss, Oxford, 1934. 623 pp.

SKOOG, WEST, HOLLER, CROUCH, Fundamentos de Química Analítica, Tradução da 8ª Edição norte-americana, Editora Thomson, São Paulo-SP, 2006.

SOARES, Cristina Pondé Prisco Paraíso Sarno. Avaliação do teor de manganês em alimentos procedentes do município de Simões Filho - BA / Cristina Ponde Prisco Paraíso Sarno Soares - 2009. (Dissertação de Mestrado – UFBA).

SRINIVASAN, Damodaran; **PARKIN,** Kirk L.; **FENNEMA,** Owen R. **Quimica de Alimentos de Fennema**, Artmed, 2010 ISBN 8-536-32334-5

STEPHENSON, Frank H., Calculations for Molecular Biology and Biotechnology: A Guide to Mathematics in the Laboratory 2thEd., Academic Press, 2010 ISBN 0-123-75691-X

STERNBERG, Hilgard O'Reilly. The Amazon River of Brazil (GEOGRAPHISCHE ZEITSCHRIFT). Franz Steiner Verlag Gmbh – Wiesbaden, 1975.

STUMM, W. and **MORGAN**, J. J. (1981). Aquatic Chemistry. An Introduction Emphasizing Chemical equilibria in Natural Water. New York: John Wiley & Sons.

THOMÉ-SOUZA, Mário J. F. Estatística Pesqueira do Amazonas e Pará - 2004 / Mario J. F. Thomé-Souza... [et al.]. – Manaus: Ibam/ProVárzea, 2007. 74 p. : il. color.; 20,8x29,7 cm. Instituto Brasileiro do Meio Ambiente e dos Recursos Naturais Renováveis.

VAL, Adalberto Luís e **ALMEIDA-VAL,** Vera Maria Fonseca. Biology of Tropical Fishes, INPA, Manaus, 1999.

VALLADARES SOARES, P., **YOSHINAGA PEREIRA** S., **SIMÕES** S J C., **BERNARDES** G P., Aplicação do Conceito de Geoindicadores na Avaliação da Disponibilidade Hídrica em Bacias Hidrográficas – Uma Abordagem Introdutória. RBRH – Revista Brasileira de Recursos Hídricos Volume 11 n.1 Jan/Mar 2006, 111-117.

VOET, Donald, **G. VOET**, Judith, **PRATT,** Charlotte W. Fundamentos de Bioquímica - 4.ed.: A Vida em Nível Molecular; Artmed Editora, 2014, ISBN 8-582-71066-6.

WHITE, Robert. Chromatography/Fourier Transform Infrared Spectroscopy and its Applications, CRC Press, 1989 ISBN 0-824-78191-0.

WHO - World Health Organizatio: technical report series; no. 960. Evaluation of certain food additives and contaminants: seventy-third report of the Joint FAO/WHO, 2010.

YALIN, Mehmet Selim. River Mechanics. Permanon Press. 219 p.

Community on the bank of the Madeira River in the El Niño period, when the river is at an elevation of approximately 12 m with the upper edge of *Terra Firme (solid ground)* (July, 2017).

Observations with operational research on the connection of the 11-year Solar Cycle and the El Niño and La Niña phenomena and rainfall in the Amazon (1980-2030).

Newton Silva de Lima[*††], Eriberto Façanha[*††], Alan dos Santos Ferreira[*], Aldemir Malveira[† ††], José Cavalcante[††], Roseilson Souza do Vale[‡], [#]Daniel Valentim Mansur

[*]Lutheran University Center of Manaus (Geosciences - Mathematics) / [†]Federal University of Amazonas (Mathematics)/ [‡]Federal University of West of Pará (Geosciences), [††] (Secretary of Education and Quality of Teaching of the State of Amazonas), # Martha Falcão College - Wyden.
[†† * †]Manaus/ [‡]Santarém (Brazil)

(newtonulbra@gmail.com, eribertofacanha@seduc.net, alans_ferreira@hotmail.com, amoliveira@gmail.com, psi.josecavalcante@gmail.com, roseilsondovale@gmail.com, danielvmansur@gmail.com)

Abstract- The stochastic bias was used to describe the correlation between the 11-year solar cycle compared to the El Niño Southern Oscillation (ENSO) time series and rainfall over the city of Manaus (Brazil), looking for a connection between these events. For this, the time series of Solar Spots and El Niño and La Niña events and rainfall over Manaus were studied by means of the time series tools for the investigated periods. This operational research work shows that from 1980 until the 2030 projection, there is a strong correlation of connection of these data to the observed phenomena.

Keywords - Connection, Solar Cycle 11 years, El Niño, La Niña, Amazon.

INTRODUCTION

Changes in atmospheric circulation in the tropical zone (Walker cell) induce change in rainfall patterns, devastating floods, and severe droughts that can drastically affect the lives of millions of people [1]. In the mosaic of landscapes that is tropical South America the tendencies for rainfall, in the Amazon in eastern Brazil, to the northwest of Peru are well-defined by long-term hydrological data for the Amazon basin that were recorded during the 20th century. During this period the tendency for rainfall during the three most humid months and for the subsequent superficial runoff rate during the three months with the greatest runoff for the northeastern region of Brazil demonstrated a slow increase over long periods [2]. In 2016 the Amazon River Expedition from Peru to Brazil observed tendencies in which a prolonged ENSO (El Niño Southern Oscillation), event combined with a trend of regional warming increased the demand for water from the reservoirs of Brazilian hydroelectric plants in the Northeast, Central-West, and Southeastern regions of Brazil [3], and caused strong rains in the Southern region of Brazil [4]. According to [5] [6] [7], this event was associated with warming that was without precedent and an extreme drought in the Amazon, compared to other strong ENSO events in 1982/83 and 1997/98. The typical conditions of drought caused by the ENSO were observed and described by [5], as occurring only in the eastern Amazon, while in the western region of the Amazon there prevailed an uncommon level of humidity. For researchers this situation can be attributed to the humid-dry dipole at the location of maximum warming of the surface of the equatorial central Pacific Ocean. About the causes of these changes are analyzed over the last two decades the average SST (Sea Surface Temperature), anomalies are weakened towards the west, in direction of the central Pacific, and this represents an indicator that needs more observation [8].

The sun emits radiation along the entire electromagnetic spectrum. The solar structure can be understood from the point of view of two regions; the interior, which goes from its center to the surface and divided into layers, while the second is the external atmosphere of constant activity in the emission of radiation and mass in the interplanetary environment. When there is an increase in the speed and concentration of the solar wind and upon reaching the earth, it causes sudden ionospheric disturbances (SID), which constitute true ionospheric storms or magnetic storms. The electromagnetic waves, UVE and X-R, do not interact with the magnetosphere and pass through it normally, but the solar wind consisting of particles (electrons and He+) collides with the magnetosphere causing a compression in the field lines, [9].

The variation between the phases of solar activity is 11 years, in energetic and transient phenomena since the number of explosions as well as coronal mass ejections that will constitute solar wind and the number of sunspots that is related to the polarity inversion. However, the number of dark spots on the surface, the brightness of X-rays, is more intense during half of the cycle and the other half of the cycle is less intense, [9].

MATERIAL AND METHODS

The variables involved are the number of sunspots observed from 1980 to the 2013 projection, sea surface temperature (TSM) Figs.1 and 2, variations that influence ENSO and precipitation over the city of Manaus. To show the connection between the upper and lower atmosphere, linear regression is used to obtain the interaction between the phenomena, showing through Operational Research (OR) the points of optimal connection solution within the period from 1980 to 2030.

The coincident points on the Optimal Solution Line validate the solution that is on the resonance of phenomena over the observed period. Using statistical moments and linear regression, [10].

Sample Measures

Sample Avarege (*N samples*):

$$\bar{X} = \frac{1}{N}\sum_{k=1}^{N} x_k \qquad (1)$$

Sample Variance:

$$\sigma^2 = \frac{1}{N-1}\sum_{k=1}^{N}(x^k - \bar{x})^2 \qquad (2)$$

Sample Standard Deviation:

$$\sigma = \sqrt{\sum_{k=1}^{N}\frac{1}{N-1}(x^k - \bar{x})^2} \qquad (3)$$

Sample Covariance:

$$\sigma_{ij} = \frac{1}{N-1}\sum_{k=1}^{N}(x_{ij} - \bar{x}_i)(x_{jk} - \bar{x}_j) \qquad (4)$$

Sample Correlation Coefficient:

$$r_{ij} = \frac{\sigma_{ij}}{\sigma_i\,\sigma_j} \qquad (5)$$

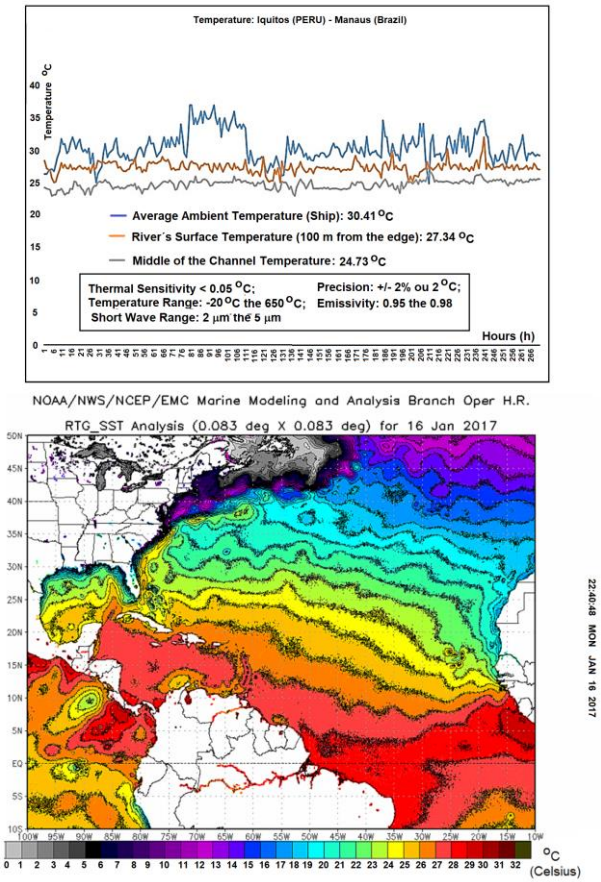

Figure. 1: Time series of temperature along the Amazon River during the first stage of the Expedition (Iquitos/Peru – Manaus/Brazil), and compared to data from the *Marine Modeling and Analysis Branch Oper. H. R.* (Verification Ensembles) of NOAA/NWS/NCEP/EMC. Source: Amazon River Expedition and NOAA, [11] [12]. 2016.

RESULTS AND DISCUSSION

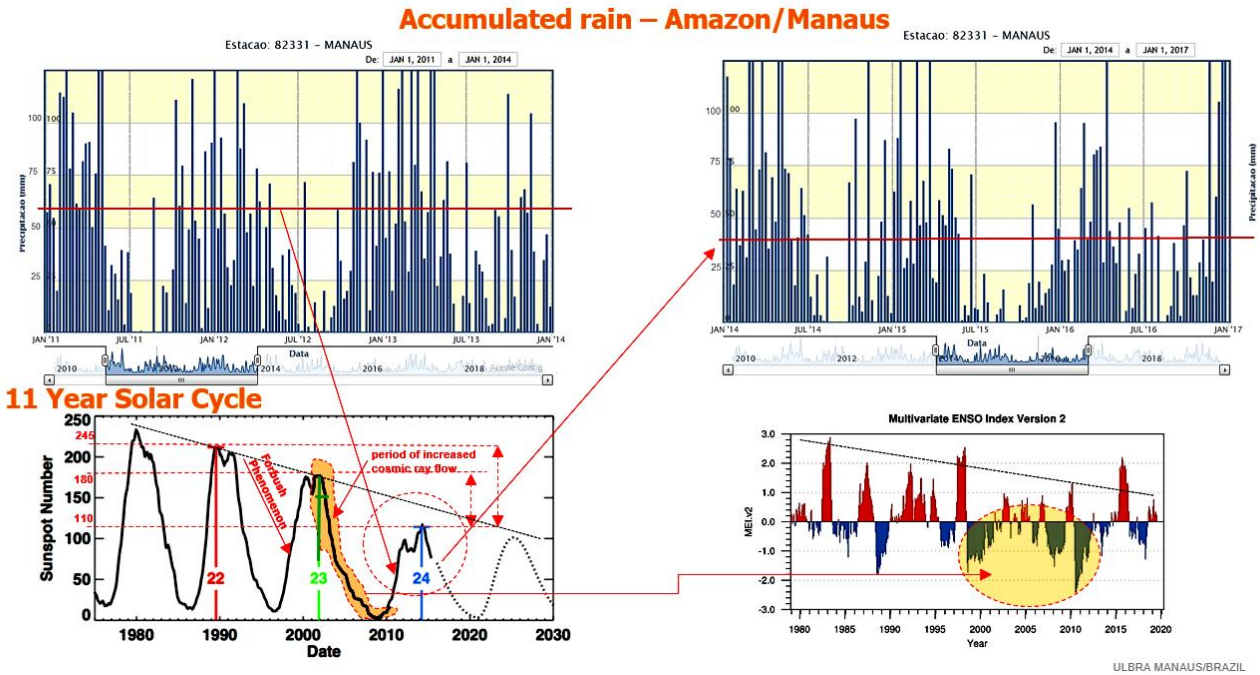

Figure. 2: Precipitation Time Series Panel, 11 Year Solar Cycle and ENSO.

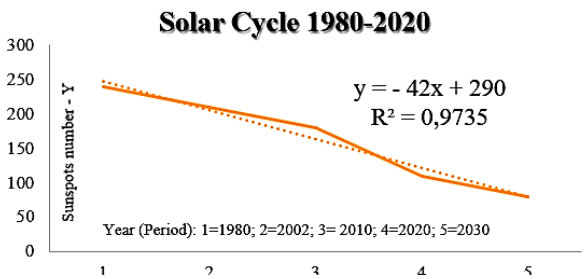

Regression Statistics	
R multiple	0,9913744
R-Square	0,982823202
R-square adjusted	0,977097602
Standard Error	10,18566944

Predicted Y	Residue
246,1153034	-6,11530335
209,4566858	0,543314217
165,4663447	14,5336553
117,8101419	-7,810141865
81,1515243	-1,151524298

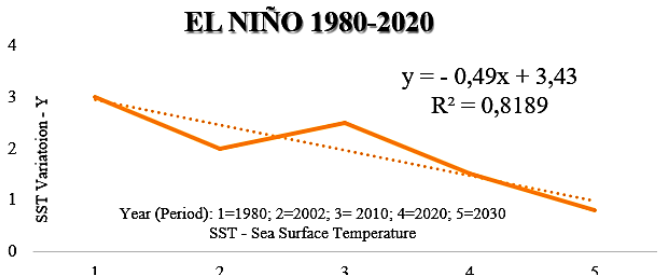

Regression Statistics	
R multiple	0,898711725
R-Square	0,807682765
R-square adjusted	0,74357702
Standard Error	0,433541283

Predicted Y	Residue
2,906912164	0,093087836
2,484183519	-0,484183519
1,976909146	0,523090854
1,427361908	0,072638092
1,004633263	-0,204633263

Figure. 3: Climate Statistics between 11-year Solar Cycle and ENSO (El Niño).

Figures 2 and 3 show the interrelationships between the precipitation time series over the city of Manaus (Amazonia-Brazil), the 11-year sunspot index from 1980 to 2019, and also the ENSO Multivariate index from the same period. In the comparison through investigation by operational research, it is found the strong correlation of the observed phenomena within the considered range, configuring to a tendency that the rains in the Amazon suffer from the solar cycle of 11 years of the Sun.

Recommendation

At the site [13], there is more information about the "actual state" of the Amazon River in 2016, not only with respect to climatology, but also with respect to the life of people in the communities in this region.

CONCLUSION

Although the statistical methods lead us to a great operational solution, we must always understand the method uncertainties, because we work with approximations and averages. However, the method shows a strong correlation between the phenomena.

ACKNOWLEDGEMENTS

The authors are grateful to the Lutheran University Center of Manaus, the Foundation for the Support of Research of the State of Amazonas (FAPEAM) that provided a scholarship student to conduct the water analyses, the Max Planck Chemistry Institute (Mainz-Germany) for support with the chemical analyses, and the Mauá group at INPA in Manaus/Brazil. Furthermore, we thank the Secretary of Education and Quality of Teaching of the State of Amazonas.

REFERENCES

M. Mohtadi; M. Prange; E. Scfub; T. Jennerjahn. Circulation in Southeastern South America and it's influence from El Niño events. Journal of the Meteorological Society of Japan, 80, 21-22. Article number: 1015 (2017) doi: 10.1038/s41467-017-00855-3n, *Nature Communications*.

J. A. Marego; J. Tomasella; C. R. Uvo. Trends in streamflow and rainfall in tropical South America, eastern Brazil, and northwestern. Journal of Geophysical Research Atmospheres. 103: (D2) 1775-1783 (1998).

CCEE – Electric Energy Trading Chamber. https://economia.uol.com.br/noticias/Reuters/2017/09/20

CPTEC – INPE: Center for Weather Forecasting and Climate Studies - NATIONAL INSTITUTE OF SPACIAL RESEARCH: (Access in: http://satelite.cptec.inpe.br/home/index.jsp , (Access in: 2016, july and december).

J. Jiménez-Muñoz; C. Mattar; J. Barichivich; A.Santamaria-Artigas; K. Takahashi; Y. Malhi; J. A. Sobrino; G. Schrier. Record-breaking warming and extreme drought in the Amazon rainforest during course of El Niño 2015-2016. Scientific Reports. 33130 (2016) doi: 10.1038/srep33130.

A. Erfanian; G. Wang; L. Fomenko. Unprecedented drought over tropical South América in 2016:significantly under-predicted by tropical SST. Scientific Reports. 5811(2017) doi: 10.1038/s415998-017-05373-2.

G. Poveda; O. J. Mesa. Feedbacks between hydrological processes in tropical South America and large-scale ocean-atmospheric phenomena. Journal of Climate. 2690-2702 (1997).

S. Hu; A. V. Fedorov. Cross-equatorial winds control El Niño diversity and change, *Nature Climate Change* volume 8, pages798–802 (2018).

ANA – CPRM - SIPAM: Hydrological Monitoring. National Water Agency - Geological Survey of Brazil - Protection System of the Amazon. Bulletin no. 18 (2016). (Access in; https://www.cprm.gov.br/sace/boletins/Amazonas/20160513_19-20160513%20-%20191650.pdf.

A. Roque da Silva. Nossa Estrela O SOL. Ed. Livraria da Física. Sociedade Brasileira de Física – SBF. São Paulo, 1a. Edição. (2006).

Von Zuben. EA932 - DCA/FEEC/Unicamp. Tópico 8 - Fundamentos para Processos Estocásticos. (2016).

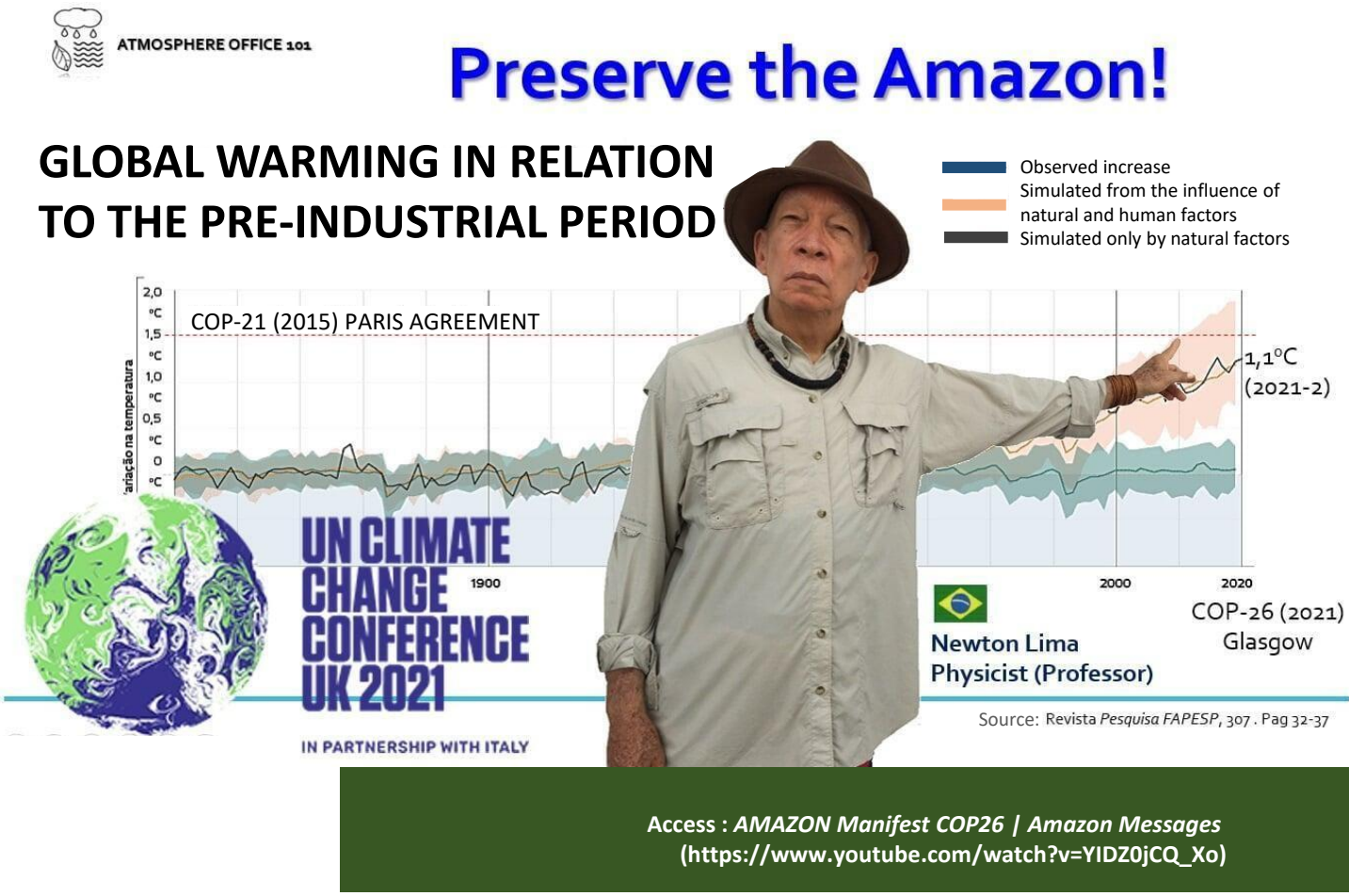

Access : *AMAZON Manifest COP26 | Amazon Messages*
(https://www.youtube.com/watch?v=YIDZ0jCQ_Xo)

SCIENTIFIC COMMITTEE PRESIDENT

- Aldemir Malveira de Oliveira

Final considerations

In its epistemology, this journal could be characterized as an investigation effort into the possibility of presenting a collection of articles on the consequences of climatic phenomena observed in the Amazon. However, starting from a reflection on each article that composes this work, it is concluded that this collection becomes a contribution to those who research on the subject around the planet. Even knowing all the difficulties that emerged in the course of each investigation, the authors of the research did not bend towards decline, but transformed each casualty into an observatory filled with energies and concerns that can only be explained by the researchers of “Climatology”. However, in essence, this magazine and its collection of articles will help those who seek to better understand atmospheric conditions, not only in the Amazon, but their interference in the planet's climate. Also, it is noteworthy that none of the works presented here do not constitute closed investigations, but seek to open a range of options for researchers who wish to embark on confronting and/or refuting the phenomena described throughout the journal.

Climate

Guatavita Lagoon National Park (Colombia), in this place we find the famous Frailejon (Big Monk) that captures water from the clouds in its plumes that condenses and converts into water for the Guatavita Chief Lagoon (3,683 m), located in the Eastern Cordillera of the Colombian Andes, in the municipality of Sesquilé, 57 km northeast of Bogotá, capital of Colombia (2022, April).

Collaborator Julio Escobar (Colombia-Bogotá)